UNIVERSITÀ DEGLI STUDI DI PADOVA

Dipartimento di Fisica e Astronomia “Galileo Galilei”

Master Degree in Astrophysics and Cosmology

Final Dissertation

Non-Gaussian signatures in a string-inspired model for the onset of inflation

Thesis supervisor

Prof. Sabino Matarrese

Thesis co-supervisors

Prof. Nicola Bartolo

Prof. Augusto Sagnotti

Candidate

Eleonora Vanzan

Academic Year 2020/21

Contents

Chapter 1

Introduction

Inflation has been widely accepted as a key ingredient of our models for the Universe. The crucial feature is a phase of accelerated expansion in the early Universe, lasting long enough to solve the horizon and flatness problems, and setting the seeds for the subsequent structure formation. This scenario is very generic and it can be realized through a variety of different models. A problem that we are confronted with is finding observables that allow us to discriminate among these models.

We are in the era of precision Cosmology and many new experiments will take data in the following decade, spanning from the Cosmic Microwave Background to Large-Scale Structure surveys. The precision of the new data will allow us to employ higher order theoretical predictions, that could give us precious information in our hunt for the best inflationary model. An observable that has a lot of potential in this direction is non-Gaussianity.

Non-Gaussianity is an "umbrella term" that covers everything that goes beyond the free field case. A completely Gaussian field is a collection of harmonic oscillator, all the information is contained in the two-point function or equivalently its Fourier transform, the power-spectrum:

$$\langle \zeta_{\vec{k}} \zeta_{\vec{k}'} \rangle = \delta^{(3)}(\vec{k} + \vec{k}') P_\zeta(k) \tag{1.1}$$

Higher order n-point correlation functions are trivial: they vanish identically for odd n and they are products of a suitable number of power-spectra for even n.
Not so for a non-Gaussian field. The first order statistics that is capable of discriminating between the Gaussian and non-Gaussian case is the three-point function or equivalently its Fourier transform, the bispectrum:

$$\langle \zeta_{\vec{k}_1} \zeta_{\vec{k}_2} \zeta_{\vec{k}_3} \rangle = \frac{1}{(2\pi)^{3/2}} \delta^{(3)}(\vec{k}_1 + \vec{k}_2 + \vec{k}_3) B_\zeta(k_1, k_2, k_3) \tag{1.2}$$

The three-point function would contain information on the particle physics aspects of the early Universe: we could learn about self interactions of the inflaton, or interactions of the inflaton with other fields, if present. This would shed light on the nature of inflation. Furthermore, different models predict different amplitudes and shapes of the bispectrum: therefore if we have models that give the same predictions at the level of the power-spectrum, for the scalar spectral index n_s and the tensor-to-scalar ratio r, they may be distinguishable in terms of non-Gaussian features.

A complementary piece of information for the inflationary puzzle would come from detecting or constraining primordial gravitational waves. An almost scale-invariant stochastic background of relic gravitational waves would fix the energy scale of inflation.

The goal of this project is to focus on a particular inflationary model and study its predictions for non-Gaussianity at the level of the bispectrum of primordial curvature perturbation. The model is motivated by the phenomenon of "climbing scalars" in String Theory [1, 2] and presents fascinating links with the CMB anomalies, in particular the lack of power on the largest angular scales [3].

This thesis is divided into two main parts. First we will focus on the attractor solution, that is power-law inflation [4], and compute the bispectrum. The calculation will be carried out without making any approximation in the slow-roll parameters, which has never been done before in the literature. Second, we will study a particular model that experiences the climbing, at the level of the power-spectrum; this prepares the ground to explore the predictions for the bispectrum, in a future work.

More in detail, the structure is the following.
The first chapter briefly recalls some basics of Cosmology, the shortcomings of the Big-Bang model and the inflationary solution. The next chapters are devoted to introducing the main quantities that come into play: second quantization in a curved spacetime, perturbation theory and the comoving curvature perturbation, n-point correlation functions. The whole chapter 7 focuses on the in-in formalism, which is a tool that is peculiar to Cosmology. The core of this first part of the thesis are chapter 8 and chapter 9: the computation of the bispectrum is carried out, trying two different approaches and finally obtaining an analytic result only in a particular configuration, the squeezed limit for the bispectrum. This configuration is, however, the one that enters in Maldacena's consistency relation, which will be explored in chapter 9. We will see that, in the case of power-law inflation, the consistency relation is satisfied even if one does not make the slow-roll assumption. This is the result one would expect, but it has never been shown before in the literature, outside the slow-roll regime.
The second part of the thesis focuses on a particular model, inspired by String Theory, which is based on the phenomenon of "climbing scalars". The attractor solution at late times is Lucchin-Matarrese power-law inflation, but at early times there is a pre-inflationary kinetic dominated phase which can leave imprints in the power-spectrum on the largest observable scales. There are many analytic models in which this can be realized, in chapter 12 we will focus on a particular one and compute the power-spectrum numerically. We recover the qualitative behaviour that has already been observed in other systems that experience the climbing. This will serve as a basis, in future works, to study the bispectrum.

Chapter 2

Inflation

In this chapter we briefly introduce the basic ingredients of the ΛCDM model. Then we review the shortcomings of the hot Big-Bang model and the inflationary solution. See [5–7] for more details.

2.1 Notation

We will use natural units $c = \hbar = 1$, unless otherwise specified.
The metric signature is the "mostly positive" one $(- + ++)$. Greek indices run from 0 to 3, Latin indices run on spatial coordinates from 1 to 3.
The reduced Planck mass is defined as $M_P^2 \equiv (8\pi G)^{-1}$. Its value is $M_P \simeq 2.4 \times 10^{18}$ GeV.

Conformal time will be denoted by τ. Dots will represent derivatives with respect to cosmic time, primes will represent derivatives with respect to conformal time.

2.2 Brief introduction to Cosmology

On sufficiently large scales, of order 100 Mpc, our Universe appears homogeneous and isotropic, a statement known as the Cosmological Principle. This properties lead to the Friedmann-Lemaître-Robetrson Walker metric (FRW in the following), which describes the background spacetime:

$$ds^2 = -dt^2 + a^2(t)\left[\frac{dr^2}{1-kr^2} + r^2\left(d\theta^2 + \sin^2\theta d\varphi^2\right)\right] \tag{2.1}$$

The spatial curvature k is a constant that can describe a flat ($k = 0$), close ($k = +1$) or open ($k = -1$) spatial geometry. The scale factor $a(t)$ only depends on time, due to homogeneity, and it accounts for the expansion of the Universe. The coordinates r are comoving coordinates, which can be though of as coordinates on a grid that is expanding together with the Universe: they are related to physical distances via $\vec{x}_{\rm phys}(t) = a(t)\vec{x}_{\rm com}$.

We define the Hubble parameter as the expansion rate:

$$H \equiv \frac{\dot{a}}{a} \tag{2.2}$$

It has units of inverse time and it sets the fundamental scale of the FRW spacetime: in units where $c = 1$, the characteristic time-scale is $t \sim H^{-1}$, setting the scale for the age of the Universe, while the characteristic length-scale is $d \sim H^{-1}$, setting the size of the observable Universe.

We introduce conformal time as:

$$d\tau = \frac{dt}{a(t)} \tag{2.3}$$

The background spacetime and the matter content living on it can be described by the action:

$$S = \int d^4x\sqrt{-g}\left(\frac{1}{16\pi G}R + \mathcal{L}_m(g_{\mu\nu},\dots)\right) \tag{2.4}$$

The first part is the Einstein-Hilbert action, the second piece accounts for the rest of the Universe. Varying the action with respect to the metric, we obtain the Einstein's field equations:

$$G_{\mu\nu} \equiv R_{\mu\nu} - \frac{1}{2}g_{\mu\nu}R = 8\pi G T_{\mu\nu} \tag{2.5}$$

where the energy-momentum tensor is defined as:

$$T_{\mu\nu} = -\frac{2}{\sqrt{-g}}\frac{\delta\left(\sqrt{-g}\mathcal{L}_m\right)}{\delta g^{\mu\nu}} \tag{2.6}$$

To describe the background spacetime, homogeneous and isotropic, we can assume the energy-momentum tensor to have the form of the perfect fluid one:

$$T_{\mu\nu} = u_\mu u_\nu(\rho + P) + P g_{\mu\nu} \tag{2.7}$$

with u^μ the 4-velocity of the fluid $g^{\mu\nu}u_\mu u_\nu = -1$, ρ the background energy density and P the background isotropic pressure.

Equations (2.5) for the metric (2.1) with the energy-momentum tensor (2.7) give the Friedmann equations:

$$H^2 = \left(\frac{\dot a}{a}\right)^2 = \frac{8\pi G}{3}\rho - \frac{k}{a^2} \tag{2.8}$$

$$\frac{\ddot a}{a} = -\frac{4\pi G}{3}\left(\rho + 3P\right) \tag{2.9}$$

From Bianchi identities $\nabla_\mu G^{\mu\nu} = 0$ we obtain the continuity equation:

$$\dot\rho + 3H(\rho + P) = 0 \tag{2.10}$$

Only two out of these three equations are actually independent. In order to solve the system for a, ρ, P as a function of t we specify the equation of state for a barotropic fluid:

$$\rho = wP \tag{2.11}$$

For matter $w = 0$, for radiation $w = 1/3$, for a cosmological constant $w = -1$.

From the continuity equation we can read the behaviour of the energy density with the scale factor:

$$\rho(a) = \rho_0\left(\frac{a}{a_0}\right)^{-3(1+w)} \tag{2.12}$$

The energy density of matter is diluted as $\rho_m \propto a^{-3}$ due to the expansion. In the case of radiation we have the combined effect of dilution ($\propto a^{-3}$) due to the expansion of the volume and of redshift ($\propto a^{-1}$), therefore the energy density of radiation goes as $\rho_r \propto a^{-4}$. A cosmological constant instead is characterized by ρ_Λ =constant.

For each species we can define the present ratio of the energy density to the critical energy density:

$$\Omega_{i,0} \equiv \frac{\rho_{i,0}}{\rho_{\text{crit},0}} \qquad \rho_{\text{crit}} \equiv \frac{3H_0^2}{8\pi G} \tag{2.13}$$

The evolution of the three components as a function of the scale factor is shown in Figure 2.1, notice that the normalization for the three curves is set by present day observations.

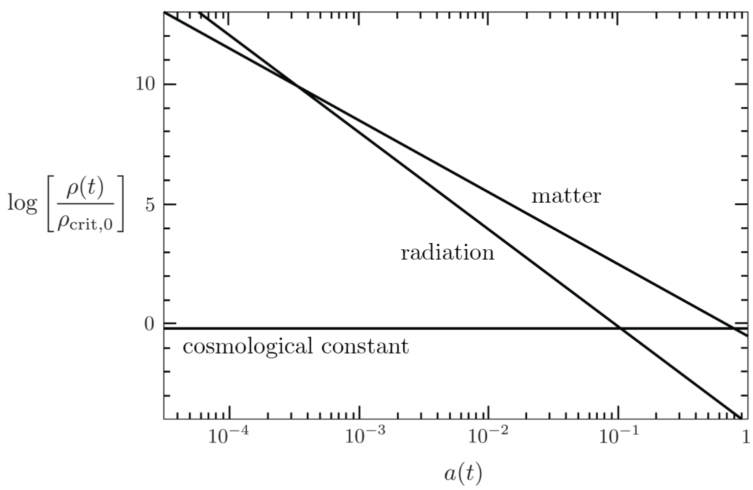

Figure 2.1: Evolution of the energy densities for the three different fluid components. From D. Baumann, Cosmology Part III Mathematical tripos.

2.3 Inflation

2.3.1 Shortcomings of the Big-Bang model

The hot Big-Bang model is affected by a few shortcomings:

- horizon problem: we observe the CMB to be very homogeneous on scales encompassing regions that at the epoch of last-scattering should have been causally disconnected. Define the (comoving) particle horizon as the maximum distance that can be covered between time 0 and t:

$$d_p(t) \equiv \int_0^t \frac{dt'}{a(t')} = \int_0^a \frac{1}{aH} d\ln a \propto \begin{cases} a & \text{radiation epoch} \\ a^{1/2} & \text{matter epoch} \end{cases} \tag{2.14}$$

  This sets the scale above which particles never had the chance to communicate with one another. The quantity $(aH)^{-1}$ is the comoving Hubble radius: for the conventional components of the fluid, with equation of state $w \geq 0$, it grows monotonically with time.

- flatness problem: in order for the Universe to be as close to spatial flatness as we observe it today, an extreme fine-tuning of Ω close to 1 in the early Universe is required. In fact, we can rewrite the first Friedmann equation (2.8) as:

$$1 - \Omega = -\frac{k}{(aH)^2} \qquad\qquad \Omega \equiv \frac{\rho}{\rho_{\rm crit}} \tag{2.15}$$

  Since the comoving Hubble radius $(aH)^{-1}$ grows with time, the quantity $|1 - \Omega|$ increases as well, unless $k = 0$ exactly which is a null-measure case.

- monopole or unwanted relics problem: during phase transitions, topological defects can be produced, and we should observe them today because not enough time has elapsed in order for the expansion to dilute them enough;

- we need a mechanism to provide the seeds for structure formation.

The horizon and flatness problems are not actual inconsistencies. We should simply accept that very special, fine-tuned initial conditions are required, in order to obtain the Universe we observe today. The large-scale homogeneity and the flatness of our Universe must be assumed, it is not predicted by the model. Instead, one would like a theory that explains these features dynamically [5].

Inflation provides a solution to these shortcomings and a way to set the seeds for structure formation. We now briefly review these two points.

2.3.2 The inflationary solution

Inflation is a phase of accelerated expansion in the very early Universe, around $\sim 10^{-34}$ s, lasting "long enough" to solve the horizon and flatness problems. The key idea is: we need the comoving Hubble radius to decrease with time. Three equivalent conditions for this to happen, related by the Friedmann equations, are:

$$\frac{d}{dt}\left(\frac{1}{aH}\right) < 0 \qquad \frac{d^2a}{dt^2} > 0 \qquad w < -\frac{1}{3} \tag{2.16}$$

The effect of a decreasing comoving Hubble radius can be appreciated in Figure 2.2.

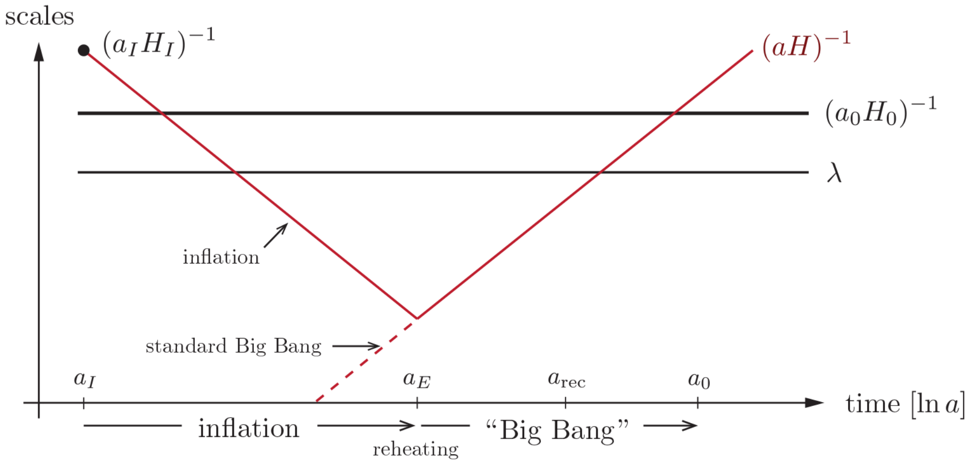

Figure 2.2: Plot of the comoving Hubble radius and comoving wavelength as a function of time. Scales of cosmological interest were larger than the Hubble radius until $a \approx 10^{-5}$ if $a_0 = 1$ today. But at very early times, before inflation, all scales of interest were smaller than the Hubble radius and therefore susceptible to microphysical processing. Similarly, at very late times, the scales of cosmological interest are back within the Hubble radius. Figure from [8].

2.3.3 Single field slow-roll scenario

So far, inflation is a generic recipe. It can be realized in a variety of ways. The simplest model involves one single scalar field, dominating the energy budget of the Universe during inflation, and with potential energy dominating over kinetic energy in such a way that $w \simeq$constant. In other words, we want this system to mimic the behaviour of a cosmological constant: in order to do this, the potential for the scalar field must be flat enough and the field must be slowly rolling. These requirements are usually encoded in the slow-roll parameters:

$$\epsilon \equiv -\frac{\dot{H}}{H^2} \qquad \eta \equiv -\frac{\ddot{\varphi}}{H\dot{\varphi}} \tag{2.17}$$

The equation of motion for the scalar field is the usual Klein-Gordon equation:

$$\ddot{\varphi} + 3H\dot{\varphi} + \frac{\partial V}{\partial \varphi} = 0 \tag{2.18}$$

Inflation only requires $\epsilon < 1$, to satisfy (2.16). However, both ϵ and η are usually required to be small, in this case we are in the so-called slow-roll regime:

$$w \simeq -1 \qquad H \simeq \text{const} \qquad a(t) \propto e^{Ht} \tag{2.19}$$

The spacetime is approximately de Sitter and the background equations (2.8), (2.18) become:

$$H^2 \simeq \frac{1}{3M_P^2} V \tag{2.20}$$

$$3H\dot{\varphi} + \frac{\partial V}{\partial \varphi} \simeq 0 \tag{2.21}$$

One can introduce two slow-roll parameters that are related to the shape of the potential:

$$\epsilon_V \equiv \frac{M_P^2}{2}\left(\frac{V'}{V}\right)^2 \qquad \eta_V \equiv M_P^2 \frac{V''}{V} \tag{2.22}$$

$$\epsilon \approx \epsilon_V \qquad \eta \approx \eta_V - \epsilon_V \tag{2.23}$$

where a prime here stands for derivative with respect to the field, and the last two relations hold in the slow-roll approximation only.

There is another set of slow-roll parameters one can introduce, the so-called "Hubble slow-roll parameters" [9]:

$$\epsilon_H \equiv -\frac{\dot{H}}{H^2} \qquad \eta_H \equiv \frac{\dot{\epsilon}}{\epsilon H} \tag{2.24}$$

They are related to the previous definitions as follows:

$$\eta_H = 2\epsilon - 2\eta \qquad \eta \approx \eta_V - \epsilon \qquad \eta_H \approx 4\epsilon - 2\eta_V \tag{2.25}$$

where the approximated relations hold in the slow-roll limit.

It is important to stress that slow-roll is not mandatory. However, it is usually assumed because physical results are more transparent in this regime. Besides, many complicated aspects of the calculations can be dropped off, if one assumes smallness of ϵ and η and works at leading order in the slow-roll parameters.

In order to quantify the amount of inflation, we can introduce the number of e-folds [6]:

$$N \equiv \ln\frac{a(t_{\rm end})}{a(t)} = \int_t^{t_{\rm end}} H dt \tag{2.26}$$

Inflation needs to last for at least 60 e-folds in order for all the wavelengths we observe today to have been in causal contact early on. The number comes from requiring that inflation solves the horizon and flatness problems [6, 10]. Many models easily predict much more than this minimum amount, however we have reasons to suspect that inflation did not last much longer than needed. One of these is the "η-problem": if we circumvent our ignorance on the ultraviolet theory by taking an effective field theory approach to inflation, even Planck mass-suppressed operators can give rise to $\mathcal{O}(1)$ corrections to the slow-roll parameter η. Roughly speaking, it is difficult to maintain η small enough for a long time [11].

2.3.4 Quantum fluctuations as seeds for structure formation

The other and more important aspect of inflation is that it provides a mechanism to set the seeds for the formation of structure. Quantum fluctuations are produced in the early Universe on small scales and inflation stretches them to superhorizon scales: after horizon crossing, the amplitude of fluctuations remains nearly frozen, until it enters the horizon again during radiation or matter domination. From the particle point of view, the picture is intuitively the following. Particle-antiparticle pairs are created and annihilated all the time, but during inflation the distance between particle and antiparticle is stretched exponentially and the pair may not be able to meet and annihilate: this results in a net number of particle being created. The appearance of these frozen fluctuations is equivalent to the appearance of a classic field whose vacuum expectation value does not vanish when we average over some macroscopic interval of time [12]. The production of quantum fluctuations during an inflationary epoch is not a peculiar to the inflaton only: it is a feature of any generic scalar field evolving in an accelerated background. The inflation plays a special role in that it dominates the energy density.

2.4 Power-law inflation

Inflation does not necessarily mean exponential expansion. One could take the ansatz:

$$a(t) \propto t^p \tag{2.27}$$

which defines power-law inflation [4, 13]. It can be realized with a single-exponential potential:

$$V(\varphi) = V_0 e^{\frac{\sqrt{6}\gamma}{M_P}\varphi} = V_0 e^{\Gamma\varphi} \tag{2.28}$$

where we have written $\sqrt{6}\gamma/M_P \equiv \Gamma$ for simplicity. The link between the slope of the potential and the exponent of the scale factor is a well-known result in the literature [14, 15]:

$$p = \frac{2}{M_P^2\Gamma^2} = \frac{1}{3\gamma^2} \tag{2.29}$$

In the following chapters we will switch among p, γ, Γ, according to what is needed to simplify calculations.

2.4.1 Background evolution

In cosmic time t, the e.o.m. (2.18) is:

$$\ddot{\varphi}_0 + \frac{3p}{t}\dot{\varphi}_0 + V_0\Gamma e^{\Gamma\varphi_0} = 0 \tag{2.30}$$

whose solution is:

$$\varphi_0(t) = -\frac{2}{\Gamma}\log t + \text{const} \tag{2.31}$$

In conformal time:

$$\boxed{\varphi_0(\tau) = \frac{2}{\Gamma(p-1)}\log|\tau| + \text{const}} \qquad p = \frac{2}{M_P^2\Gamma^2} \tag{2.32}$$

We will come back on this solution later.

2.4.2 On the slow-roll parameters in power-law inflation

We defined the slow-roll parameters in (2.17) and (2.22). In conformal time:

$$\epsilon = -\frac{\mathcal{H}'}{\mathcal{H}^2} + 1 \qquad \eta = -\frac{\varphi''}{\mathcal{H}\varphi'} + 1$$

On the attractor, with $a(\tau) = A(-\tau)^{\frac{p}{1-p}}$ and so on:

$$\epsilon = \eta = \frac{1}{p} = 3\gamma^2 \tag{2.33}$$

So that the requirement that they be smaller than 1 translates into:

$$\boxed{\gamma < \frac{1}{\sqrt{3}}} \tag{2.34}$$

As for the other two definitions:

$$\epsilon_V = 3\gamma^2 \qquad \eta_V = 6\gamma^2 \tag{2.35}$$

therefore we have the link $\eta_V = 2\epsilon_V$ in power-law inflation.

Chapter 3

QFT in curved spacetime

We briefly review how to deal with second quantization in a curved spacetime. See [16] and [12] for more details.

3.1 Second quantization

Consider a scalar field φ. We split it into the background field, corresponding to its homogeneous classical value, and the fluctuations:

$$\varphi(\tau, \vec{x}) = \varphi_0(\tau) + \delta\varphi(\tau, \vec{x}) \tag{3.1}$$

To quantize the field, we first rescale:

$$\delta\widetilde{\varphi} = a\delta\varphi \tag{3.2}$$

that is, we work on the conformal metric, with the "conformal field".
The canonical conjugated momentum is:

$$\pi = \delta\widetilde{\varphi}' \tag{3.3}$$

The small fluctuations field is promoted to operator, satisfying the standard equal time commutation relations:

$$[\delta\hat{\widetilde{\varphi}}(\tau, \vec{x}), \hat{\widetilde{\pi}}(\tau, \vec{x}')] = i\hbar\delta^{(3)}(\vec{x} - \vec{x'}) \qquad \text{others vanishing} \tag{3.4}$$

Notice that the background is a c-number, it does not play a role in the commutators.
We can expand the field in Fourier space as usual:

$$\delta\hat{\widetilde{\varphi}}(\tau, \vec{x}) = \int \frac{d^3\vec{k}}{(2\pi)^{3/2}} \left[u_k(\tau)\hat{a}_{\vec{k}}e^{i\vec{k}\cdot\vec{x}} + u_k^*(\tau)\hat{a}^\dagger_{\vec{k}}e^{-i\vec{k}\cdot\vec{x}}\right] \tag{3.5}$$

where k is the comoving wavevector. We have already enforced isotrpy in the assumption that the modefunctions only depend on the modulus of the wavevector k.
The creation and annihilation operators satisfy the standard commutation relations:

$$[\hat{a}_{\vec{k}}, \hat{a}^\dagger_{\vec{k}'}] = \delta^{(3)}(\vec{k} - \vec{k'}) \qquad \text{others vanishing} \tag{3.6}$$

which follows from (3.4), if the modefunctions are normalized as[1]:

$$u_k^* u_k' - u_k u_k^{*\prime} = -i \tag{3.7}$$

[1] In fact the conjugated momentum is

$$\tilde{\pi}(\tau, \vec{x}) \equiv \delta\tilde{\varphi}'(\tau, \vec{x}) = \int \frac{d^3\vec{k}}{(2\pi)^{3/2}} \left[u_k'(\tau)\hat{a}_{\vec{k}}e^{i\vec{k}\cdot\vec{x}} + u_k^{*\prime}(\tau)\hat{a}^\dagger_{\vec{k}}e^{-i\vec{k}\cdot\vec{x}}\right]$$

3.2 Equation of motion

The evolution equation for the scalar field $\varphi(\tau, \vec{x})$ is the Klein-Gordon equation:

$$g^{\mu\nu}\nabla_\mu\nabla_\nu\varphi = \frac{\partial V}{\partial\varphi} \tag{3.8}$$

The unperturbed background field only depends on conformal time, thus the e.o.m. is:

$$\varphi_0'' + 2\mathcal{H}\varphi_0' = -a^2\frac{\partial V}{\partial\varphi_0} \tag{3.9}$$

with $\mathcal{H} \equiv \dfrac{a'}{a}$.

Now we perturb the scalar field but not the metric, also including the spatial dependence of the field in the Klein-Gordon equation.

$$\delta\widetilde{\varphi}'' - \frac{a''}{a}\delta\widetilde{\varphi} + m^2a^2\delta\widetilde{\varphi} - \nabla^2\delta\widetilde{\varphi} = 0 \qquad \left.\frac{\partial^2 V}{\partial\varphi^2}\right|_{\delta\widetilde{\varphi}=0} \equiv m^2 \tag{3.10}$$

where we defined the effective mass of the scalar field m.

Going to Fourier space as in (3.5) we find how the modes $u_k(\tau)$ evolve.

$$\boxed{u_k'' + \left(k^2 - \frac{a''}{a} + m^2a^2\right)u_k = 0} \tag{3.11}$$

3.2.1 Choice of the vacuum state

A crucial feature of dealing with second quantization in a curved spacetime is the ambiguity in the choice of vacuum [16, 17]. The usual definitions of vacuum and of particles with momentum $\vec{k}$ in Minkowski are based on the decomposition of the field into plane waves $e^{-i(\omega_k t - \vec{k}\cdot\vec{x})}$. A particle with momentum p corresponds to a wavepacket with spread Δp, therefore it should be $\Delta p \ll p$ for the momentum of the particle to be well-defined. Roughly, if the spatial size of the wavepacket is λ such that $\lambda\Delta p \sim 1$ this means requiring $\lambda \gg 1/p$. But the geometry of a curved spacetime may vary significantly across a region of size λ: the notion of a particle with momentum p and solving the wave equation in terms of plane waves is only meaningful if the spacetime is very close to Minkowski on distances and on timescales of order p^{-1}. Notice that spatial flatness alone is not sufficient: the relevant quantity is the four-dimensional curvature.
For example, assume that in equation (3.11) the scale factor is such that at some time $\omega_k^2(\tau) = k^2 - \frac{a''}{a} + m^2a^2 < 0$. In this case the modes $u_k(\tau)$ do not oscillate, they behave as growing and decaying exponentials. Formally, we can still define a mode expansion, a set of creation and annihilation operators, a vacuum state, the corresponding excited states... but we could not interpret these states as physical vacuum and particle number states! Moreover, the expectation value of the energy density is not necessarily positive if $\omega_k^2(\tau) < 0$, so we cannot even interpret it as an energy density. The

therefore

$$\begin{aligned}[\delta\hat{\widetilde{\varphi}}(\tau,\vec{x}), \delta\hat{\widetilde{\varphi}}'(\tau,\vec{x}')] &= \int \frac{d^3\vec{k}d^3\vec{k}'}{(2\pi)^3}\Big[u_k(\tau)\hat{a}_{\vec{k}}e^{i\vec{k}\cdot\vec{x}} + u_k^*(\tau)\hat{a}^\dagger_{\vec{k}}e^{-i\vec{k}\cdot\vec{x}},\\ &\qquad u_k'(\tau)\hat{a}_{\vec{k}'}e^{i\vec{k}'\cdot\vec{x}'} + u_k^{*\prime}(\tau)\hat{a}^\dagger_{\vec{k}'}e^{-i\vec{k}'\cdot\vec{x}'}\Big]\\ &= \int \frac{d^3\vec{k}}{(2\pi)^3}\quad\left(u_k(\tau)u_k^{*\prime}(\tau)e^{i\vec{k}\cdot(\vec{x}-\vec{x}')} - u_k^*(\tau)u_k'(\tau)e^{-i\vec{k}\cdot(\vec{x}-\vec{x}')}\right)\end{aligned}$$

send $\vec{k}$ into $-\vec{k}$ in the second piece and this must be equal to $i\delta^{(3)}(\vec{x}-\vec{x}')$, from which the normalization (3.7) follows.

ultimate reason of this ambiguity in the definition of vacuum and particle states is to be attributed to the action being explicitly time-dependent, so the energy of the field is generally not conserved. In quantum theory this leads to the possibility of particle creation, where the energy for new particles is supplied by the gravitational field. A very instructive example of this is the Unruh effect, in which the ground state of an inertial observer in Minkowski is detected as a non-vanishing particle number state by an accelerated observer.

A quick way to appreciate the ambiguity is the following. Imagine we choose two different sets of modefunctions and corresponding operators:

$$\delta\hat{\widetilde{\varphi}}(\tau,\vec{x}) = \int \frac{d^3\vec{k}}{(2\pi)^{3/2}} \left[u_k(\tau)\hat{a}_{\vec{k}}e^{i\vec{k}\cdot\vec{x}} + u_k^*(\tau)\hat{a}_{\vec{k}}^\dagger e^{-i\vec{k}\cdot\vec{x}}\right] \tag{3.12}$$

$$= \int \frac{d^3\vec{k}}{(2\pi)^{3/2}} \left[v_k(\tau)\hat{b}_{\vec{k}}e^{i\vec{k}\cdot\vec{x}} + v_k^*(\tau)\hat{b}_{\vec{k}}^\dagger e^{-i\vec{k}\cdot\vec{x}}\right] \tag{3.13}$$

Since v_k, v_k^* are a basis, the function u_k is a linear combination:

$$u_k^*(\tau) = \alpha_k v_k^*(\tau) + \beta_k v_k(\tau) \tag{3.14}$$

If both sets are normalized by (3.7), then:

$$|\alpha_k|^2 - |\beta_k|^2 = 1 \qquad\qquad |\alpha_k| \geq 1 \tag{3.15}$$

The complex coefficients α_k, β_k are called the Bogolyubov coefficients. Their meaning is the following. The two sets of creation and annihilation operators define two different vacua $\hat{a}_{\vec{k}}|0_a\rangle = 0 \;\forall\; \vec{k}$ and $\hat{b}_{\vec{k}}|0_b\rangle = 0 \;\forall\; \vec{k}$, which are related through the Bogolyubov coefficients. If we compute the expectation value of the b-particle number in the a-vacuum state, we find:

$$\langle 0_a|\hat{N}_b|0_a\rangle = \langle 0_a|\hat{b}_{\vec{k}}^\dagger \hat{b}_{\vec{k}}|0_a\rangle = |\beta_k|^2\, \delta^{(3)}(0) \tag{3.16}$$

If we quantized the field in a finite box, the divergent factor $\delta^{(3)}(0)$ would be replaced by the box volume. Therefore we can interpret $|\beta_k|^2 = n_k$ as a mean number density of b-particles.

Ultimately the choice of vacuum is determined by experiment: the correct vacuum state must be such that the theoretical predictions agree with the available experimental data [17].

In our case, at very short distances, when the modes are well within the horizon, we want to recover the usual flat spacetime theory. This translates into the requirement that, well within the horizon, the modes approach the usual Minkowski plane waves:

$$\boxed{\frac{k}{aH} \to \infty \qquad\qquad u_k(\tau) \to \frac{1}{\sqrt{2k}}e^{-ik\tau}} \tag{3.17}$$

This is called the Bunch-Davies vacuum choice.

3.2.2 Limiting behaviours

Subhorizon scales

Well within the horizon $k \gg aH$, therefore k^2 dominates over both a''/a and the mass term. Equation (3.11) becomes:

$$u_k'' + k^2 u_k = 0 \tag{3.18}$$

whose solutions are plane waves $u_k \propto e^{-ik\tau}$, in agreement with (3.17). We are recovering the Minkowski limit, as expected.

Superhorizon scales

On superhorizon scales $k \ll aH$, therefore k^2 is negligible. Equation (3.11) becomes:

$$u_k'' - \left(\frac{a''}{a} - m^2 a^2\right) u_k = 0 \tag{3.19}$$

In the case of a massless field $m = 0$, we can look for power-law solutions of (3.19) of the form $u_k \propto a^\beta$:

$$u_k = B_+(k)a + B_-(k)\frac{1}{a^2} \tag{3.20}$$

There are a growing mode and a decaying mode.
Now we fix the amplitude of the growing mode by matching this solution (3.20) to the plane wave solution (3.17) when the fluctuation with wavenumber k leaves the horizon ($k = aH$):

$$|B_+(k)| = \frac{1}{a\sqrt{2k}} = \frac{H}{\sqrt{2k^3}} \tag{3.21}$$

On superhorizon scales, fluctuations are frozen, the original scalar field has the constant amplitude:

$$|\delta\varphi_k| = \frac{|u_k|}{a} = \frac{H}{\sqrt{2k^3}} \tag{3.22}$$

When we average over large intervals of time, $\delta\varphi \neq 0$. As a result of the exponential expansion of the Universe, a classical fluctuation has been generated, the net result is a state with a non-vanishing number of particles. It is a mechanism of gravitational amplification whose key point is H =constant.

3.3 Exact solution in a de Sitter stage

In a de Sitter Universe:

$$H = \text{const} \qquad a(\tau) = -\frac{1}{H\tau} \tag{3.23}$$

equation (3.11) becomes:

$$u_k'' + \left(k^2 - \frac{\nu^2 - \frac{1}{4}}{\tau^2}\right) u_k = 0 \qquad \nu^2 \equiv \frac{9}{4} - \frac{m^2}{H^2} \tag{3.24}$$

This is a Bessel equation, a linear second order ODE of the type:

$$x^2\frac{d^2y}{dx^2} + x\frac{dy}{dx} + (x^2 - \alpha^2)y = 0 \tag{3.25}$$

If $\nu \in \mathbb{R}$, as is the case, then the exact solution is given in terms of Bessel and Neumann functions, or of Hankel functions of first and second order:

$$u_k(\tau) = \sqrt{-\tau}\left[c_1(k)H_\nu^{(1)}(-k\tau) + c_2(k)H_\nu^{(2)}(-k\tau)\right] \tag{3.26}$$

We match solutions in the ultraviolet regime by using the asymptotic form of the Hankel functions (A.5) and applying the Bunch-Davies vacuum prescription (3.17):

$$c_1(k)\sqrt{\frac{2}{\pi k}}e^{-ik\tau + i\left(\nu-\frac{1}{2}\right)\frac{\pi}{2}} + c_2(k)\sqrt{\frac{2}{\pi k}}e^{ik\tau - i\left(\nu-\frac{1}{2}\right)\frac{\pi}{2}} \equiv \frac{1}{\sqrt{2k}}e^{-ik\tau} \tag{3.27}$$

$$c_1(k) = \sqrt{\frac{\pi}{4}}e^{i\left(\nu+\frac{1}{2}\right)\frac{\pi}{2}} \qquad c_2(k) = 0 \tag{3.28}$$

The exact solution becomes:

$$\boxed{u_k(\tau) = \frac{\sqrt{\pi}}{2} e^{i\left(\nu+\frac{1}{2}\right)\frac{\pi}{2}} \sqrt{-\tau} H_\nu^{(1)}(-k\tau)} \tag{3.29}$$

Notice that if $m = 0$ then $\nu = \frac{3}{2}$ exactly.

We obtain the fluctuation for the original field by dividing by the scale factor $\delta\varphi_k = u_k/a$. On superhorizon scales:

$$|\delta\varphi_k| = 2^{\nu-\frac{3}{2}} \frac{\Gamma(\nu)}{\Gamma(\frac{3}{2})} \frac{H}{\sqrt{2k^3}} \left(\frac{k}{aH}\right)^{\frac{3}{2}-\nu} \tag{3.30}$$

Chapter 4

The primordial curvature perturbation

In the previous chapter, we have only focused on the fluctuations of the scalar field, neglecting perturbations in the metric. However, in the case of the inflaton, it is crucial to account for metric perturbations as well. As a matter of fact, the inflaton dominates the energy budget of the Universe during inflation and perturbations in the energy-momentum tensor generate perturbations in the FRW metric through Einstein's equations (2.5). On the other hand, metric fluctuations affect the evolution of the inflaton perturbations since they appear in the perturbed Klein-Gordon equation. Therefore field and metric perturbations are deeply intertwined and are to be studied together [12].
To keep track of non-Gaussianities, the analysis must be performed up to second order in perturbation theory.

4.1 The gauge issue

The starting point is perturbing the quantities appearing in Einstein's field equations (2.5): the matter and energy content on one side, the geometry on the other side.

When dealing with perturbation theory in General Relativity, a crucial point to keep in mind is that we are also perturbing the geometry. On the one hand we have the physical spacetime, on which the physical quantity T lives; on the other hand there is the unperturbed background spacetime, on which T_0 is defined. We would like to define the perturbation as:

$$\text{“}\delta T = T - T_0\text{”} \tag{4.1}$$

but we cannot directly compare the two quantities T and T_0 since they are defined on different spacetimes. We first need a map, a one-to-one correspondence between the physical and the background spacetimes. A *gauge choice* is the choice of such a map. Changing the map amounts to a gauge transformation. There is not a unique choice of the map, and this introduces an ambiguity in the definition of the perturbations. This problem is called the *gauge issue*. We refer to [18–20] for a detailed discussion.

There are two main ways to deal with this problem. One possibility is to make a gauge choice that simplifies the calculations, then in the end perform a gauge transformation if needed and go to a gauge where physical results are easier to interpret. Another option, which was first introduced by Bardeen [21], is to work with gauge-invariant quantities.
We will use the gauge-invariant curvature perturbation, which is a “mixed variable” containing both matter and metric perturbations. Such a quantity is the most natural way to study the problem, because Einstein's equations themselves couple the metric and the inflaton fluctuations, as we already mentioned. Therefore these objects that we define separately are actually very deeply intertwined from a physical point of view.

4.2 Cosmological perturbations

We explicitly write down the metric perturbations and the energy-momentum tensor perturbations in full generality, with no gauge choice. The notation in recent works is quite unified, we mostly follow [12].

If δ is a generic perturbation, our convention will be:

$$\delta = \sum_{r=1}^{+\infty} \frac{1}{r!}\delta^{(r)} = \delta^{(1)} + \frac{1}{2}\delta^{(2)} + \dots \tag{4.2}$$

We can use Helmholtz theorem to separate scalar, vector and tensor degrees of freedom. Vector quantities can be split into a curl-free part and a divergence-free part:

$$\hat{\omega}_i = \partial_i \omega + \omega_i \qquad \partial^i \omega_i = 0 \tag{4.3}$$

Similarly, tensors can be decomposed as:

$$\hat{\chi}_{ij} = \mathrm{D}_{ij}\chi + \partial_i \chi_j + \partial_j \chi_i + \chi_{ij} \qquad \partial^i \chi_{ij} = 0 \qquad \chi^i_i = 0 \tag{4.4}$$

where $\mathrm{D}_{ij} = \partial_i \partial_j - \frac{1}{3}\delta_{ij}\nabla^2$.

The advantage of these splittings is that scalar, vector and tensor perturbations evolve independently at linear order, therefore they can be studied separately. When going to higher order in perturbation theory, it is still true that n-th order modes evolve independently, but they receive contributions from all kinds of lower order modes. This phenomenon is called *mode-mixing*, because higher-order perturbations are coupled, in the sense that they are sourced by lower-order perturbations.

4.2.1 Metric perturbations

We perturb around the FRW background:

$$\begin{aligned} g_{00} &= -a^2(\tau)\left(1 + 2\phi(\vec{x},\tau)\right) \\ g_{0i} &= a^2(\tau)\hat{\omega}_i(\vec{x},\tau) \\ g_{ij} &= a^2(\tau)\left[(1 - 2\psi(\vec{x},\tau))\delta_{ij} + \hat{\chi}_{ij}(\vec{x},\tau)\right] \end{aligned} \tag{4.5}$$

For our purposes, we can simplify the metric (4.5).
First-order vector perturbations are not generated in the presence of scalar fields, and in any case they have decreasing amplitudes, hence we can safely neglect them.
The first-order tensor gives a negligible contribution to second-order perturbations.
Therefore:

$$\begin{aligned} g_{00} &= -a^2(\tau)\left(1 + 2\phi^{(1)} + \phi^{(2)}\right) \\ g_{0i} &= a^2(\tau)\left(\partial_i \omega^{(1)} + \frac{1}{2}\partial_i \omega^{(2)} + \frac{1}{2}\omega_i^{(2)}\right) \\ g_{ij} &= a^2(\tau)\left[(1 - 2\psi^{(1)} - \psi^{(2)})\delta_{ij} + \mathrm{D}_{ij}\left(\chi^{(1)} + \frac{1}{2}\chi^{(2)}\right) + \frac{1}{2}\left(\partial_i \chi_j^{(2)} + \partial_j \chi_i^{(2)} + \chi_{ij}^{(2)}\right)\right] \end{aligned} \tag{4.6}$$

The contravariant metric is obtained by requiring, up to second order, that $g_{\mu\nu}g^{\nu\lambda} = \delta^\lambda_\mu$.

With the perturbed $g_{\mu\nu}$ one can compute the Christoffel symbols $\Gamma^\alpha_{\beta\gamma}$ and the components of the Einstein tensor G^μ_ν up to second order. The computation is very long, the full expressions can be found in [22].

4.2.2 Energy-momentum tensor perturbations

Making the hypothesis of a perfect fluid, the energy-momentum tensor is (2.7). The velocity can be perturbed as:

$$u^\mu = \frac{1}{a}\left(\delta^\mu_0 + v^\mu_{(1)} + \frac{1}{2}v^\mu_{(2)}\right) \tag{4.7}$$

and the energy density:

$$\rho(\tau,\vec{x}) = \rho_0(\tau) + \delta^{(1)}\rho(\tau,\vec{x}) + \frac{1}{2}\delta^{(2)}\rho(\tau,\vec{x}) \tag{4.8}$$

4.2.3 Perturbed Einstein equations in Poisson gauge

We will now write down the perturbed Einstein equations at the background level, at first order, at second order. Following [22], we work in the Poisson gauge or generalized longitudinal gauge:

$$\boxed{\omega = 0,\ \chi = 0} \tag{4.9}$$

The metric (4.6) in the Poisson gauge becomes:

$$\begin{aligned} g_{00} &= -a^2\left(1 + 2\phi^{(1)} + \phi^{(2)}\right) \\ g_{0i} &= 0 \\ g_{ij} &= a^2\left[\left(1 - 2\psi^{(1)} + \psi^{(2)}\right)\delta_{ij} + \frac{1}{2}\left(\partial_i\chi^{(2)}_j + \partial_j\chi^{(2)}_i + \chi^{(2)}_{ij}\right)\right] \end{aligned} \tag{4.10}$$

The inverse metric can be found by requiring $g^{\mu\lambda}g_{\lambda\nu} = \delta^\mu_\nu$ up to second order:

$$\begin{aligned} g^{00} &= -\frac{1}{a^2}\left(1 - 2\phi^{(1)} - \phi^{(2)} + 4(\phi^{(1)})^2\right) \\ g^{0i} &= 0 \\ g^{ij} &= \frac{1}{a^2}\left[\left(1 + 2\psi^{(1)} + \psi^{(2)} + 4(\psi^{(1)})^2\right)\delta^{ij} - \frac{1}{2}\left(\partial^i\chi^{(2)j} + \partial^j\chi^{(2)i} + \chi^{(2)ij}\right)\right] \end{aligned} \tag{4.11}$$

The field is split into a homogeneous background and a perturbation:

$$\varphi(\vec{x},\tau) = \varphi_0(\tau) + \delta^{(1)}\varphi(\vec{x},\tau) + \frac{1}{2}\delta^{(2)}\varphi(\vec{x},\tau) \tag{4.12}$$

We now have to perturb Einstein equations (2.5) up to second order. The calculation can be found in [22] and in the Appendix therein one can find the full expressions for the perturbed Einstein tensor.

First order

The equations of motion are hidden in the trace of the spatial part of Einstein equations.

We start with five scalar variables: the metric perturbations ϕ, ω, ψ, χ and the scalar field $\delta\varphi$. Two scalars are eliminated with the gauge choice, in our case ω and χ. At first order there is a further simplification because we are dealing with a single scalar field and there is no anisotropic stress, this is given by the traceless spatial part of the Einstein equations: this results in the two gravitational potential being equal $\phi^{(1)} = \psi^{(1)}$. So we are left with two variables only.

From a physical point of view, actually, the variable must be one, because the gravitational potential feeds on the scalar field perturbation. They are related through Einstein equations. Hence we must be able to use the energy constraint or the momentum constraint to express one as a function of the other.

The perturbed Einstein equations are [22]:

$$\text{energy constraint } \delta^{(1)}G^0_0 = 8\pi G\delta^{(1)}T^0_0 \tag{4.13}$$
$$6\left(\frac{a'}{a}\right)^2\phi^{(1)} + 6\frac{a'}{a}\psi^{(1)\prime} - 2\partial_i\partial^i\psi^{(1)} = 8\pi G\left(\phi^{(1)}\varphi_0'^2 - \delta^{(1)}\varphi'\varphi_0' - \delta^{(1)}\varphi\frac{\partial V}{\partial\varphi}a^2\right)$$

$$\text{momentum constraint } \delta^{(1)}G^0_i = 8\pi G\delta^{(1)}T^0_i \tag{4.14}$$
$$-2\frac{a'}{a}\partial_i\phi^{(1)} - 2\partial_i\psi^{(1)} = -8\pi G\varphi_0'\partial_i\delta^{(1)}\varphi$$

$$\text{spatial part } \delta^{(1)}G^i_j = 8\pi G\delta^{(1)}T^i_j \tag{4.15}$$
$$\left(2\frac{a'}{a}\phi^{(1)\prime} + 4\frac{a''}{a}\psi^{(1)} - 2\left(\frac{a'}{a}\right)^2\phi^{(1)} + \partial_k\partial^k\phi^{(1)} + 4\frac{a'}{a}\psi^{(1)\prime} + 2\psi^{(1)\prime\prime} - \partial_k\partial^k\psi^{(1)}\right)\delta^i_j$$
$$-\partial^i\partial_j\phi^{(1)} + \partial^i\partial_j\psi^{(1)} = 8\pi G\left(-\phi^{(1)}\varphi_0'^2 + \delta^{(1)}\varphi'\varphi_0' - \delta^{(1)}\varphi\frac{\partial V}{\partial\varphi}a^2\right)\delta^i_j$$

From the traceless part of the $i - j$ equation:

$$\boxed{\phi^{(1)} = \psi^{(1)}} \tag{4.16}$$

The trace gives:

$$2\frac{a'}{a}\phi^{(1)\prime} + 4\frac{a''}{a}\phi^{(1)} - 2\left(\frac{a'}{a}\right)^2\phi^{(1)} + 4\frac{a'}{a}\phi^{(1)\prime} + 2\phi^{(1)\prime\prime} =$$
$$= 8\pi G\left(-\phi^{(1)}\varphi_0'^2 + \delta^{(1)}\varphi'\varphi_0' - \delta^{(1)}\varphi\frac{\partial V}{\partial\varphi}a^2\right)$$

We need now the background results:

$$\frac{a''}{a} = \mathcal{H}^2 + \mathcal{H}' \qquad 4\pi G\varphi_0'^2 = \mathcal{H}^2 - \mathcal{H}' \tag{4.17}$$

By substituting the last term $-8\pi G\delta^{(1)}\varphi\frac{\partial V}{\partial\varphi}a^2$ from $0 - 0$ and using $0 - i$ to eliminate $\delta^{(1)}\varphi$:

$$\partial_i\left(\frac{a'}{a}\phi^{(1)} + \phi^{(1)\prime}\right) = \partial_i\left(4\pi G\varphi_0'\delta^{(1)}\varphi\right)$$
$$\boxed{\delta^{(1)}\varphi = \frac{1}{4\pi G\varphi_0'}\left(\mathcal{H}\phi^{(1)} + \phi^{(1)\prime}\right)} \tag{4.18}$$

For the gravitational potential we find:

$$\boxed{\phi^{(1)\prime\prime} + 2\left(\mathcal{H} - \frac{\varphi_0''}{\varphi_0'}\right)\phi^{(1)\prime} + 2\left(\mathcal{H}' - \mathcal{H}\frac{\varphi_0''}{\varphi_0'}\right)\phi^{(1)} - \partial_i\partial^i\phi^{(1)} = 0} \tag{4.19}$$

Alternatively we could have eliminated $\phi^{(1)}$ with the momentum constraint and obtained an equation for $\delta^{(1)}\varphi$.

Second order

When we go to second order, the most remarkable effect is mode-mixing: we find quantities that are intrinsically second order and quantities that are products of first order fluctuations. As we have already mentioned, first order perturbations act as a source for second order ones.

The unknowns are: $\phi^{(2)}$, $\psi^{(2)}$, $\chi_i^{(2)}$, $\chi_{ij}^{(2)}$, $\delta^{(2)}\varphi$. In the following we will already set $\psi^{(1)} = \phi^{(1)}$.

Taking the divergence of the $0-i$ equation we get rid of the vector mode and we get an expression for $\delta^{(2)}\varphi$:

$$\boxed{\frac{1}{2}\delta^{(2)}\varphi = \frac{\psi^{(2)\prime} + \mathcal{H}\phi^{(2)} + \Delta^{-1}\alpha}{8\pi G\varphi_0'} - \frac{\Delta^{-1}\beta}{\varphi_0'}} \tag{4.20}$$

$$\alpha \equiv 2\phi^{(1)\prime}\partial_i\partial^i\phi^{(1)} + 10\partial_i\phi^{(1)\prime}\partial^i\phi^{(1)} + 8\phi^{(1)}\partial_i\partial^i\phi^{(1)\prime} \tag{4.21}$$

$$\begin{aligned}\beta \equiv& \left(\partial_i\partial^i\delta^{(1)}\varphi\right)\delta^{(1)}\varphi' + \partial^i\delta^{(1)}\varphi\partial_i\delta^{(1)}\varphi' \\ &+ 2\phi^{(1)}\partial_i\partial^i\delta^{(1)}\varphi\varphi_0' + 2\partial_i\phi^{(1)}\partial^i\delta^{(1)}\varphi\varphi_0'\end{aligned} \tag{4.22}$$

Similarly we take the trace of the $i-j$ equation:

$$\begin{aligned}&\partial_i\partial^i\phi^{(2)} + 3\mathcal{H}\phi^{(2)\prime} + 3\frac{a''}{a}\phi^{(2)} + 3\mathcal{H}^2\phi^{(2)} - \partial_i\partial^i\psi^{(2)} + 6\mathcal{H}\psi^{(2)\prime} + 3\psi^{(2)\prime\prime} + \\ &- 24\frac{a''}{a}\left(\phi^{(1)}\right)^2 + 12\mathcal{H}^2\left(\phi^{(1)}\right)^2 - 24\mathcal{H}\phi^{(1)}\phi^{(1)\prime} + \\ &- 7\partial_i\phi^{(1)}\partial^i\phi^{(1)} - 8\phi^{(1)}\partial_i\partial^i\phi^{(1)} - 3\left(\phi^{(1)\prime}\right)^2 = \\ &= 3(8\pi G)\left[\frac{1}{2}\delta^{(2)}\varphi'\varphi_0' - \frac{1}{2}\delta^{(2)}\varphi\frac{\partial V}{\partial\varphi}a^2 + \frac{1}{2}\left(\delta^{(1)}\varphi'\right)^2 - \frac{1}{2}\left(\delta^{(1)}\varphi\right)^2\frac{\partial^2 V}{\partial\varphi^2}a^2 + \right. \\ &\left. -2\phi^{(1)}\delta^{(1)}\varphi'\varphi_0' + 2\left(\phi^{(1)}\right)^2\varphi_0'^2 - \frac{1}{6}\partial_i\delta^{(1)}\varphi\partial^i\delta^{(1)}\varphi\right]\end{aligned}$$

Then we substitute $\delta^{(2)}\varphi$ and $\delta^{(2)}\varphi'$ and we use the background eom where needed:

$$\varphi_0'' + 2\mathcal{H}\varphi_0' + a^2\frac{\partial V}{\partial\varphi} = 0$$

Finally:

$$\boxed{\phi^{(2)} - \psi^{(2)} = \Delta^{-1}\gamma} \tag{4.23}$$

$$\begin{aligned}\frac{1}{3}\gamma \equiv& \Delta^{-1}\left(\alpha' - 8\pi G\beta'\right) + 2\mathcal{H}\Delta^{-1}\left(\alpha - 8\pi G\beta\right) + 8\frac{a''}{a}\left(\phi^{(1)}\right)^2 + 8\mathcal{H}\phi^{(1)}\phi^{(1)\prime} + \\ &- 4\mathcal{H}^2\left(\phi^{(1)}\right)^2 + \left(\phi^{(1)\prime}\right)^2 + \frac{7}{3}\partial_i\phi^{(1)}\partial^i\phi^{(1)} + \frac{8}{3}\phi^{(1)}\partial_i\partial^i\phi^{(1)} + \\ &+ 8\pi G\left[\frac{1}{2}\left(\delta^{(1)}\varphi'\right)^2 - \frac{1}{2}\left(\delta^{(1)}\varphi\right)^2\frac{\partial^2 V}{\partial\varphi^2}a^2 - 2\phi^{(1)}\delta^{(1)}\varphi'\varphi_0' + \right. \\ &\left. +2\left(\phi^{(1)}\right)^2\varphi_0'^2 - \frac{1}{6}\partial_i\delta^{(1)}\varphi\partial^i\delta^{(1)}\varphi\right]\end{aligned} \tag{4.24}$$

This leaves one unknown only: $\phi^{(2)}$.

Substituting everything in the $0-0$ equation we find:

$$\begin{aligned}
&\phi^{(2)\prime\prime} + 2\left(\mathcal{H} - \frac{\varphi_0''}{\varphi_0'}\right)\phi^{(2)\prime} + 2\left(\mathcal{H}' - \mathcal{H}\frac{\varphi_0''}{\varphi_0'}\right)\phi^{(2)} - \partial_i\partial^i\phi^{(2)} = \\
&= 12\mathcal{H}^2\left(\phi^{(1)}\right)^2 + 3\left(\phi^{(1)\prime}\right)^2 + 8\phi^{(1)}\partial_i\partial^i\phi^{(1)} + 3\partial_i\phi^{(1)}\partial^i\phi^{(1)} - \gamma + \Delta^{-1}\gamma'' + \\
&\quad + \left(\mathcal{H} - 2\frac{\varphi_0''}{\varphi_0'}\right)\Delta^{-1}\gamma' - \Delta^{-1}\left(\alpha' - 8\pi G\beta'\right) + 2\left(\mathcal{H} + \frac{\varphi_0''}{\varphi_0'}\right)\Delta^{-1}\left(\alpha - 8\pi G\beta\right) + \\
&\quad + 8\pi G\left[-\frac{1}{2}\left(\delta^{(1)}\varphi'\right)^2 - \frac{1}{2}\left(\delta^{(1)}\varphi\right)^2\frac{\partial^2 V}{\partial\varphi^2}a^2 + 2\phi^{(1)}\delta^{(1)}\varphi'\varphi_0' + 2\left(\phi^{(1)}\right)^2\varphi_0'^2 + \right. \\
&\quad \left. -\frac{1}{2}\partial_i\delta^{(1)}\varphi\partial^i\delta^{(1)}\varphi\right]
\end{aligned} \tag{4.25}$$

which is master equation (47) in Acquaviva *et al.* [22].

4.3 The gauge-invariant curvature perturbation

Following [12], we introduce the gauge-invariant curvature perturbation on spatial slices of uniform density, at linear order. We will need to generalize it to second order, in order to deal with non-Gaussianity.

The intrinsic spatial curvature on hypersurfaces of constant τ in a flat Universe ($k=0$) is:

$$^{(3)}R = \frac{4}{a^2}\Delta^2\hat{\psi}^{(1)} \tag{4.26}$$

where

$$\hat{\psi}^{(1)} = \psi^{(1)} + \frac{1}{6}\Delta^2\chi^{(1)} \tag{4.27}$$

is the curvature perturbation.

Let's make a gauge transformation:

$$x^\mu \longmapsto \tilde{x}^\mu = x^\mu + \xi^\mu \tag{4.28}$$

with $\xi^\mu = (\xi^0, \partial^i\xi)$. The scalar functions ξ^0 and ξ are arbitrary and they determine the choice of constant-τ hypersurfaces (time-slicing) and the spatial coordinates on these hypersurfaces respectively.

We can verify that $\hat{\psi}^{(1)}$ is not gauge-invariant, in fact if we change the slicing:

$$\tau \longmapsto \tau + \alpha^{(1)} \qquad\qquad \psi^{(1)} \longmapsto \widetilde{\psi}^{(1)} = \psi^{(1)} - \mathcal{H}\alpha^{(1)} \tag{4.29}$$

Any scalar quantity φ which is homogeneous in the background can be written as $\varphi(\tau, x^i) = \varphi_0(\tau) + \delta\varphi(\tau, x^i)$ and the perturbation transforms as:

$$\widetilde{\delta\varphi} = \delta\varphi - \xi^0\varphi_0' \tag{4.30}$$

Notice that scalars are independent of the function ξ, that is, they do not depend on the choice of coordinates on the three-dimensional spatial hypersurfaces. The function ξ can only affect the components of 3-vectors or 3-tensors on the hypersurfaces.

Bardeen in his seminal work [21] showed that any unambiguous choice of time-slicing can be used to define explicitly gauge-invariant perturbations.
If we use the value of any physical scalar to unambiguously specify the gauge function ξ^0, and hence the time-slicing of the perturbed spacetime, then we can write the resulting scalar metric perturbations or any matter perturbation on this hypersurface in a manifestly gauge-invariant way *by explicitly including the transformation from an arbitrary coordinate system.* If in addition we make an unambiguous choice of the spatial coordinates on these hypersurfaces, through the gauge function ξ, then all the 3-tensor components also become gauge-invariant.

For example, one can use the matter content to pick out uniform density hypersurfaces, and this gives an unambiguous time-slicing on which to define perturbed quantities [12]. The perturbation in the density transforms as in (4.30), so $\widetilde{\delta^{(1)}\rho} = \delta^{(1)}\rho + \rho_0'\alpha^{(1)}$. We want $\widetilde{\delta^{(1)}\rho} = 0$ so it must be:

$$\alpha^{(1)} = -\frac{\delta^{(1)}\rho}{\rho_0'} \tag{4.31}$$

The curvature perturbation on uniform density hypersurfaces is:

$$\begin{aligned} \widetilde{\widehat{\psi}^{(1)}}\Big|_{\rho} &= \widehat{\psi}^{(1)} - \mathcal{H}\alpha^{(1)} \\ &= \widehat{\psi}^{(1)} + \mathcal{H}\frac{\delta^{(1)}\rho}{\rho_0'} \end{aligned} \tag{4.32}$$

Now this quantity is indeed gauge-invariant (the two new terms that would come from the gauge transformation would cancel out exactly) and it is indicated with:

$$\boxed{-\zeta^{(1)} \equiv \widetilde{\widehat{\psi}^{(1)}}\Big|_{\rho} = \widehat{\psi}^{(1)} + \mathcal{H}\frac{\delta^{(1)}\rho}{\rho_0'}} \tag{4.33}$$

This combination can also be interpreted as the density perturbation on uniform curvature slices or spatially-flat gauge, such that $\psi^{(1)} = \chi^{(1)} = 0$. This procedure is an example of how to find a gauge-invariant quantity by selecting a proper time-slicing in an unambiguous way.

Let's see a more intuitive link between inflaton, density and curvature perturbations.
The inflaton dominates the energy budget of the Universe during inflation, and its energy density is mainly potential energy $\rho \sim V$. So the energy density fluctuations are:

$$\delta\rho \simeq V'(\varphi)\delta\varphi \tag{4.34}$$

which using the equation of motion in the slow-roll regime $3H\dot{\varphi} + V' \simeq 0$ becomes:

$$\delta\rho \simeq -3H\dot{\varphi}\delta\varphi \tag{4.35}$$

Fluctuations in the inflaton produce fluctuations in the Universe expansion from place to place. Each region in the Universe goes through the same expansion history, but at different times.

$$\delta t = \frac{\delta t}{\delta\varphi}\delta\varphi = -\frac{\delta\varphi}{\dot{\varphi}} \tag{4.36}$$

to be connected to the number of e-foldings:

$$N = \int_{t_i}^{t_f} H dt = \ln\frac{a_f}{a_i} \qquad\qquad \delta N = H\delta t \tag{4.37}$$

We can define δN to be the "additional expansion":

$$\begin{aligned} \zeta \equiv \delta N = H\delta t &= -H\frac{\delta\varphi}{\dot{\varphi}} = -H\frac{1}{\dot{\varphi}}\left(-\frac{\delta\rho}{3H\dot{\varphi}}\right) \\ &= -H\frac{\delta\rho}{V'\dot{\varphi}} = -H\frac{\delta\rho}{\dot{\rho}} \end{aligned} \tag{4.38}$$

hence

$$\zeta = \delta N \simeq -H\frac{\delta\rho}{\dot{\rho}} \tag{4.39}$$

Of course $\delta\rho/\rho$ is not a gauge invariant quantity. The correct definition is the one given above.

The time evolution of the curvature perturbation can be derived from the continuity equation for the energy density [12, 23]: one starts from the Bianchi identities for the energy momentum tensor part $\nabla_\mu T^\mu_\nu = 0$ and projects it onto a time-like vector field $u^\nu \nabla_\mu T^\mu_\nu = 0$. The result is (neglecting spatial gradients):

$$\zeta^{(1)\prime} = -\frac{\mathcal{H}}{\rho + P}\delta^{(1)} P_{\text{non-adiabatic}} \tag{4.40}$$

So the curvature perturbation evolves being sourced by the non-adiabatic pressure. In particular, for purely adiabatic perturbations it is conserved on large scales: hence $\zeta^{(1)}$ is the proper quantity to use in order to characterize the amplitude of adiabatic perturbations. This is the case for single field slow-roll inflation.

Observationally, ζ is the physical quantity that we can measure by looking at the temperature anisotropies in the CMB:

$$\zeta \approx -5\frac{\Delta T}{T} \tag{4.41}$$

The statistical properties of this variables encode informations on inflation.

Another gauge-invariant quantity is given by:

$$\boxed{\mathcal{R}^{(1)} = \psi^{(1)} + \mathcal{H}\frac{\delta^{(1)}\varphi}{\varphi_0'}} \tag{4.42}$$

On superhorizon scales, both $\mathcal{R}^{(1)}$ and $\zeta^{(1)}$ are nearly constant and

$$\mathcal{R}^{(1)} \approx -\zeta^{(1)} \qquad \text{on superhorizon scales} \tag{4.43}$$

In order to deal with non-Gaussianity, this discussion must be generalized to second order.
The second order extension of (4.33) is [24]:

$$\begin{aligned} -\zeta^{(2)} \equiv & \left.\widetilde{\widehat{\psi}^{(2)}}\right|_\rho \\ = & \widehat{\psi}^{(2)} + \mathcal{H}\frac{\delta^{(2)}\rho}{\rho_0'} - 2\mathcal{H}\frac{\delta^{(1)}\rho'}{\rho_0'}\frac{\delta^{(1)}\rho}{\rho_0'} - 2\frac{\delta^{(1)}\rho}{\rho_0'}\left(\widehat{\psi}^{(1)\prime} + 2\mathcal{H}\widehat{\psi}^{(1)}\right) \\ & + \left(\frac{\delta^{(1)}\rho}{\rho_0'}\right)^2\left(\mathcal{H}\frac{\rho_0''}{\rho_0'} - \mathcal{H}' - 2\mathcal{H}^2\right) \end{aligned} \tag{4.44}$$

with $\widehat{\psi}^{(2)} \equiv \psi^{(2)} + \frac{1}{6}\nabla^2\chi^{(2)}$.
Going beyond linear order, [22] showed that the second order generalization of (4.42) is:

$$\mathcal{R}^{(2)} = \mathcal{H}\frac{\delta^{(2)}\varphi}{\varphi_0'} + \psi^{(2)} + \frac{\left(\psi^{(1)\prime} + 2\mathcal{H}\psi^{(1)} + \mathcal{H}\frac{\delta^{(1)}\varphi'}{\varphi_0'}\right)^2}{\mathcal{H}' + 2\mathcal{H}^2 - \mathcal{H}\frac{\varphi_0''}{\varphi_0'}} - \frac{1}{3}\partial_i\omega^{(1)}\partial^i\omega^{(1)} \tag{4.45}$$

We will be interested in the three-point function of primordial curvature perturbations $\langle\zeta\zeta\zeta\rangle$. There are many approaches to compute it. In the following chapters we will sketch two of them: one relies on standard field theory techniques and follows the steps of Acquaviva *et al.* [22], the other one is the in-in formalism which is the most common approach nowadays for n-point functions in Cosmology.
Before doing this, the next chapter will be devoted to introducing more in detail the power-spectrum and the bispectrum.

Chapter 5

Power-spectrum and beyond: non-Gaussianity

In this chapter we set the conventions for the correlation functions, introduce the power-spectrum and the bispectrum. We briefly review the main predictions for the observables.

5.1 Power-spectrum

Consider a random field $f(t,\vec{x})$ which can be expanded in Fourier space:

$$f(t,\vec{x}) = \int \frac{d^3\vec{k}}{(2\pi)^{3/2}} e^{i\vec{k}\cdot\vec{x}} f_{\vec{k}}(t) \tag{5.1}$$

The power-spectrum is the Fourier transform of the two-point function:

$$\boxed{\langle f_{\vec{k}_1} f^*_{\vec{k}_2} \rangle = P_f(k)\delta^{(3)}(\vec{k}_1 - \vec{k}_2)} \tag{5.2}$$

The Dirac delta enforces momentum conservation, the function P_f only depends on the modulus due to anisotropy. The power-spectrum measures the amplitude of the fluctuations at a given scale k. We can define the dimensionless power-spectrum $\mathcal{P}_f(k)$ as:

$$P_f(k) \equiv \frac{2\pi^2}{k^3}\mathcal{P}_f(k) \tag{5.3}$$

The mean square value of $f(t,\vec{x})$ in real space is:

$$\langle f^2(t,\vec{x}) \rangle = \int \frac{dk}{k}\mathcal{P}_f(k) \tag{5.4}$$

We can see that the meaning of $\mathcal{P}_f(k)$ is that of contribution to the variance per unit logarithmic interval in the wavenumber k.

To describe the slope of the power-spectrum we introduce the spectral index $n_f(k)$:

$$\boxed{n_f(k) - 1 \equiv \frac{d\log\mathcal{P}_f(k)}{d\log k}} \tag{5.5}$$

The quantity $n_f(k) - 1$ parametrizes the deviation from scale invariance: $n_f = 1$ corresponds to an exact scale-invariant or Harrison-Zel'dovich power-spectrum; $n_f > 1$ corresponds to a blue tilt, which means perturbations have more power on smaller scales; $n_f < 1$ corresponds to a red tilt, thus perturbations have less power on smaller scales.

5.1.1 Power-spectrum for the inflaton fluctuations

The power-spectrum for inflation fluctuations is given by:

$$\langle \delta\varphi_{\vec{k}_1}, \delta\varphi^*_{\vec{k}_2} \rangle = \frac{1}{a^2} \langle \delta\tilde{\varphi}_{\vec{k}_1}, \delta\tilde{\varphi}^*_{\vec{k}_2} \rangle \equiv \frac{2\pi^2}{k^3} \mathcal{P}_{\delta\varphi}(k) \delta^{(3)}(\vec{k}_1 - \vec{k}_2) \tag{5.6}$$

The left-hand side, the average on the vacuum, gives:

$$\frac{1}{a^2} u_{k_1} u^*_{k_2} \delta^{(3)}(\vec{k}_1 - \vec{k}_2) = \frac{|u_k|^2}{a^2} \delta^{(3)}(\vec{k}_1 - \vec{k}_2) \tag{5.7}$$

so:

$$\mathcal{P}_{\delta\varphi}(k) = \frac{k^3}{2\pi^2} \frac{|u_k|^2}{a^2} = \frac{k^3}{2\pi^2} |\delta\varphi_k|^2 \tag{5.8}$$

In the case of a massless field, $\nu = \frac{3}{2}$ exactly. The fluctuation $\delta\varphi_k$ has the constant amplitude (3.22) on superhorizon scales, therefore the two-point function in this limit approaches $\frac{H^2}{2k^3}$ and we find the well-known result:

$$\mathcal{P}_{\delta\varphi}(k) = \left(\frac{H}{2\pi} \right)^2 \tag{5.9}$$

The scalar spectral index is $n_{\delta\varphi} = 1$: we are in the case of a perfect scale invariance, or Harrison-Zel'dovich power-spectrum.

For a light scalar field, instead, the amplitude of the fluctuations is given by (3.30) and:

$$\mathcal{P}_{\delta\varphi}(k) = \frac{H^2}{(2\pi)^2} \left(\frac{k}{aH} \right)^{3-2\nu} \tag{5.10}$$

The spectral index is:

$$n_{\delta\varphi} - 1 = 3 - 2\nu \tag{5.11}$$

so it follows that $n_{\delta\varphi} \sim 1$. There is a deviation from perfect scale invariance.

See [12] for a more detailed discussion.

5.2 Non-Gaussianity

The non-Gaussianity we observe today in the sky is mainly due to the highly non-linear gravitational evolution and structure formation later in the history of the Universe. It may be that, below and before that, there was some primordial contribution to non-Gaussianity, which is the aspect we are focusing on now.

Primordial non-Gaussianity can be caused by intrinsic non-linearities in the scalar field already during inflation.
We considered the evolution on a single scalar field on the background spacetime. The simplest case is that of a Gaussian field, whose expression in momentum space is $\sim u\hat{a} + u^*\hat{a}^\dagger$. In that case, all the information is contained in the power-spectrum: n-point correlation functions are vanishing for odd n and are products of the two-point correlation functions for even n. The power-spectrum completely characterizes the field from a statistical point of view.

But if there is an interaction term in the Lagrangian, then the field can no longer be written as sum of harmonic oscillators.
The three-point function or its Fourier transform, the bispectrum, is the lowest-order statistics able to distinguish non-Gaussian from Gaussian perturbations [12].

There can be many sources of non-Gaussianity. Simplest inflation models generate a negligible amount of non-Gaussianities, where "simplest" means [9]:

- single scalar field
- with canonical kinetic term
- always slow-rolls
- in Bunch-Davies vacuum
- in Einstein gravity

Any violation of the above condition could generate some non-Gaussianity.

5.3 The bispectrum

The bispectrum is the Fourier transform of the three-point function. With our Fourier convention (5.1):

$$\langle \zeta_{\vec{k}_1} \zeta_{\vec{k}_2} \zeta_{\vec{k}_3} \rangle = \frac{1}{(2\pi)^{3/2}} \delta^{(3)}(\vec{k}_1 + \vec{k}_2 + \vec{k}_3) B_\zeta(k_1, k_2, k_3) \tag{5.12}$$

The Dirac delta enforces momentum conservation, so that the three wavevectors $\vec{k}_i$ form a triangle. Due to isotropy, B_ζ only depends on the moduli of the momenta.
We can split the bispectrum into an *amplitude* and a *shape*:

$$B_\zeta(k_1, k_2, k_3) = f_{\rm NL} F(k_1, k_2, k_3) \tag{5.13}$$

Now we will analyze these two components more in detail.

The naive expectation is that the bispectrum should be proportional to $1/\epsilon^2$. The reason is that the power-spectrum for single-field slow-roll inflation is proportional to $1/\epsilon$ and, schematically, the bispectrum is proportional to the product of two power-spectra. Falk *et al.* [25] computed $f_{\rm NL} \propto \epsilon^2$, due to non-linearity in the inflaton potential in a fixed de Sitter space. However, it was shown later [26] that $f_{\rm NL} \sim \epsilon, \eta$ because of second order gravitational corrections during inflation: so it is gravity that gives the most important contribution, such that non-Gaussianity is not second order in the slow-roll parameters but first order. This estimate was later confirmed with a full second order approach in [22, 27].

5.3.1 $f_{\rm NL}$

The non-Gaussianity parameter $f_{\rm NL}$ is a measure of the amplitude of the bispectrum with respect to the power-spectrum squared.
There are many conventions in the literature to define it, we follow [28] and parametrize:

$$\boxed{B_\zeta(k_1, k_2, k_3) = -\frac{6}{5} f_{\rm NL} \left[P_\zeta(k_1) P_\zeta(k_2) + P_\zeta(k_1) P_\zeta(k_3) + P_\zeta(k_2) P_\zeta(k_3) \right]} \tag{5.14}$$

The numerical factor comes from the relation between the curvature perturbation ζ on superhorison scales and the Bardeen potential Φ [21], that is $\Phi = \frac{3}{5}\zeta$ [29].

For single-field slow-roll inflation, see [27, 28]:

$$B_\zeta^{\rm M}(k_1, k_2, k_3) = \frac{H_{\rm DS}^4}{32 k_1^3 k_2^3 k_3^3 M_P^4 \epsilon^2} \cdot \Bigg[-2(\eta_V - \epsilon)(k_1^3 + k_2^3 + k_3^3) + 2\epsilon \Bigg(\frac{k_1^3 + k_2^3 + k_3^3}{2} + \frac{1}{2} \left(k_1 k_2^2 + k_1^2 k_2 + k_1 k_3^2 + k_1^2 k_3 + k_2 k_3^2 + k_2^2 k_3 \right) + + \frac{4}{k_1 + k_2 + k_3} \left(k_1^2 k_2^2 + k_1^2 k_3^2 + k_2^2 k_3^2 \right) \Bigg) \Bigg] \tag{5.15}$$

According to (5.14), the non-Gaussianity parameter is:

$$f_{\rm NL} = \frac{5}{12}\left(2\eta_V - 6\epsilon - 2\epsilon f(k_1,k_2,k_3)\right) \tag{5.16}$$

where $f(k_1,k_2,k_3)$ is a function of the three momenta such that $0 \leq f(k_1,k_2,k_3) \leq 5/6$, in particular it goes to zero when one side of the triangle is much smaller than the other two and it goes to 5/6 in the equilateral case.

$$\begin{aligned} f(k_1,k_2,k_3) =& \frac{1}{2(k_1+k_2+k_3)\left(k_1^3+k_2^3+k_3^3\right)}\cdot \\ &\Bigg[-3(k_1^4+k_2^4+k_3^4) - 2(k_1^3k_2+k_1k_2^3+k_1^3k_3+k_1k_3^3+k_2^3k_3+k_2k_3^3)+ \\ &+10(k_1^2k_2^2+k_1^2k_3^2+k_2^2k_3^2)+2k_1k_2k_3(k_1+k_2+k_3)\Bigg] \end{aligned} \tag{5.17}$$

Specializing these results to the case of power-law inflation, where $\eta_V = 2\epsilon$:

$$\begin{aligned} B_\zeta^{\rm M}(k_1,k_2,k_3) =& -\frac{V_0^2}{288M_P^8\epsilon k_1^3k_2^3k_3^3(k_1+k_2+k_3)}\cdot \\ &\left(k_1^4+k_2^4+k_3^4-10(k_1^2k_2^2+k_1^2k_3^2+k_2^2k_3^2)-2k_1k_2k_3(k_1+k_2+k_3)\right) \end{aligned} \tag{5.18}$$

and:

$$f_{\rm NL} = -\frac{5}{6}\epsilon\left(1+f(k_1,k_2,k_3)\right) \tag{5.19}$$

Some care is needed. Detecting non-zero $f_{\rm NL}$ proves that the initial seeds were non-Gaussian, but not detecting it does not prove Gaussianity. Indeed, primordial non-Gaussianity may evade observational bounds that are optimized to search for $f_{\rm NL}$.

5.3.2 Shapes

The shape function contains information on how much power is associated to a given triangle shape, keeping the overall scale $k_1+k_2+k_3$ fixed. Figure 5.1 illustrates the possible configurations. Since the three wavevectors are bound to form a triangle, the function $F(k_1,k_2,k_3)$ only has two degrees of freedom.

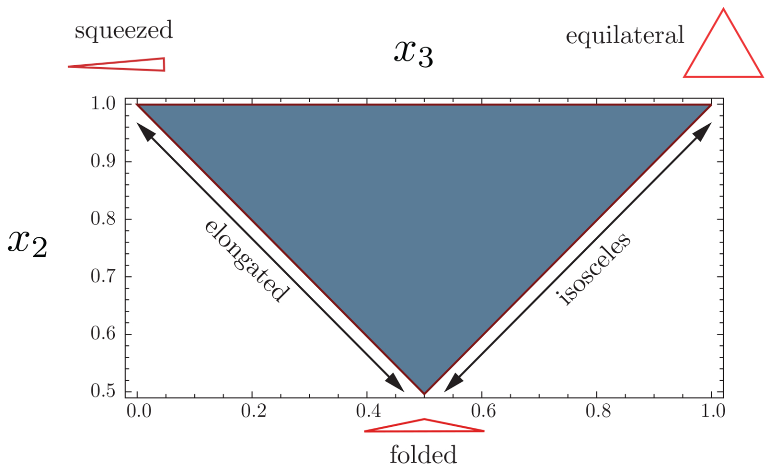

Figure 5.1: Parameter space for the three momenta, rescaled so that $x_2 \equiv k_2/k_1$ and $x_3 \equiv k_3/k_1$. They are ordered $x_3 < x_2 < 1$ and satisfy the triangle inequality $x_2 + x_3 > 1$. Figure from [5].

Shapes are a powerful tool because different inflationary models predict bispectra that peak at different shapes. As someone once said, "there are more shapes of non-Gaussianity from inflation than... stars in the sky"[1]. Below we only list two of them, the equilateral shape and the squeezed shape, because they will be relevant for our discussion. For more details, we refer to [30].

- **Equilateral shape**
  We choose $k_1 = k_2 = k_3 \equiv k$.

$$F_{\text{equil}}(k_1,k_2,k_3) = \frac{18}{5}A^2\left[-\frac{1}{k_1^{4-n_s}k_2^{4-n_s}} - \frac{1}{k_1^{4-n_s}k_3^{4-n_s}} - \frac{1}{k_2^{4-n_s}k_3^{4-n_s}} - \frac{2}{(k_1k_2k_3)^{2(4-n_s)/3}} + \left(\frac{1}{(k_1k_2^2k_3^3)^{(4-n_s)/3}} + 5 \text{ permutations}\right)\right] \tag{5.20}$$

  This type of non-Gaussianity is associated to non-canonical kinetic terms for the inflaton.

- **Local or squeezed shape**
  In this case, one of the sides of the triangle is much smaller than the other two $k_3 \ll k_1,\ k_2$.

$$F_{\text{local}}(k_1,k_2,k_3) = \frac{6}{5}A^2\left(\frac{1}{k_1^{4-n_s}k_2^{4-n_s}} + \frac{1}{k_1^{4-n_s}k_3^{4-n_s}} + \frac{1}{k_2^{4-n_s}k_3^{4-n_s}}\right) \tag{5.21}$$

  where the constant is the normalization of the power-spectrum $P_\zeta(k) = Ak^{n_s-4}$.

  Multi-field models usually predict a large amount of non-Gaussianity of this type. Also for single-field slow-roll inflation some non-Gaussianity of the local type is expected, but its amplitude is suppressed by the slow-roll parameters $f_{\text{NL}} = \mathcal{O}(\epsilon, \eta)$.

  In Fourier space, when taking the squeezed limit we are looking at correlations between long and short wavelength modes. This configuration will be very important in the following since, for single-field models, there is a consistency relation linking the bispectrum in the squeezed limit with the scalar spectral index of the power-spectrum. We will come back on this point later on and examine it in the case of power-law inflation.

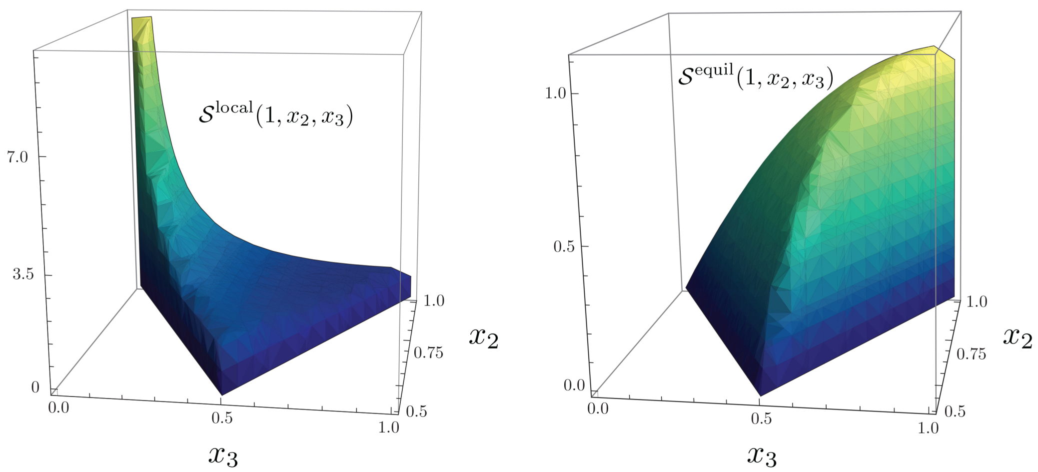

Figure 5.2: Plots of the local and equilateral bispectra. Again, the coordinates x_2 and x_3 are the rescaled momenta. Figure from [5].

5.4 Experimental constraints

Experimental constraints on the power-spectrum have been obtained by the Planck mission [31]. If we parametrize the primordial power-spectrum in terms of an amplitude A_s and a tilt $n_s - 1$, then:

$$\mathcal{P}_\zeta(k) = A_s\left(\frac{k}{k_*}\right)^{n_s-1} \tag{5.22}$$

[1]Sabino Matarrese, paraphrasing Saint Augustine.

$$A_s = \left(2.101^{+0.031}_{-0.034}\right) \times 10^{-9} \qquad n_s = 0.9649 \pm 0.0042 \qquad \text{at } 68\%,\ k_* = 0.05\ \text{Mpc}^{-1} \tag{5.23}$$

Experimental constraints on non-Gaussianity are usually given in terms of the amplitude parameter $f_{\rm NL}$.
There is a critical sensitivity $f_{\rm NL} \sim 1$, which is set by non-Gaussian contributions from ubiquitous second-order perturbations [12]. Ideally, we would like to reach this threshold. In fact, the slow-roll parameters are of order $\mathcal{O}(0.01)$, so $f_{\rm NL} \sim \mathcal{O}(0.01)$ for these models; but even if we start with Gaussian primordial perturbations, nonlinear effects in CMB evolution will generate $f_{\rm NL} \sim \mathcal{O}(1)$, and a similar number for large-scale structures due to the nonlinear gravitational evolution or the galaxy bias [9]. We should be able to disentangle all these contributions.
Unfortunately, the data at hand do not provide definitive conclusions.

The best results so far have been obtained by looking at the CMB: in this area, the Planck experiment is currently the state of the art and it has been able to set the most stringent constraints to date [30]. The bounds depend on the specific template one is looking for in the data:

$$\begin{aligned} f_{\rm NL}^{\rm local} &= -0.9 \pm 5.1 \\ f_{\rm NL}^{\rm equil} &= -26 \pm 47 \\ f_{\rm NL}^{\rm ortho} &= -38 \pm 24 \end{aligned} \tag{5.24}$$

at 68% confidence level.

The Planck constraints are close to what is ultimately possible from using CMB temperature data alone. When measuring the angular CMB power-spectrum, there is always a fractional error of $\sqrt{\frac{2}{2\ell+1}}$ in the measurement of each C_ℓ. The crucial limit is set at low ℓ by cosmic variance, due to the fact that we only have one realization of the CMB at our disposal, and this greatly dominates the error bars at the lowest multipoles [32, 33]. In particular, the signal for $f_{\rm NL} = 1$, which is the watershed that would rule out single-field models of inflation, is smaller than cosmic variance. Therefore, distinguishing $|f_{\rm NL}| \ll 1$ from $|f_{\rm NL}| \sim 1$ is a key target to observationally distinguish single-field, slow-roll inflation from other scenarios.

The next challenge is looking at the large-scale structure: improvements in this direction are expected in the next decades.

Chapter 6

Power-law inflation

We now specialize the results of the previous chapters to power-law inflation [4, 13]. We go through the perturbed Einstein equations for this model, we introduce the Mukhanov-Sasaki variable which greatly simplifies the problem, we compute the power-spectrum.

6.1 Background dynamics

Power-law inflation is defined by $a(t) \propto t^p$. In conformal time, the scale factor becomes $a(\tau) = A(-\tau)^{\frac{p}{1-p}}$ where A is some normalization constant.
The solution for the background field is (2.32):

$$\varphi_0(\tau) = M_P \frac{\sqrt{2p}}{p-1} \log(-\tau) + \mathrm{C} \tag{6.1}$$

where C is the integration constant.

Following [13], the definition of the scale factor should be, more rigorously:

$$a(t) = a_* \left[1 + \frac{H_*(t - t_*)}{p}\right]^p \tag{6.2}$$

since this returns exactly de Sitter in the $p \to \infty$ limit.
In conformal time:

$$\begin{aligned} \tau &= \int \frac{dt}{a(t)} \\ \tau - \tau_* &= -\frac{p}{a_* H_* (p-1)} \left(1 + \frac{H_*(t - t_*)}{p}\right)^{1-p} \\ a(\tau) &= a_* \left[\frac{a_* H_* (1-p)(\tau - \tau_*)}{p}\right]^{\frac{p}{1-p}} \end{aligned} \tag{6.3}$$

What is a_*? Another way to fix the normalization, that is more convenient for our purposes, is via the background equation of motion for the field (2.18), with $a(\tau) = A(-\tau)^{\frac{p}{1-p}}$:

$$\varphi_0'' + 2\mathcal{H}\varphi_0' + a^2 \frac{\partial V}{\partial \varphi} = 0 \tag{6.4}$$

This way we find:

$$A = e^{-\frac{\mathrm{C}}{M_P}\frac{1}{\sqrt{2p}}} \frac{M_P}{\sqrt{V_0}} \frac{\sqrt{p(3p-1)}}{p-1} \tag{6.5}$$

Finally, recall the relations:

$$\nu = \frac{3p-1}{2(p-1)} \qquad\qquad p = \frac{1}{3\gamma^2} = \frac{1}{\epsilon} \tag{6.6}$$

with ϵ the slow-roll parameter.

6.2 Perturbed Einstein equations in power-law inflation

6.2.1 First order

The equation is (4.19):

$$\begin{aligned}
&\phi^{(1)\prime\prime} + 2\left(\mathcal{H} - \frac{\varphi_0''}{\varphi_0'}\right)\phi^{(1)\prime} + 2\left(\mathcal{H}' - \mathcal{H}\frac{\varphi_0''}{\varphi_0'}\right)\phi^{(1)} - \partial_i\partial^i\phi^{(1)} = 0\\
&\phi^{(1)\prime\prime} + \frac{2}{\tau}\left(\frac{p}{1-p}+1\right)\phi^{(1)\prime} + \frac{2}{\tau^2}\left(-\frac{p}{1-p}+\frac{p}{1-p}\right)\phi^{(1)} - \partial_i\partial^i\phi^{(1)} = 0\\
&\phi^{(1)\prime\prime} + \frac{2}{(1-p)\tau}\phi^{(1)\prime} + k^2\phi^{(1)} = 0
\end{aligned} \tag{6.7}$$

where in the last step we also went to Fourier space.

The solutions are Bessel functions of first and second kind:

$$\phi^{(1)}(\tau) = 2^\alpha\left((1-p)\tau\right)^\alpha\left[c_J(k)J_\alpha(-k\tau) + c_Y(k)Y_\alpha(-k\tau)\right] \tag{6.8}$$

having introduced:

$$\alpha \equiv \frac{1+p}{2(p-1)} \qquad\qquad \alpha = \nu - 1 \tag{6.9}$$

Now we plug this solution in (4.18) to get $\delta^{(1)}\varphi$:

$$\begin{aligned}
\phi^{(1)\prime} &= 2^\alpha k\left((1-p)\tau\right)^\alpha\left[c_J(k)J_{\alpha-1}(-k\tau) + c_Y(k)Y_{\alpha-1}(-k\tau)\right]\\
\mathcal{H}\phi^{(1)} &= 2^\alpha p\left((1-p)\tau\right)^{\alpha-1}\left[c_J(k)J_\alpha(-k\tau) + c_Y(k)Y_\alpha(-k\tau)\right]
\end{aligned}$$

$$\begin{aligned}
\delta^{(1)}\varphi &= \frac{1}{4\pi G\varphi_0'}\left(\mathcal{H}\phi^{(1)} + \phi^{(1)\prime}\right)\\
&= \frac{1}{8\pi G}2^\alpha\Gamma\left((1-p)\tau\right)^\alpha\Big[c_J(k)\left((p-1)(-k\tau)J_{\alpha-1}(-k\tau) - pJ_\alpha(-k\tau)\right) +\\
&\qquad c_Y(k)\left((p-1)(-k\tau)Y_{\alpha-1}(-k\tau) - pY_\alpha(-k\tau)\right)\Big]\\
&= \sqrt{\frac{2}{p}}M_P 2^\alpha(p-1)^\alpha(-\tau)^\alpha\Big[c_J(k)\left((p-1)(-k\tau)J_{\alpha-1}(-k\tau) - pJ_\alpha(-k\tau)\right) +\\
&\qquad c_Y(k)\left((p-1)(-k\tau)Y_{\alpha-1}(-k\tau) - pY_\alpha(-k\tau)\right)\Big]
\end{aligned} \tag{6.10}$$

6.2.2 Second order

The equation is (4.25):

$$\phi^{(2)\prime\prime} + 2\left(\mathcal{H} - \frac{\varphi_0''}{\varphi_0'}\right)\phi^{(2)\prime} + 2\left(\mathcal{H}' - \mathcal{H}\frac{\varphi_0''}{\varphi_0'}\right)\phi^{(2)} - \partial_i\partial^i\phi^{(2)} = S$$

It looks like the first order equation (4.19) except that on the right hand side we have a source term $S = S(\vec{x},\tau)$ that has the form $A(\vec{x},\tau)B(\vec{x},\tau)$ with A, B first order quantities. When we go to Fourier space, the product becomes a convolution[1]:

$$\phi_{\vec{k}}^{(2)\prime\prime} + 2\left(\mathcal{H} - \frac{\varphi_0''}{\varphi_0'}\right)\phi_{\vec{k}}^{(2)\prime} + 2\left(\mathcal{H}' - \mathcal{H}\frac{\varphi_0''}{\varphi_0'}\right)\phi_{\vec{k}}^{(2)} + k^2\phi_{\vec{k}}^{(2)} = \int\frac{d^3\vec{k}'}{(2\pi)^{3/2}}A_{\vec{k}'}B_{\vec{k}-\vec{k}'} \tag{6.11}$$

[1] In our convention (5.1):

$$\phi^{(2)}(\vec{x},\tau) = \int\frac{d^3\vec{k}}{(2\pi)^{3/2}}\phi_{\vec{k}}^{(2)}(\tau)e^{i\vec{k}\cdot\vec{x}}$$

The solutions will be given by the solutions of the homogeneous equation, which is analogous to the first order one, and a particular solution. The main difficulty in this calculation will be dealing with the convolution kernel in the particular solution and computing that time integral.
If we work in the slow-roll approximation as in [22] a lot of terms in (4.25) can be dropped, and we are able to recast it as a first order equation. This way we never have to deal with the kernel.
The homogeneous solution is (6.8):

$$\phi^{(2)}_{\text{hom}}(\tau) = 2^{\alpha}\left((1-p)\tau\right)^{\alpha}\left[b_J(k)J_\alpha(-k\tau) + b_Y(k)Y_\alpha(-k\tau)\right] \tag{6.12}$$

To find the particular solution, we should integrate[2]:

$$\phi^{(2)}_{\text{part}}(\tau) = \int_{\tau_i}^{\tau} d\eta\left(-\frac{\phi^{(2)}_1(\tau)\phi^{(2)}_2(\eta)}{\det W(\eta)}S_{\vec{k}}(\eta) + \frac{\phi^{(2)}_1(\eta)\phi^{(2)}_2(\tau)}{\det W(\eta)}S_{\vec{k}}(\eta)\right) \tag{6.13}$$

where:

$$\begin{aligned}
\phi^{(2)}_1(\tau) &= c_1(k)2^{\alpha}\left((1-p)\tau\right)^{\alpha}J_\alpha(-k\tau)\\
\phi^{(2)}_2(\tau) &= c_2(k)2^{\alpha}\left((1-p)\tau\right)^{\alpha}Y_\alpha(-k\tau)\\
\det W &= \phi^{(2)}_1\phi^{(2)\prime}_2 - \phi^{(2)\prime}_1\phi^{(2)}_2 = \frac{2^{1+2\alpha}c_1(k)c_2(k)}{\pi}\frac{(p-1)^{2\alpha}(-\tau)^{2\alpha}}{(-\tau)}
\end{aligned} \tag{6.14}$$

We obtain:

$$\phi^{(2)}_{\text{part}}(\tau) = \int_{\tau_i}^{\tau} d\eta\frac{\pi}{2}\left(\frac{\tau}{\eta}\right)^{\alpha}(-\eta)\left[J_\alpha(-k\tau)Y_\alpha(-k\eta) - J_\alpha(-k\eta)Y_\alpha(-k\tau)\right]S_{\vec{k}}(\eta) \tag{6.15}$$

Or in terms of Hankel functions:

$$\phi^{(2)}_{\text{part}}(\tau) = \frac{\pi}{4i}(-\tau)^{\alpha}\int_{\tau_i}^{\tau} d\eta(-\eta)^{1-\alpha}\left[H^{(1)}_\alpha(-k\eta)H^{(2)}_\alpha(-k\tau) - H^{(1)}_\alpha(-k\tau)H^{(2)}_\alpha(-k\eta)\right]S_{\vec{k}}(\eta) \tag{6.16}$$

Notice that the Green's functions inside the time integral for $\phi^{(2)}$ are classical, so we can use Bessel and Neumann or we can use Hankel of first and second kind, at will. Instead, when quantizing $\mathcal{R}^{(1)}$ and writing the mode functions θ_k, those must be Hankel of first and second kind, because that is the framework in which we can locally recover the harmonic oscillator with the Bunch-Davies prescription for the vacuum. For this reason, the modefunction associated to the annihilation operator $\hat{a}_{\vec{k}}$ must be $H^{(1)}(-k\tau)$ so that it will have the correct $e^{-ik\tau}$ behaviour (positive frequency), while the modefunction associated to the creation operator $\hat{a}^{\dagger}_{\vec{k}}$ must be $H^{(2)}(-k\tau)$ and locally will go like $e^{ik\tau}$ (negative frequency). In other words, $\theta_k \propto H^{(1)}$ and $\theta^*_k \propto H^{(2)}$ [34,35].
It is be more convenient to work with Hankel functions, especially when approximating to super-horizon scales.

$$\begin{aligned}
&\int \frac{d^3\vec{k}}{(2\pi)^{3/2}}e^{i\vec{k}\cdot\vec{x}}\left(\phi^{(2)\prime\prime}_{\vec{k}} + 2\left(\mathcal{H} - \frac{\varphi_0''}{\varphi_0'}\right)\phi^{(2)\prime}_{\vec{k}} + 2\left(\mathcal{H}' - \mathcal{H}\frac{\varphi_0''}{\varphi_0'}\right)\phi^{(2)}_{\vec{k}} + k^2\phi^{(2)}_{\vec{k}}\right)\\
&= \int \frac{d^3\vec{k}}{(2\pi)^{3/2}}\frac{d^3\vec{k}'}{(2\pi)^{3/2}}e^{i(\vec{k}+\vec{k}')\cdot\vec{x}}A_{\vec{k}}B_{\vec{k}'}
\end{aligned}$$

Multiplying by $e^{-i\vec{p}\cdot\vec{x}}$ and integrating in $d^3\vec{x}$:

$$\int d^3\vec{x}\ d^3\vec{k}(\dots)e^{i(\vec{k}-\vec{p})\cdot\vec{x}} = \int d^3\vec{x}\ \frac{d^3\vec{k}\ d^3\vec{k}'}{(2\pi)^{3/2}}(\dots)e^{i(\vec{k}+\vec{k}'-\vec{p})\cdot\vec{x}}$$

Recall that $\int d^3\vec{x}\ e^{i(\vec{k}-\vec{p})\cdot\vec{x}} = (2\pi)^3\delta^{(3)}(\vec{k}-\vec{p})$:

$$\int d^3\vec{k}\ \delta^{(3)}(\vec{k}-\vec{p})(\dots) = \int \frac{d^3\vec{k}\ d^3\vec{k}'}{(2\pi)^{3/2}}\delta^{(3)}(\vec{k}+\vec{k}'-\vec{p})A_{\vec{k}}B_{\vec{k}'} = \int \frac{d^3\vec{k}}{(2\pi)^{3/2}}A_{\vec{k}}B_{\vec{p}-\vec{k}}$$

[2]Notice that here η inside the integral is conformal time, not to be confused with the second slow-roll parameter.

6.3 Mukhanov-Sasaki variable

The quickest way to deal with equations (4.16), (4.18), (4.19) is to introduce a mixed variable. We introduce the Mukhanov-Sasaki variable [36]:

$$v = a\left(\delta\varphi + \frac{\varphi_0'}{\mathcal{H}}\phi\right) \tag{6.17}$$

This variable mixes together perturbations in the field and perturbations in the metric. At first it may seem that we are complicating matters but, as we have already mentioned, a mixed variable is actually the most natural way to formulate the problem because these objects are deeply intertwined from a physical point of view. As a matter of fact, the equations we obtain for v are much more elegant than the ones for the single variables alone.

The e.o.m. for v can be obtained from the second-order action (as will be sketched in the in-in formalism framework, see (8.8)):

$$v_k'' + \left(k^2 - \frac{z''}{z}\right)v_k = 0 \tag{6.18}$$

with:

$$z = \frac{a\varphi_0'}{\mathcal{H}} \tag{6.19}$$

The Mukhanov-Sasaki variable is linked to the curvature perturbation (4.42) through[3]:

$$v(\vec{x},\tau) = z(\tau)\mathcal{R}(\vec{x},\tau) \qquad \text{with } z = \frac{a\varphi_0'}{\mathcal{H}} \tag{6.20}$$

We only need to compute the background dependent term z''/z. Using (2.32) and the background evolution:

$$\frac{z''}{z} = \frac{p(2p-1)}{(p-1)^2\tau^2} \tag{6.21}$$

The solutions of (8.9) are:

$$\boxed{v_k(\tau) = \sqrt{-\tau}\left[c_J(k)J_\nu(-k\tau) + c_Y(k)Y_\nu(-k\tau)\right]} \qquad \nu = \frac{3p-1}{2(p-1)} \tag{6.22}$$

We can also check that inserting our first order solutions (6.10) and (6.8) into the definition of v we recover the same result, up to a redefinition of the coefficients $c_J(k)$ and $c_Y(k)$. To perform this check we need some properties of the Bessel functions like the recurrence relations (A.2).

Let us mention that working with v is not the only possibility. For example, [2] choose another way, that proves more convenient when one deals with the problem numerically in a more generic model:

$$Q \equiv \frac{v}{a} = \frac{\varphi_0'}{\mathcal{H}}\mathcal{R} \tag{6.23}$$

The advantage of working with the rescaled Mukhanov-Sasaki variable is that *it is constant on superhorizon scales and it remains well-defined throughout the evolution of* φ_0. Naively, if $\delta\varphi$ is frozen on superhorizon scales and $\mathcal{R} \approx \mathcal{H}\delta\varphi/\varphi_0'$, then $\mathcal{R}\varphi_0'/\mathcal{H}$ is frozen. So working with Q is analogous to what we did in chapter 3, in a quasi-de Sitter stage and neglecting metric perturbations, when we worked

[3] In fact:

$$v = a\left(\delta\varphi + \frac{\varphi_0'}{\mathcal{H}}\phi\right) = a\frac{\varphi_0'}{\mathcal{H}}\left(\phi + \mathcal{H}\frac{\delta\varphi}{\varphi_0'}\right) \underset{\uparrow}{=} \frac{a\varphi_0'}{\mathcal{H}}\left(\hat{\psi} + \mathcal{H}\frac{\delta\varphi}{\varphi_0'}\right) = \frac{a\varphi_0'}{\mathcal{H}}\mathcal{R}$$

in Poisson gauge where $\chi = 0$

with the fluctuations of the field $\delta\varphi$ and computed $\langle\delta\varphi\delta\varphi\rangle$. Instead v would be the analogous of the rescaled field that we called $\delta\widetilde{\varphi}$.

In our case:

$$Q_k(\tau) = (-\tau)^\nu \left[c_J(k) J_\nu(-k\tau) + c_Y(k) Y_\nu(-k\tau)\right] \tag{6.24}$$

where we can reabsorb the normalization of the scale factor into a redefinition of the coefficients $c_J(k)$, $c_Y(k)$.

To fix the coefficients $c_J(k)$ and $c_Y(k)$ we have to choose the vacuum according to the Bunch-Davies prescription. In order to do this, it is best to rewrite everything in terms of Hankel functions, because it will be useful to study the asymptotic behaviour:

$$v_k(\tau) = \sqrt{-\tau}\left[c_1(k) H_\nu^{(1)}(-k\tau) + c_2(k) H_\nu^{(2)}(-k\tau)\right] \tag{6.25}$$

Using the asymptotic expansion of the Hankel functions (A.5) well inside the horizon, for $-k\tau \gg 1$, we obtain:

$$v_k(\tau) \sim \sqrt{-\tau}\sqrt{\frac{2}{-\pi k\tau}}\left[c_1(k) e^{-ik\tau} e^{-i\left(\nu\frac{\pi}{2}+\frac{\pi}{4}\right)} + c_2(k) e^{ik\tau} e^{i\left(\nu\frac{\pi}{2}+\frac{\pi}{4}\right)}\right]$$

As usual, the Hankel function of second kind has the wrong asymptotic behaviour, so we need to choose $c_2(k) = 0$. The other coefficient is fixed by asking that we recover the Minkowski behaviour:

$$\sqrt{\frac{2}{\pi k}} e^{-i\left(\nu\frac{\pi}{2}+\frac{\pi}{4}\right)} c_1(k) e^{-ik\tau} = \frac{1}{\sqrt{2k}} e^{-ik\tau}$$

$$c_1(k) = \sqrt{\frac{\pi}{4}} e^{i\left(\nu\frac{\pi}{2}+\frac{\pi}{4}\right)} \tag{6.26}$$

Finally:

$$\boxed{v_k(\tau) = \sqrt{\frac{\pi}{4}} e^{i\left(\nu\frac{\pi}{2}+\frac{\pi}{4}\right)} \sqrt{-\tau} H_\nu^{(1)}(-k\tau)} \qquad \nu = \frac{3p-1}{2(p-1)} \tag{6.27}$$

6.3.1 Modefunctions for $\mathcal{R}$ or ζ

Equation (6.20) gives the link between comoving curvature perturbation and Mukhanov-Sasaki variable, therefore we are in the position to write down the modefunctions for $\mathcal{R}$ or for ζ.

Using $a(\tau) = A(-\tau)^{\frac{p}{1-p}}$, with the normalization A defined in (6.5):

$$z = \frac{a\varphi_0'}{\mathcal{H}} = -\sqrt{\frac{2}{p}} A M_P (-\tau)^{\frac{p}{1-p}} \tag{6.28}$$

With the normalized solution for v (6.27) we find:

$$\zeta_k(\tau) = -\sqrt{\frac{p}{2}}\frac{1}{A M_P}\sqrt{\frac{\pi}{4}} e^{i\left(\nu\frac{\pi}{2}+\frac{\pi}{4}\right)} (-\tau)^\nu H_\nu^{(1)}(-k\tau) \tag{6.29}$$

Let's write the modefunction of ζ as:

$$\boxed{\theta_k(\tau) = c(-\tau)^\nu H_\nu^{(1)}(-k\tau)} \tag{6.30}$$

where we have called the constant c for simplicity.

6.4 Power-spectrum in power-law inflation

With the convention (5.2), the dimensionless power-spectrum, defined in (5.3), for ζ or $\mathcal{R}$ is:

$$P_\zeta(k,\tau)) = \langle \hat{\zeta}_{\vec{k}}(\tau)\hat{\zeta}_{\vec{k}'}(\tau)\rangle = \frac{1}{|z(\tau)|^2} v_k(\tau)v_k^*(\tau)\delta^{(3)}(\vec{k}+\vec{k}') \tag{6.31}$$

On superhorizon scales, if we approximate the Hankel functions as in (A.6):

$$\mathcal{P}_\zeta(k) = \frac{2^{\frac{1-3\epsilon}{-1+\epsilon}} e^{\frac{C}{M_P}\sqrt{2\epsilon}}}{\pi^3} \frac{V_0}{M_P^4} \frac{(1-\epsilon)^2 \left(\Gamma\left(\frac{3-\epsilon}{2(1-\epsilon)}\right)\right)^2}{(3-\epsilon)\epsilon} k^{\frac{2\epsilon}{-1+\epsilon}} \tag{6.32}$$

In the slow-roll limit $\epsilon \to 0$ we recover the known result:

$$\mathcal{P}_\mathcal{R}(k) \xrightarrow{\epsilon \to 0} \frac{H_{\rm DS}^2}{8M_P^2\pi^2\epsilon} \tag{6.33}$$

where we have introduced the would-be de Sitter Hubble parameter $H_{\rm DS}^2 = \frac{1}{3M_P^2}V_0$.

Defining the scalar spectral index as in (5.5):

$$n_s - 1 = \frac{d\log\mathcal{P}_\mathcal{R}(k)}{d\log k} = 3 - 2\nu = -\frac{2\epsilon}{1-\epsilon} \simeq -2\epsilon + \mathcal{O}(\epsilon^2) \tag{6.34}$$

In the slow-roll limit, we recover the standard result.

Chapter 7

In-in formalism

If we are interested in studying n-point correlation functions with $n > 2$, a powerful tool in cosmology is the in-in formalism. This chapter is devoted to introducing the formalism, we refer to [5, 37, 38] for more details.

In full generality, let's say we want to compute expectation values of operators $\hat{Q}$ which in general are products of the field $\delta\phi_a$ and its conjugate momentum $\delta\pi_a$, typically evaluated at the end of inflation.

There is a crucial difference with respect to the particle physics case. In particle physics, the main observable is the S-matrix, i.e. the transition probability for a given state $|in\rangle$ in the far past to become some state $|out\rangle$ in the far future:

$$\langle out|S|in\rangle = \langle out(+\infty)|in(-\infty)\rangle \tag{7.1}$$

The states are taken to be asymptotically free in the far past and again in the far future.

In cosmology instead one is interested in expectation values at a fixed time. We want to compute:

$$\langle\hat{Q}(\tau)\rangle = \langle in|\hat{Q}(\tau)|in\rangle \tag{7.2}$$

The boundary conditions are only imposed at early times, when the wavelengths are well inside the Hubble radius and we expect the fields to behave as if they were in Minkowski space. This is the essence of the Bunch-Davies vacuum choice.

(a) Particle physics in-out transition amplitudes.

(b) Cosmology in-in expectation values.

Figure 7.1: Comparison between the particle physics and the cosmology approach. From [39].

The time evolution is governed by the Hamiltonian of the system, which is a functional of the fields $\phi_a(\vec{x},\tau)$ and their conjugate momenta $\pi_a(\vec{x},\tau)$ at a fixed time t:

$$H[\phi(\tau),\pi(\tau)] \equiv \int d^3\vec{x}\mathcal{H}[\phi_a(\vec{x},\tau),\pi_a(\vec{x},\tau)] \tag{7.3}$$

with ϕ and π satisfying the canonical commutation relation:

$$[\phi_a(\vec{x},\tau),\pi_b(\vec{x}',\tau)] = i\delta_{ab}\delta^{(3)}(\vec{x}-\vec{x}') \tag{7.4}$$

7.0.1 Interaction picture

Assume that we can split the Hamiltonian for perturbations $H[\phi(\vec{x},\tau),\pi(\vec{x};\tau),\tau]$ as:

$$H = H_0 + H_{INT} \tag{7.5}$$

The interaction term would lead to nonlinear equations of motion. It is convenient to put ourselves in the interaction picture: we evolve operators as in the free theory, and move all the complications into the evolution of states.

- Physical states evolve with a Schroedinger equation with H_{INT}:

$$i\partial_\tau |\psi(\tau)\rangle^I = \hat{H}^I_{INT}(\tau)|\psi(\tau)\rangle^I \tag{7.6}$$

- Operators evolve with a Heisenberg equation with H_0:

$$i\partial_\tau \hat{O}^I(\tau) = \left[\hat{O}^I(\tau), \hat{H}^I_0(\tau)\right] \tag{7.7}$$

Therefore:

$$|\psi(\tau)\rangle^I = e^{-iH_{INT}\tau}|\psi(0)\rangle \qquad\qquad \hat{O}^I(\tau) = e^{iH_0\tau}\hat{O}(0)e^{-iH_0\tau}$$

The link with the Schroedinger picture for states is given by:

$$|\psi(\tau)\rangle^I = e^{iH_0\tau}|\psi(\tau)\rangle^S$$

The key point is that the field operator evolves like in the free theory: thus the plane wave expansion is still valid [37]. Corrections arising from the interaction are then treated perturbatively, as a power series in H_{INT} [39].

7.0.2 Interaction picture fields

According to the split of the Hamiltonian into H_0 and H_{INT}, the interaction picture fields are defined as [38]:

$$\phi^{I\prime} \equiv i\left[H_0[\phi^I(\tau),\pi^I(\tau);\tau],\phi^I\right] \quad\longrightarrow\quad \phi^I(\tau) = U_0^{-1}(\tau,\tau_0)\phi^I(\tau_0)U_0(\tau,\tau_0) \tag{7.8}$$

$$\pi^{I\prime} \equiv i\left[H_0[\phi^I(\tau),\pi^I(\tau);\tau],\pi^I\right] \quad\longrightarrow\quad \pi^I(\tau) = U_0^{-1}(\tau,\tau_0)\pi^I(\tau_0)U_0(\tau,\tau_0) \tag{7.9}$$

where $U_0(\tau,\tau_0)$ is the time evolution operator in the free theory, coming from the free Hamiltonan H_0:

$$\frac{\partial}{\partial\tau}U_0(\tau,\tau_0) = -iH_0(\tau)U_0(\tau,\tau_0) \qquad U_0(\tau_0,\tau_0) = \mathbb{1} \tag{7.10}$$

In order to fix ϕ^I completely, we also need to specify the initial conditions.

An operator in the Heisenberg picture evolves with the interaction Hamiltonian as [37, 38]:

$$\hat{O}(\tau) = \left(T - e^{i\int_{\tau_0}^{\tau}\hat{H}_{INT}(\tau')d\tau'}\right)^{-1}\hat{O}^I(\tau)\left(T - e^{i\int_{\tau_0}^{\tau}\hat{H}_{INT}(\tau')d\tau'}\right) \tag{7.11}$$

7.0.3 In-in master formula

The n-point correlation functions can be expressed perturbatively in terms of the free field ones.

It is necessary to compute expectation values *for the actual vacuum state*, the interacting vacuum state, not the free one $|0\rangle$ for which $a_{\vec{k}}|0\rangle = 0\ \forall\ \vec{k}$.
Let $|\Omega\rangle$ be the vacuum of the interacting theory. Using the interaction picture, if the vacuum coincides with the free vacuum at time τ_0 then:

$$\langle Q_n(\tau)\rangle = \langle\Omega(\tau)|Q^I_n(\tau)|\Omega(\tau)\rangle = \langle\Omega|U^{-1}(\tau,\tau_0)Q^I_n(\tau)U(\tau,\tau_0)|\Omega\rangle \tag{7.12}$$

where the time evolution operator $U(\tau, \tau_0)$ evolves the vacuum state from τ_0 up to τ. Again, notice that this does not correspond to a scattering amplitude because when we compute scattering amplitudes in particle physics the initial $t \to -\infty$ and final $t \to +\infty$ states are free states.
From the evolution of a generic state in the interaction picture, the vacuum will obey:

$$\partial_\tau |\Omega(\tau)\rangle = -i\hat{H}^I_{INT}(\tau)|\Omega(\tau)\rangle \qquad |\Omega(\tau)\rangle \equiv \hat{U}(\tau,\tau_0)|\Omega\rangle \tag{7.13}$$

$$\hat{U}(\tau,\tau_0) = T - \exp\left(-i\int_{\tau_0}^{\tau} \hat{H}^I_{INT}(\tau')d\tau'\right) \tag{7.14}$$

In order to connect the vacuum of the interacting theory $|\Omega\rangle$ to the vacuum of the free theory $|0\rangle$, let's expand $|0\rangle$ by inserting a complete state of energy eigenstates of the full theory [38, 39]:

$$|0\rangle = |\Omega\rangle\langle\Omega|0\rangle + \sum_n |n\rangle\langle n|0\rangle \tag{7.15}$$

$$e^{-iH(\tau-\tau_0)}|0\rangle = e^{-iE_\Omega(\tau-\tau_0)}|\Omega\rangle\langle\Omega|0\rangle + \sum_{n'} e^{-iE_{n'}(\tau-\tau_0)}|n'\rangle\langle n'|0\rangle \tag{7.16}$$

Now we require that in the far past the vacuum coincides with the one of the free theory. This is achieved via the $i\epsilon$ prescription:

$$\boxed{\tau_0 \longmapsto -\infty(1-i\epsilon)} \tag{7.17}$$

This projects out all the excited states and leaves us with the free vacuum only. As [38] points out, this implies some assumptions, that are difficult to explicitly verify. We need the interacting vacuum to have some projection onto the free vacuum $\langle\Omega|0\rangle \neq 0$, which is fine as long as H_{INT} is a small perturbation (see also the remarks in [27]). We are also assuming that, if $\langle\Omega|0\rangle$ grows with time, the growth near $\tau \to -\infty$ is slower than exponential, so that it does not overcome the suppression factor coming from the $i\epsilon$ trick.
We obtain:

$$e^{-iH(\tau-\tau_0)}|\Omega\rangle = \frac{e^{-iH(\tau-\tau_0)}|0\rangle}{\langle\Omega|0\rangle} \quad \longrightarrow \quad \hat{U}(\tau,\tau_0)|\Omega\rangle = \frac{\hat{U}(\tau,\tau_0)|0\rangle}{\langle\Omega|0\rangle} \tag{7.18}$$

where the $i\epsilon$ prescription is understood.
This prescription translates into a choice of contour for the time integration, as shown in Figure 7.2.

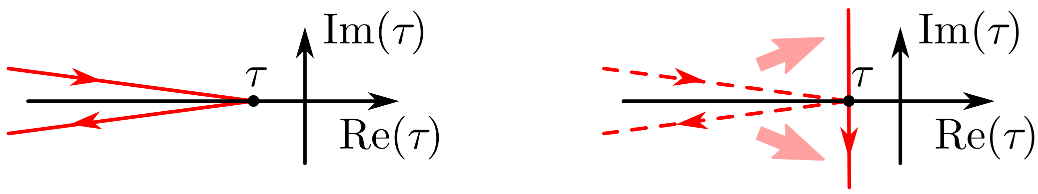

Figure 7.2: Contour of integration in the in-in formalism. In numerical calculations, the contour is often deformed to a vertical line, as in the right panel. From [38].

So our expectation value is:

$$\langle\hat{Q}_n(\tau)\rangle = \frac{\langle 0|\left(T - e^{\left(-i\int_{\tau_0}^{\tau}\hat{H}^I_{INT}(\tau')d\tau'\right)}\right)^{-1}\hat{Q}^I_n(\tau) T - e^{\left(-i\int_{\tau_0}^{\tau}\hat{H}^I_{INT}(\tau')d\tau'\right)}|0\rangle}{|\langle 0|\Omega\rangle|^2} \tag{7.19}$$

If we require both vacuum states to be normalized, the denominator is 1 (this can be seen by taking $\hat{Q}$ to be the identity matrix, [38]). Hence:

$$\boxed{\langle\hat{Q}_n(\tau)\rangle = \langle 0|\left(T - e^{\left(-i\int_{\tau_0}^{\tau}\hat{H}^I_{INT}(\tau')d\tau'\right)}\right)^{-1}\hat{Q}^I_n(\tau) T - e^{\left(-i\int_{\tau_0}^{\tau}\hat{H}^I_{INT}(\tau')d\tau'\right)}|0\rangle} \tag{7.20}$$

This is our master formula. A few variants exist, for example the *commutator form*:

$$\langle\Omega|\hat{Q}(\tau)|\Omega\rangle = \sum_{n=0}^{\infty} i^n \int_{\tau_0}^{\tau} d\tau_1 \int_{\tau_0}^{\tau_1} d\tau_2 \cdots \int_{\tau_0}^{\tau_{n-1}} d\tau_n \\ \langle \Big[\hat{H}_{INT}(\tau_n), \Big[\hat{H}_{INT}(\tau_{n-1}), \dots \Big[\hat{H}_{INT}(\tau_1), \hat{Q}^I(\tau)\Big] \dots\Big]\Big]\rangle \tag{7.21}$$

To first order in the interaction Hamiltonian, we can expand:

$$\hat{U}(\tau,\tau_0) = \mathbb{1} - i\int_{\tau_0}^{\tau} \hat{H}^I_{INT}(\tau')d\tau' \tag{7.22}$$

and substituting back in the expectation value:

$$\boxed{\langle Q_n(\tau)\rangle = -i\int_{\tau_0}^{\tau} d\tau' \langle 0| \left[Q_n^I(\tau), H^I_{INT}(\tau')\right]|0\rangle} \tag{7.23}$$

The general recipe for dealing with this computation in the in-in formalism is [9]:

- perturb the Lagrangian around the homogeneous solutions of the classical e.o.m.;
- write down the Lagrangian and/or the Hamiltonian for the perturbations;
- split the Hamiltonian into a quadratic kinematic part H_0, describing free fields in the time-dependent background, and and interaction part H_{INT};
- quantize the fluctuation fields in terms of the annihilation and creation operators;
- the mode functions $u_{\vec{k}}(\tau)$ are solutions of the e.o.m., properly normalized, and specified by an initial condition such as the Bunch-Davies vacuum;
- the correlation function is given by (7.20);
- series-expand the integrand in powers of H_{INT} to the desired order;
- perform contractions for each term in the expansion: each term gives a non-zero contribution only when all fields are contracted;
- sum over all possible contractions and perform the time-ordered integrations.

Chapter 8

Going to second order in the action

In order to compute the bispectrum, we need to perturb the action up to third order. The calculation is very long, we will only sketch the main steps. See the original work by Maldacena [27] and a detailed review of his computation in [40] and in [38].

8.1 The ADM formalism

A convenient framework to perform the computation is the Arnowitt, Desner and Misner (ADM) decomposition of the metric. The advantage of this choice is that, in the perturbed action, some variables will not be dynamical, i.e. their e.o.m. will be purely algebraic and they will act as constraints, thus reducing the difficulty of the problem. Furthermore, within this formalism the Einstein equations assume manifestly the form of a time-evolution equation.

We start by splitting the spacetime $\mathcal{M}$ into a spatial part and time, or $(3+1)$-splitting. This can be done for any spacetime that is globally hyperbolic, that is it admits a spacelike surface Σ called Cauchy surface such that every timelike or null curve without endpoints intersects Σ once and only once. Practically, this condition is almost always satisfied in the cases of interest in cosmology. In this case, we can foliate $\mathcal{M}$ into a family of spacelike hypersurfaces $\{\Sigma_t\}$ at constant $t \in \mathbb{R}$. Hence we can write the manifold $\mathcal{M}$ as product $\mathbb{R} \times \Sigma$. The "time flow" vector field will have a component that is normal to the surfaces Σ_t and a component that is tangential to them [41].
We write the metric as:

$$ds^2 = -N^2 dt^2 + h_{ij}(dx^i + N^i dt)(dx^j + N^j dt) \tag{8.1}$$

$$g_{\mu\nu} = \begin{pmatrix} -N^2 + N^k N_k & N_j \\ N_i & h_{ij} \end{pmatrix} \qquad g^{\mu\nu} = \begin{pmatrix} -\frac{1}{N^2} & \frac{N^j}{N^2} \\ \frac{N^i}{N^2} & h^{ij} - \frac{N^i N^j}{N^2} \end{pmatrix} \tag{8.2}$$

The quantity $N(t, \vec{x})$ is the *lapse function* which measures the rate of flow of proper time with respect to coordinate time t, as one moves normally to Σ_t. The quantity $N^i(t, \vec{x})$ is the *shift vector* which measures the amount of "shift" tangential to Σ_t contained in the time flow vector field. See Figure 8.1. The effect of "moving forward in time" can be seen as that of changing the spatial metric on some abstract three-dimensional manifold Σ: the globally hyperbolic spacetime $(\mathcal{M}, g_{\mu\nu})$ can be seen as time development of a Riemannian metric on a fixed three-dimensional manifold [41].

8.2 Perturbed action

8.2.1 Second order

The action for gravity and a scalar field is:

$$S = \int d^4x \sqrt{-g} \left(\frac{1}{16\pi G} R - \frac{1}{2} g^{\mu\nu} \partial_\mu \varphi \partial_\nu \varphi - V(\varphi) \right) \tag{8.3}$$

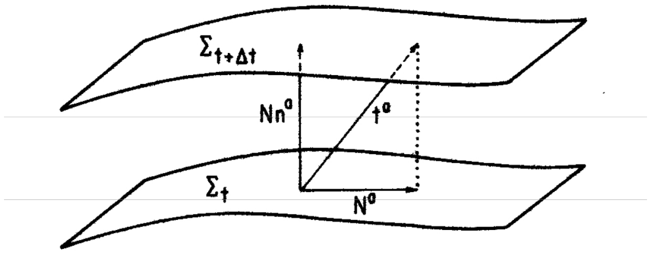

Figure 8.1: Illustration of the lapse function and the shift vector. From [41].

When substituting the metric (8.1) into the action (8.3), h_{ij} and φ are the dynamical variables while N and N^i are Lagrange multipliers. The e.o.m. for N and N^i are the hamiltonian and momentum contstraints. A gauge choice for h_{ij} and φ is necessary in order to fix time and space reparametrization. Maldacena in [27] sets, to second order:

$$\delta\varphi = 0 \qquad h_{ij} = a^2 e^{2\zeta}\left(\delta_{ij} + \gamma_{ij} + \frac{1}{2}\gamma_{il}\gamma_{lj}\right) \qquad \text{with } \partial^i\gamma_{ij} = 0,\ \gamma^i_i = 0 \tag{8.4}$$

so that ζ and γ are the physical degrees of freedom, which oarametrize the scalar and tensor fluctuations respectively.
The lapse function and shift vector are perturbed as:

$$N(t,\vec{x}) = 1 + \alpha(t,\vec{x}) \qquad N_i(t,\vec{x}) = \partial_i\beta(t,\vec{x}) \tag{8.5}$$

In computing both second and third order action, it is only necessary to know N and N^i to first order. Their second-order and third-order perturbations would be multiplying the first-order and zeroth-order constraints respectively.

In the following, we will use the definitions of the slow-roll parameters as given in (2.17):

$$\epsilon = \frac{1}{2M_P^2}\frac{\dot{\varphi}^2}{H^2} \qquad \eta = -\frac{\ddot{\varphi}}{\dot{\varphi}H} \tag{8.6}$$

but we will not make the slow-roll approximation, we will just use them to keep the notation lighter and compare the results with the approximated case. In the end, if needed, we can always rewrite explicitly the coefficients.

Introducing the curvature perturbation (4.33), the action to second order is:

$$S_2 = M_P^2 \int dt d^3\vec{x} \frac{1}{2}\frac{\dot{\varphi}^2}{H^2}\left(a^3\dot{\zeta}^2 - a\partial_i\zeta\partial^i\zeta\right) \tag{8.7}$$

In terms of the Mukhanov-Sasaki variable $v = -z\zeta$:

$$S_2 = M_P^2 \int d\tau d^3\vec{x} \frac{1}{2}\left((v')^2 + \partial_i v\partial^i v + \frac{z''}{z}v^2\right) \tag{8.8}$$

leading to an e.o.m. that resembles a harmonic oscillator, with a time-dependent frequency term:

$$v_k'' + \left(k^2 - \frac{z''}{z}\right)v_k = 0 \tag{8.9}$$

8.2.2 Third order

When going to third order, a lot of integration by parts is necessary (see [40]). In the gauge (8.4):

$$\begin{aligned} S_3 =& M_P^2 \int dt d^3\vec{x} \Big\{ \frac{1}{4}\left(\frac{\dot\varphi^2}{H^2}\right)^2 \left(a^3\dot\zeta^2\zeta + a\partial_i\zeta\partial^i\zeta\zeta\right) - \frac{\dot\varphi^2}{H^2}a^3\dot\zeta\partial_i\chi\partial^i\zeta + \\ & -\frac{1}{16}\left(\frac{\dot\varphi^2}{H^2}\right)^3 a^3\dot\zeta^2\zeta + \frac{\dot\varphi^2}{H^2}a^3\dot\zeta\zeta^2\frac{d}{dt}\left(\frac{1}{2}\frac{\ddot\varphi}{\dot\varphi H}+\frac{1}{4}\frac{\dot\varphi^2}{H^2}\right) + \\ & + \frac{1}{4}\frac{\dot\varphi^2}{H^2}a^3\partial_i\partial_j\chi\partial^i\partial^j\chi\zeta + f(\zeta)\left.\frac{\delta L}{\delta\zeta}\right|_1 + \\ & + \mathcal{L}_b \Big\} \end{aligned} \tag{8.10}$$

where:

$$\nabla^2\chi = \frac{1}{2}\frac{\dot\varphi^2}{H^2}\dot\zeta \tag{8.11}$$

$$\frac{\delta L}{\delta\zeta} = -\frac{d}{dt}\left(\frac{\dot\varphi^2}{H^2}a^3\dot\zeta\right) + \frac{\dot\varphi^2}{H^2}a\nabla^2\zeta \tag{8.12}$$

$$\begin{aligned} -f(\zeta) =& \left(\frac{1}{2}\frac{\ddot\varphi}{\dot\varphi H}+\frac{1}{4}\frac{\dot\varphi^2}{H^2}\right)\zeta^2 + \frac{1}{H}\dot\zeta\zeta - \frac{1}{4}\frac{1}{H^2a^2}\partial_i\zeta\partial^i\zeta + \frac{1}{2H}\partial_i\chi\partial^i\zeta + \\ & + \frac{1}{4}\frac{1}{H^2a^2}\Delta^{-1}\partial_i\partial_j\left(\partial^i\zeta\partial^j\zeta\right) - \frac{1}{2H}\Delta^{-1}\partial_i\partial_j\left(\partial^i\chi\partial^j\zeta\right) \end{aligned} \tag{8.13}$$

The first line in (8.10) is of order ϵ^2 and would give the leading contribution in the slow-roll parameters. Notice that the main contribution comes from the gravitational interaction, not from V''' which is subleading in the slow-roll parameters [27].

The last line in (8.10) contains boundary terms, arising from the integration by parts, and it is given explicitly in [42]. It is of the form:

$$\mathcal{L}_b = \partial_t(\dots) + \partial_i(\dots) \tag{8.14}$$

As pointed out in [38, 42, 43] the total spatial derivative do not contribute. To see this, one can think that there is no "spatial boundary" in our inflationary Universe [38], or alternatively that the interaction Hamiltonian of these terms would be proportional to the total momentum $\vec{k}_1+\vec{k}_2+\vec{k}_3$ which vanishes thanks to the Dirac delta imposing momentum conservation [42].
However, the total time derivative terms can not, in general, be neglected. For the in-in formalism we do have a "time boundary" [38], typically chosen at a time such that ζ becomes conserved after that. Since we will be interested in the superhorizon regime, the contribution from the boundary terms will be just:

$$\mathcal{L}_b \simeq \frac{d}{dt}\left(-\left(\frac{\ddot\varphi}{\dot\varphi H}+\frac{1}{2}\frac{\dot\varphi^2}{H^2}\right)a^3\zeta^2\nabla^2\chi\right) = \frac{d}{dt}\left(\epsilon(\eta-2\epsilon)a^3\dot\zeta\zeta^2\right) \tag{8.15}$$

Furthermore, in the superhorizon regime we can neglect those terms in (8.13) which contain at least one derivative of ζ, since they should be vanishing. We can approximate:

$$f(\zeta) \simeq -\left(\frac{1}{2}\frac{\ddot\varphi}{\dot\varphi H}+\frac{1}{4}\frac{\dot\varphi^2}{H^2}\right)\zeta^2 = -\frac{\epsilon-\eta}{2}\zeta^2 \tag{8.16}$$

The last term in the action (8.10) is proportional to the first order equations of motion. We are doing perturbation theory, hence we are allowed to use the linear equations of motion in the third or higher order actions and simplify out that term [38]. However, if we do this, we must keep in mind the contribution from the boundary terms (8.14). This is well explained in [42]. The boundary terms are

necessary to erase from the action the terms with second order time derivative on ζ contained in the second to last term in (8.10). Without these boundary terms, the second order time derivative terms remain in the action. The reason why we have such problematic interactions is that these terms are generated by the integration by parts, and therefore the inclusion of the boundary terms naturally takes care of them.
Another way to take care of the term proportional to the e.o.m. is removing it by performing a field redefinition:

$$\boxed{\zeta = \zeta_n - f(\zeta_n)} \tag{8.17}$$

As pointed out in [27], it does not matter whether we write ζ or ζ_n in $f(\zeta)$ since it is quadratic in the field[1].
If we perform this redefinition, the $\ddot{\zeta}$ terms would be eliminated without using the equations of motion, in the following manner. The cubic terms in the action S_3 are not affected by the field redefinition, since we would only get quartic corrections. Only the second-order terms S_2 change, and the extra terms we get cancel exactly the last term in (8.10).

$$\begin{aligned}
S_2 &= \int dt d^3\vec{x} \left(\epsilon a^3 \dot{\zeta}^2 - \epsilon a \partial_i \zeta \partial^i \zeta \right) \longmapsto \\
&= \int dt d^3\vec{x} \left(\epsilon a^3 \left(\dot{\zeta}_n - \dot{f}(\zeta_n) \right)^2 - \epsilon a \partial_i \left(\zeta_n - f(\zeta_n) \right) \partial^i \left(\zeta_n - f(\zeta_n) \right) \right) \\
&= \int dt d^3\vec{x} \left(\epsilon a^3 \dot{\zeta}_n^2 - 2\epsilon a^3 \dot{\zeta}_n \dot{f}(\zeta_n) - \epsilon a \partial_i \zeta_n \partial^i \zeta_n + 2\epsilon a \partial_i \zeta_n \partial^i f(\zeta_n) + \mathcal{O}(\zeta_n^4) \right) \\
&= S_2[\zeta_n] + \int dt d^3\vec{x} \left\{ \frac{d}{dt} \left(-2\epsilon a^3 \dot{\zeta}_n f(\zeta_n) \right) + f(\zeta_n) \frac{d}{dt} \left(2\epsilon a^3 \dot{\zeta}_n \right) - 2\epsilon a f(\zeta_n) \nabla^2 \zeta_n \right\} \\
&= S_2[\zeta_n] + \int dt d^3\vec{x} \left\{ \frac{d}{dt} \left(-2\epsilon a^3 \dot{\zeta}_n f(\zeta_n) \right) - f(\zeta_n) \frac{\delta L}{\delta \zeta_n} \right\}
\end{aligned} \tag{8.18}$$

Where again, when integrating by parts, the total spatial derivative term can be dropped. The last term cancels exactly the term proportional to the lienar e.o.m. in (8.10). Moreover, if we approximate $f(\zeta)$ as in (8.16), then the boundary term we get from S_2 will cancel (8.15).

After we remove all terms proportional to the equations of motion, for the cubic terms $H_{INT} = -L_{INT}$ [27]. This statement holds, as long as there are no time-derivative couplings in the interaction terms.

However, the three-point function is changed by the field redefinition. The crucial point here is that $f(\zeta)$ contains time derivatives. As a consequence, ζ_n is not constant outside the horizon, unlike ζ: this comes from the fact that ζ stays constant on superhorizon scales and (8.13) contains coefficients of the quadratic terms which are time-dependent [27]. Furthermore, the redefinition changes the ground state of perturbations [44].
Schematically, if we have a field redefinition of the form $\zeta = \zeta_c + \lambda \zeta_c^2$ then the three-point correlation function changes as:

$$\begin{aligned}
\langle \zeta(x_1)\zeta(x_2)\zeta(x_3) \rangle =& \langle \zeta_c(x_1)\zeta_c(x_2)\zeta_c(x_3) \rangle \\
&+ 2\lambda \Big[\langle \zeta(x_1)\zeta(x_2) \rangle \langle \zeta(x_1)\zeta(x_3) \rangle + \text{cyclic} \Big]
\end{aligned} \tag{8.19}$$

Different field redefinitions can reshuffle the contributions between the two terms.
If we work in the superhorizon regime:

$$\zeta \simeq \zeta_n + \frac{\epsilon - \eta}{2} \zeta_n^2 \tag{8.20}$$

[1]Some care is needed with the conventions used in the literature for the sign of $f(\zeta_n)$. We are following [27], but for example [42] defines the term proportional to the e.o.m. with the opposite sign, and as a consequence also the field redefinition has the opposite sign.

hence:

$$\begin{aligned}\langle\zeta(x_1)\zeta(x_2)\zeta(x_3)\rangle =&\langle\zeta_n(x_1)\zeta_n(x_2)\zeta_n(x_3)\rangle \\ &+ 2(\epsilon-\eta)\Big[\langle\zeta(x_1)\zeta(x_2)\rangle\langle\zeta(x_1)\zeta(x_3)\rangle + \text{cyclic}\Big]\end{aligned} \tag{8.21}$$

So I now have two choices. I can either keep the whole action (8.10) and explicitly compute by hand the interaction Hamiltonian, but keep track of the boundary terms (8.15); or I can follow the field redefinition approach, this way I don't have to worry about boundaries, but I will have to correct the three-point function as in (8.21).

Chapter 9

The bispectrum: in-in formalism approach

After performing the redefinition (8.17) and switching to conformal time, the action for the field ζ_n is:

$$\begin{aligned}\mathcal{S}_3[\zeta_n] = M_P^2 \int d\tau d^3\vec{x}\Big\{&\epsilon^2 a^2 \zeta_n'^2 \zeta_n + \epsilon^2 a^2 \partial_i \zeta_n \partial^i \zeta_n \zeta_n - 2\epsilon^2 a^2 \zeta_n' \partial_i \Delta^{-1} \zeta_n' \partial^i \zeta_n + \\ &- \frac{1}{2}\epsilon^3 a^2 \zeta_n'^2 \zeta_n + \epsilon a^2 \zeta_n' \zeta_n^2 \frac{d}{d\tau}(\epsilon - \eta) + \\ &+ \frac{1}{2}\epsilon^3 a^2 \partial_i \partial_j \Delta^{-1} \zeta_n' \partial^i \partial^j \Delta^{-1} \zeta_n' \zeta_n \Big\}\end{aligned} \tag{9.1}$$

The correction to the three-point function when we go to Fourier space looks as follows. The redefinition is of the form:

$$\zeta = \zeta_n + \lambda \zeta_n^2 \longrightarrow \zeta_{\vec{k}} = \zeta_{n,\vec{k}} + \lambda \int \frac{d^3\vec{p}_1 d^3\vec{p}_2}{(2\pi)^{3/2}} \delta^{(3)}(\vec{p}_1 + \vec{p}_2 - \vec{k}) \zeta_{n,\vec{p}_1} \zeta_{n,\vec{p}_2} \tag{9.2}$$

Hence (8.21) becomes:

$$\begin{aligned}\langle \zeta_{\vec{k}_1} \zeta_{\vec{k}_2} \zeta_{\vec{k}_3} \rangle =& \langle \zeta_{n,\vec{k}_1} \zeta_{n,\vec{k}_2} \zeta_{n,\vec{k}_3} \rangle + \\ &+ \lambda \int \frac{d^3\vec{p}_1 d^3\vec{p}_2}{(2\pi)^{3/2}} \delta^{(3)}(\vec{p}_1 + \vec{p}_2 - \vec{k}_1) \langle \zeta_{n,\vec{p}_1} \zeta_{n,\vec{p}_2} \zeta_{n,\vec{k}_2} \zeta_{n,\vec{k}_3} \rangle + \text{sym.} \\ =& \langle \zeta_{n,\vec{k}_1} \zeta_{n,\vec{k}_2} \zeta_{n,\vec{k}_3} \rangle + 2\lambda \frac{1}{(2\pi)^{3/2}} \delta^{(3)}(\vec{k}_1 + \vec{k}_2 + \vec{k}_3) P_\zeta(k_2) P_\zeta(k_3) + \text{sym.}\end{aligned} \tag{9.3}$$

In our particular case, due to the relation between ϵ and η in power-law inflation, $\lambda = 0$. The correction vanishes identically.

Applying our in-in master formula (7.23), we have:

$$\begin{aligned}\langle \zeta_{n,\vec{k}_1}(\tau) \zeta_{n,\vec{k}_2}(\tau) \zeta_{n,\vec{k}_3}(\tau) \rangle &= -i \int_{\tau_0}^{\tau} d\tau' \langle 0 | \left[\zeta_{n,\vec{k}_1}(\tau) \zeta_{n,\vec{k}_2}(\tau) \zeta_{n,\vec{k}_3}(\tau), H_{INT}^I(\tau') \right] | 0 \rangle \\ &= 2\text{Im} \int_{\tau_0}^{\tau} d\tau' \langle 0 | \zeta_{n,\vec{k}_1}(\tau) \zeta_{n,\vec{k}_2}(\tau) \zeta_{n,\vec{k}_3}(\tau) H_{INT}^I(\tau') | 0 \rangle\end{aligned} \tag{9.4}$$

where $H_{INT} = -L_{INT}$ and the interaction Lagrangian for the redefined field can be read from the action (9.1).

9.1 Interaction Hamiltonian in Fourier space

Schematically:

$$\begin{aligned}
H_{INT,3} &= \int d^3\vec{x}\mathcal{H}_3 \\
&\sim \int d^3\vec{x} \int \frac{d^3\vec{p}_1 d^3\vec{p}_2 d^3\vec{p}_3}{(2\pi)^{9/2}} f(\tau)\zeta_{n,\vec{p}_1}\zeta_{n,\vec{p}_2}\zeta_{n,\vec{p}_3} e^{i(\vec{p}_1+\vec{p}_2+\vec{p}_3)\cdot\vec{x}} \\
&= \int \frac{d^3\vec{p}_1 d^3\vec{p}_2 d^3\vec{p}_3}{(2\pi)^{9/2}} (2\pi)^3 \delta^{(3)}(\vec{p}_1+\vec{p}_2+\vec{p}_3) f(\tau)\zeta_{n,\vec{p}_1}\zeta_{n,\vec{p}_2}\zeta_{n,\vec{p}_3}
\end{aligned} \tag{9.5}$$

Symmetrizing in the three momenta:

$$\begin{aligned}
H_{INT} = &\int \frac{d^3\vec{p}_1 d^3\vec{p}_2 d^3\vec{p}_3}{(2\pi)^{3/2}} \delta^{(3)}(\vec{p}_1+\vec{p}_2+\vec{p}_3)\cdot \\
&\Bigg\{\frac{1}{3}\epsilon^2 a^2 \left(\vec{p}_1\cdot\vec{p}_2+\vec{p}_1\cdot\vec{p}_3+\vec{p}_2\cdot\vec{p}_3\right)\zeta_{n,\vec{p}_1}\zeta_{n,\vec{p}_2}\zeta_{n,\vec{p}_3} + \\
&-\frac{1}{3}\epsilon a^2 \left(\epsilon-\eta\right)' \zeta'_{n,\vec{p}_1}\zeta_{n,\vec{p}_2}\zeta_{n,\vec{p}_3} + \\
&-\frac{1}{3}\epsilon a^2 \left(\epsilon-\eta\right)' \zeta_{n,\vec{p}_1}\zeta'_{n,\vec{p}_2}\zeta_{n,\vec{p}_3} + \\
&-\frac{1}{3}\epsilon a^2 \left(\epsilon-\eta\right)' \zeta_{n,\vec{p}_1}\zeta_{n,\vec{p}_2}\zeta'_{n,\vec{p}_3} + \\
&-\frac{1}{6}\epsilon^2 a^2 \frac{2p_1^2p_2^2-2p_1^2\vec{p}_2\cdot\vec{p}_3-2p_2^2\vec{p}_1\cdot\vec{p}_3+\epsilon\left(-p_1^2p_2^2+(\vec{p}_1\cdot\vec{p}_2)^2\right)}{p_1^2p_2^2}\zeta'_{n,\vec{p}_1}\zeta'_{n,\vec{p}_2}\zeta_{n,\vec{p}_3} + \\
&-\frac{1}{6}\epsilon^2 a^2 \frac{2p_1^2p_3^2-2p_1^2\vec{p}_2\cdot\vec{p}_3-2p_3^2\vec{p}_1\cdot\vec{p}_2+\epsilon\left(-p_1^2p_3^2+(\vec{p}_1\cdot\vec{p}_3)^2\right)}{p_1^2p_3^2}\zeta'_{n,\vec{p}_1}\zeta_{n,\vec{p}_2}\zeta'_{n,\vec{p}_3} + \\
&-\frac{1}{6}\epsilon^2 a^2 \frac{2p_2^2p_3^2-2p_2^2\vec{p}_1\cdot\vec{p}_3-2p_3^2\vec{p}_1\cdot\vec{p}_2+\epsilon\left(-p_2^2p_3^2+(\vec{p}_2\cdot\vec{p}_3)^2\right)}{p_2^2p_3^2}\zeta_{n,\vec{p}_1}\zeta'_{n,\vec{p}_2}\zeta'_{n,\vec{p}_3}\Bigg\}
\end{aligned} \tag{9.6}$$

Notice that in general both the scale factor and ϵ depend on time. But for Lucchin-Matarrese power-law inflation $\epsilon = 1/p$ so we can factor it out, moreover $\eta = \epsilon$ so the terms with one time derivative only cancel out.

9.2 Calculation

Substituting the interaction Hamiltonian (9.6) in (9.4) we obtain:

$$\begin{aligned}
2M_P^2\epsilon^2 \mathrm{Im} &\int d\tau' \int \frac{d^3\vec{p}_1 d^3\vec{p}_2 d^3\vec{p}_3}{(2\pi)^{3/2}} \delta^{(3)}(\vec{p}_1+\vec{p}_2+\vec{p}_3)\cdot \\
&\Bigg\{\frac{a^2(\tau')}{3} h_{000}(\vec{p}_1,\vec{p}_2,\vec{p}_3)\langle\zeta_{n,\vec{k}_1}(\tau)\zeta_{n,\vec{k}_2}(\tau)\zeta_{n,\vec{k}_3}(\tau)\zeta_{n,\vec{p}_1}(\tau')\zeta_{n,\vec{p}_2}(\tau')\zeta_{n,\vec{p}_3}(\tau')\rangle + \\
&-\frac{a^2(\tau')}{6} h_{110}(\vec{p}_1,\vec{p}_2,\vec{p}_3)\langle\zeta_{n,\vec{k}_1}(\tau)\zeta_{n,\vec{k}_2}(\tau)\zeta_{n,\vec{k}_3}(\tau)\zeta'_{n,\vec{p}_1}(\tau')\zeta'_{n,\vec{p}_2}(\tau')\zeta_{n,\vec{p}_3}(\tau')\rangle + \\
&+ \text{two derivative terms } \vec{k}_2 \longleftrightarrow \vec{k}_3 \text{ and } \vec{k}_1 \longleftrightarrow \vec{k}_3\Bigg\}
\end{aligned} \tag{9.7}$$

Using Wick's theorem and keeping only connected terms:

$$\frac{1}{(2\pi)^{3/2}}\delta^{(3)}(\vec{k}_1+\vec{k}_2+\vec{k}_3)2M_P^2\epsilon^2\mathrm{Im}\Bigg\{\theta_{k_1}(\tau)\theta_{k_2}(\tau)\theta_{k_3}(\tau)\cdot$$
$$\Bigg(\int d\tau'\theta^*_{k_1}(\tau')\theta^*_{k_2}(\tau')\theta^*_{k_3}(\tau')a^2(\tau')\left(-k_1^2-k_2^2-k_3^2\right)+$$
$$\int d\tau'\theta^{*\prime}_{k_1}(\tau')\theta^{*\prime}_{k_2}(\tau')\theta^*_{k_3}(\tau')a^2(\tau')\left(-\frac{1}{4k_1^2k_2^2}\right)\left(-4(k_1^4+k_2^4-4k_1^2k_2^2-k_1^2k_3^2-k_2^2k_3^2)+\right.$$
$$\left.+\,\epsilon(k_1^4+k_2^4+k_3^4-2k_1^2k_2^2-2k_1^2k_3^2-2k_2^2k_3^2)\right)+$$
$$+\text{ two derivative terms }\vec{k}_2\longleftrightarrow\vec{k}_3\text{ and }\vec{k}_1\longleftrightarrow\vec{k}_3\Bigg)\Bigg\} \tag{9.8}$$

Using the modefunctions (6.30) we find integrals of three Hankel functions times some power of conformal time.

$$\frac{1}{(2\pi)^{3/2}}\delta^{(3)}(\vec{k}_1+\vec{k}_2+\vec{k}_3)2M_P^2\epsilon^2A^2\left(cc^*\right)^3\mathrm{Im}\Bigg\{(-\tau)^{3\nu}H_\nu^{(1)}(-k_1\tau)H_\nu^{(1)}(-k_2\tau)H_\nu^{(1)}(-k_3\tau)\cdot$$
$$\Bigg(\int_{-\infty(1-i\epsilon)}^{\tau}d\tau'(-\tau')^{1+\nu}H_\nu^{(2)}(-k_1\tau')H_\nu^{(2)}(-k_2\tau')H_\nu^{(2)}(-k_3\tau')\left(-k_1^2-k_2^2-k_3^2\right)+$$
$$\int_{-\infty(1-i\epsilon)}^{\tau}d\tau'(-\tau')^{1+\nu}H_{\nu-1}^{(2)}(-k_1\tau')H_{\nu-1}^{(2)}(-k_2\tau')H_\nu^{(2)}(-k_3\tau')\cdot$$
$$\left(-\frac{1}{4k_1k_2}\right)\left(-4(k_1^4+k_2^4-4k_1^2k_2^2-k_1^2k_3^2-k_2^2k_3^2)\epsilon(k_1^4+k_2^4+k_3^4-2k_1^2k_2^2-2k_1^2k_3^2-2k_2^2k_3^2)\right)+$$
$$+\text{ two derivative terms }\vec{k}_2\longleftrightarrow\vec{k}_3\text{ and }\vec{k}_1\longleftrightarrow\vec{k}_3\Bigg)\Bigg\} \tag{9.9}$$

The problem we have to face now is computing the integral of three Hankel functions times some power. First of all, to get a better understanding of what is going on, we will review the computation in the standard slow-roll case, as in [27]: in this regime, the Hankel functions are assumed to be the de Sitter ones, with $\nu=\frac{3}{2}$, and we can take advantage of the explicit expression (A.7).

9.2.1 Standard slow-roll case $\nu=\frac{3}{2}$

The modefunctions for ζ are:

$$\theta_{k,\mathrm{DS}}(\tau)=c\sqrt{\frac{2}{\pi}}\frac{1}{k^{3/2}}(-i+k\tau)e^{-ik\tau} \tag{9.10}$$

The scale factor is $a(\tau)=-A/\tau$ where $A\xrightarrow{\epsilon\to0}H_{\mathrm{DS}}^{-1}$.

We will need the following integrals, see (A.8) in the Appendix:

$$\int d\tau\frac{e^{ik_T\tau}}{\tau}=-E_1(ik_T\tau) \tag{9.11}$$
$$\int d\tau\frac{e^{ik_T\tau}}{\tau^2}=-\frac{e^{ik_T\tau}}{\tau}-ik_TE_1(ik_T\tau) \tag{9.12}$$
$$\int d\tau\tau e^{ik_T\tau}=\frac{1}{k_T^2}(1-ik_T\tau)e^{ik_T\tau} \tag{9.13}$$

The term without any time derivative in (9.8):

$$\int_{-\infty(1-i\epsilon)}^{\tau} \theta^*_{k_1}(\tau')\theta^*_{k_2}(\tau')\theta^*_{k_3}(\tau')a^2(\tau')d\tau' =$$
$$= \frac{2\sqrt{2}A^2(c^*)^3}{\pi^{3/2}(k_1k_2k_3)^{3/2}} \int_{-\infty(1-i\epsilon)}^{\tau} \left[i(k_1k_2+k_1k_3+k_2k_3) + k_1k_2k_3\tau' - \frac{k_T}{\tau'} - \frac{i}{\tau'^2} \right] e^{ik_T\tau'} d\tau'$$
$$= \frac{2\sqrt{2}A^2(c^*)^3}{\pi^{3/2}(k_1k_2k_3)^{3/2}} \left(\frac{k_1k_2+k_1k_3+k_2k_3}{k_T} + \frac{k_1k_2k_3}{k_T^2} - i\frac{k_1k_2k_3}{k_T}\tau + \frac{i}{\tau} \right) e^{ik_T\tau} \tag{9.14}$$

The term with two time derivatives:

$$\int_{-\infty(1-i\epsilon)}^{\tau} \theta^{*\prime}_{k_1}(\tau')\theta^{*\prime}_{k_2}(\tau')\theta^*_{k_3}(\tau')a^2(\tau')d\tau' =$$
$$= \frac{2\sqrt{2}A^2(c^*)^3}{\pi^{3/2}(k_1k_2k_3)^{3/2}}(-k_1^2k_2^2) \int_{-\infty(1-i\epsilon)}^{\tau} (i + k_3\tau)\, e^{ik_T\tau'} d\tau'$$
$$= \frac{2\sqrt{2}A^2(c^*)^3}{\pi^{3/2}(k_1k_2k_3)^{3/2}}(-k_1^2k_2^2) \left[\frac{1}{k_T} + \frac{k_3}{k_T^2}(1 - ik_T\tau) \right] e^{ik_T\tau} \tag{9.15}$$

and analogously for the other two permutations.

Approximating the three modefunctions outside the integral with the asymptotic expression for the Hankel functions (A.6):

$$\theta_{k_1}(\tau)\theta_{k_2}(\tau)\theta_{k_3}(\tau) \simeq \frac{i8^{\frac{1}{2}+\frac{1}{1-\epsilon}} \left(\Gamma\left(\frac{1}{2} + \frac{1}{1-\epsilon} \right) \right)^3 (k_1k_2k_3)^{-\left(\frac{1}{2}+\frac{1}{1-\epsilon}\right)} c^3}{\pi^3} \tag{9.16}$$

Taking the imaginary part and then the limit for $\tau \to 0$, we find:

$$\frac{1}{(2\pi)^{3/2}}\delta^{(3)}(\vec{k}_1+\vec{k}_2+\vec{k}_3)\frac{V_0^2}{M_P^8} \frac{2^{-10+\frac{3}{1-\epsilon}} e^{\frac{2C}{M_P}\sqrt{2\epsilon}}}{\pi^{3/2}k_T^2(k_1k_2k_3)^{2+\frac{1}{1-\epsilon}}} \frac{(1-\epsilon)(1+\epsilon)^3 \left(\Gamma\left(\frac{1+\epsilon}{2(1-\epsilon)} \right) \right)^3}{(\epsilon-3)^2\epsilon}\cdot$$
$$\Big[-4(k_1+k_2+k_3)\left(k_1^4+k_2^4+k_3^4 - 2k_1^2k_2k_3 - 2k_1k_2^2k_3 - 2k_1k_2k_3^2 - 10k_1^2k_2^2 - 10k_1^2k_3^2 - 10k_2^2k_3^2 \right) +$$
$$- 4(-k_1+k_2+k_3)(k_1+k_2-k_3)(k_1-k_2+k_3)(k_1+k_2+k_3)^3\epsilon \Big] \tag{9.17}$$

Taking the limit $\epsilon \to 0$:

$$\frac{1}{(2\pi)^{3/2}}\delta^{(3)}(\vec{k}_1+\vec{k}_2+\vec{k}_3)\frac{H_{\rm DS}^4}{32M_P^4\epsilon} \frac{1}{k_1^3k_2^3k_3^3(k_1+k_2+k_3)}\cdot$$
$$\left(-k_1^4 - k_2^4 - k_3^4 + 2k_1^2k_2k_3 + 2k_1k_2^2k_3 + 2k_1k_2k_3^2 + 10k_1^2k_2^2 + 10k_1^2k_3^2 + 10k_2^2k_3^2 \right) \tag{9.18}$$

Using the definition of $f_{\rm NL}$ (5.14) with (9.17) we obtain:

$$f_{\rm NL} = \frac{5}{3} \frac{2^{-1-\frac{1}{1-\epsilon}}\sqrt{\pi}(k_1k_2k_3)^{\frac{\epsilon}{1-\epsilon}}(-1+\epsilon)\epsilon}{(k_1+k_2+k_3)(k_1^{\frac{3-\epsilon}{1-\epsilon}} + k_2^{\frac{3-\epsilon}{1-\epsilon}} + k_3^{\frac{3-\epsilon}{1-\epsilon}})(1+\epsilon)\Gamma\left(\frac{1+\epsilon}{2(1-\epsilon)} \right)}\cdot$$
$$\Big(2k_1^2k_2k_3 + 2k_1k_2^2k_3 + 2k_1k_2k_3^2 + 2k_1^2k_2^2(5-\epsilon) + 2k_1^2k_3^2(5-\epsilon) + 2k_2^2k_3^2(5-\epsilon) +$$
$$- k_1^4(1-\epsilon) - k_2^4(1-\epsilon) - k_3^4(1-\epsilon) \Big) \tag{9.19}$$

This indeed behaves as we expect to lowest order in the slow-roll limit, see (5.19).

Now we turn to the case where the index ν inside the modefunctions in the integrals is generic. This $\nu = \frac{3}{2}$ case will serve as a playground to validate procedures and test assumptions.

9.2.2 Comments on the integrals

We have to deal with the integrals of three Hankels in (9.9). There are in the literature some results for the integral of three Bessel functions. For example, Gervois [45] gives:

$$\begin{aligned}
&\int_0^\infty dt\ t^{1-\rho} J_\nu(at) J_\nu(bt) \begin{pmatrix} J_\rho(ct) \\ Y_\rho(ct) \end{pmatrix} = \qquad \text{any } a,\, b,\, c\ \in \mathbb{R} \\
&= \frac{1}{\pi}\sqrt{\frac{2}{\pi}}\frac{(ab)^{\rho-1}}{c^\rho}(\sin\varphi_c)^{\rho-\frac{1}{2}} \begin{pmatrix} \frac{\pi}{2} P^{-\rho+\frac{1}{2}}_{\nu-\frac{1}{2}}(\cos\varphi_c) \\ -Q^{-\rho+\frac{1}{2}}_{\nu-\frac{1}{2}}(\cos\varphi_c) \end{pmatrix} \\
&|a-b| < c < a+b \\
&2ab\cos\varphi_c = a^2+b^2-c^2 \qquad \frac{1}{2}ab\sin\varphi_c = \frac{1}{4}\sqrt{(c^2-(a-b)^2)\left((a+b)^2-c^2\right)} \\
&\rho > -\frac{1}{2} \qquad \begin{cases} \nu+1>0 & \text{for } J_\rho \\ \nu+1-\frac{\rho+|\rho|}{2}>0 & \text{for } Y_\rho \end{cases}
\end{aligned} \tag{9.20}$$

$$\begin{aligned}
&\int_0^\infty dt\ t^{1+\rho} J_\nu(at) J_\nu(bt) \begin{pmatrix} J_\rho(ct) \\ Y_\rho(ct) \end{pmatrix} = \qquad \text{any } a,\, b,\, c\ \in \mathbb{R} \\
&= \frac{1}{\pi}\sqrt{\frac{2}{\pi}}\frac{(ab)^{-\rho-1}}{c^{-\rho}}(\sin\varphi_c)^{-\rho-\frac{1}{2}} \begin{pmatrix} \frac{\pi}{2}\cos\pi\rho P^{\rho+\frac{1}{2}}_{\nu-\frac{1}{2}}(\cos\varphi_c) - \sin\pi\rho Q^{\rho+\frac{1}{2}}_{\nu-\frac{1}{2}}(\cos\varphi_c) \\ -\frac{\pi}{2}\sin\pi\rho P^{\rho+\frac{1}{2}}_{\nu-\frac{1}{2}}(\cos\varphi_c) - \cos\pi\rho Q^{\rho+\frac{1}{2}}_{\nu-\frac{1}{2}}(\cos\varphi_c) \end{pmatrix} \\
&|a-b| < c < a+b \\
&2ab\cos\varphi_c = a^2+b^2-c^2 \qquad \frac{1}{2}ab\sin\varphi_c = \frac{1}{4}\sqrt{(c^2-(a-b)^2)\left((a+b)^2-c^2\right)} \\
&\rho < \frac{1}{2} \qquad \begin{cases} \nu+1+\rho>0 & \text{for } J_\rho \\ \nu+1+\frac{\rho-|\rho|}{2}>0 & \text{for } Y_\rho \end{cases}
\end{aligned} \tag{9.21}$$

In a later work, Tyler [46] deals with the case where at least two functions share the same argument:

$$\begin{aligned}
&\int_0^\infty dx x^\alpha J_l(x) J_m(x) J_n(\beta x) \qquad \text{if } \frac{\beta}{2} > 1 \\
&= 2^{-l-m-1}\frac{\Gamma\left(\frac{\alpha+l+m+n+1}{2}\right)}{\Gamma(m+1)\Gamma(l+1)\Gamma\left(\frac{-\alpha-l-m+n+1}{2}\right)}\left(\frac{\beta}{2}\right)^{-\alpha-l-m-1}\cdot \\
&\quad {}_4F_3\left(\frac{l+m+1}{2}, \frac{l+m+2}{2}, \frac{\alpha+l+m+n+1}{2}, \frac{\alpha+l+m-n+1}{2};\right. \\
&\qquad \left. m+1, l+m+1, l+1; \frac{4}{\beta^2}\right)
\end{aligned} \tag{9.22}$$

$$\text{converges if } \mathrm{Re}(\alpha) < \frac{3}{2} \text{ (but } \frac{1}{2} \text{ if } \beta = 2) \qquad \mathrm{Re}(\alpha+l+m+n+1) > 0 \tag{9.23}$$

In the particular case where $\nu = \rho$:

$$\begin{aligned}
&\int_0^\infty dt\ t^{1+\nu} J_\nu(at) J_\nu(bt) \begin{pmatrix} J_\nu(ct) \\ Y_\nu(ct) \end{pmatrix} = \qquad \text{any } a,\, b,\, c\ \in \mathbb{R} \\
&= \frac{2^{-\nu-1}}{\pi\sqrt{\pi}}(abc)^\nu \Gamma\left(\nu+\frac{1}{2}\right)\frac{1}{\Delta^{2\nu+1}}\begin{pmatrix} 1 \\ 0 \end{pmatrix} \\
&|a-b| < c < a+b \\
&\Delta = \frac{1}{4}\sqrt{(c^2-(a-b)^2)\left((a+b)^2-c^2\right)} \\
&|\nu| < \frac{1}{2}
\end{aligned} \tag{9.24}$$

Among all the cases shown in the paper, we are interested in the case $|a-b| < c < a+b$ that is when the three parameters are the sides of a triangle, as is enforced by the Dirac delta.

This kind of integral has been studied also in [47]. The paper was written in jail, after his mentally unstable author had killed four people in his department. This should already ring an alarm bell.

Unfortunately, the integrals we find in (9.9) cannot be rewritten in such a way that we recover any of these cases. The problem is that we fail to reproduce the conditions on the indices of the Bessel functions. Such conditions are required to make sure that the integrals converge. In particular, problems arise for us as $\tau \to -\infty$: our integrals diverge in that limit.

This makes sense, if we recall that we need to apply the $i\epsilon$ prescription (7.17) at very early times to ensure convergence. As Maldacena points out [27], we need to deform the integration contour so that it includes some evolution in euclidean time which projects onto the true vacuum. Physically, we know that the integrals must converge because well inside the horizon we are basically in Minkowski space, the field oscillates rapidly and we expect no contribution. After we continue to euclidean time, this is exactly what happens.

At this point, one possibility is to compute again the integrals from scratch, following the methods employed in the literature but this time applying the $i\epsilon$ prescription. For example, Tyler [46] uses the Mellin transforms, taking advantage of the fact that the integral can be rewritten as two nested Mellin transforms. In our case, this cannot be done directly because of the $i\epsilon$ prescription: to follow this approach, we should be able to define a "modified" Mellin transform using this integration contour.

Another possibility is to restrict our attention to the superhorizon regime, since physically we expect to have no contribution when we are deep inside the horizon. Therefore we can approximate for $-k_i\tau$ small, and integrate from a cutoff $1/k_{\max}$ up to some τ. This cutoff has been chosen so that all the three wavelengths corresponding to k_1, k_2, k_3 are outside the horizon. In the end we will be interested in the bispectrum at the end of inflation $\tau \to 0^-$.
Hopefully, we would like to find a finite term, plus corrections depending on the cutoff. Of course this is a rough approximation, and the full result will depend on the ultraviolet cutoff that we set.
Unfortunately, we will see that the result only depends on the cutoff.

The plan is the following. We want to set:

$$\text{cutoff} \equiv -\frac{\alpha}{k_{\max}} \tag{9.25}$$

with α some numerical factor, and integrate from this cutoff to τ. Then we take the imaginary part according to (9.8), and we send $\tau \to 0^-$ to compute the bispectrum at the end of inflation.
First we will take the standard $\nu = \frac{3}{2}$ case, to validate this procedure in a framework where we have everything under control analytically. Then we repeat the same sequence of operations for generic ν.

9.2.3 Approximation on superhorizon scales: case $\nu = \frac{3}{2}$

In the standard slow-roll case, where we take the index of the modefunctions inside the integrals to be $\nu = \frac{3}{2}$, the modefunctions for ζ are:

$$\theta_{k,\mathrm{DS}}(\tau) = c\sqrt{\frac{2}{\pi}}\frac{1}{k^{3/2}}(-i + k\tau)e^{-ik\tau} \tag{9.26}$$

Approximating on superhorizon scales, for $-k\tau \ll 1$, we obtain to lowest order:

$$\theta_{k,\mathrm{DS}}(\tau) \approx -\sqrt{\frac{2}{\pi}}\frac{ic}{k^{3/2}} \tag{9.27}$$

which is purely imaginary, therefore if we substituted in (9.8) and took the imaginary part we would find zero. To obtain a non-vanishing result, we need to go to at least third order in the expansion:

$$\theta_{k,\mathrm{DS}}(\tau) \approx -\frac{ic}{3\sqrt{2\pi}k^{3/2}}\left(6 + 3k^2\tau^2 - 2ik^3\tau^3\right) \tag{9.28}$$

The scale factor is $a(\tau) = -A/\tau$.

Now we compute the integrals. For example, the first one in (9.8) becomes:

$$\int_{\text{cutoff}}^{\tau} d\tau' \theta^*_{k_1,\text{DS}}(\tau')\theta^*_{k_2,\text{DS}}(\tau')\theta^*_{k_3,\text{DS}}(\tau')a^2(\tau') = -\frac{1}{1890\sqrt{2}(k_1k_2k_3)^{3/2}\pi^{3/2}(-\tau)}\cdot$$
$$\Big(7560i - 3780i(k_1^2+k_2^2+k_3^2)(-\tau)^2 - 1260(k_1^3+k_2^3+k_3^3)(-\tau)^3 - 630i(k_1^2k_2^2+k_1^2k_3^2+k_2^2k_3^2)(-\tau)^4 +$$
$$-315(k_1^3k_2^2+k_1^2k_2^3+k_1^3k_3^2+k_1^2k_3^3+k_2^3k_3^2+k_2^2k_3^3)(-\tau)^5 + \big(168i(k_1^3k_2^3+k_1^3k_3^3+k_2^3k_3^3)+$$
$$-189ik_1^2k_2^2k_3^2\big)(-\tau)^6 - 105k_1^2k_2^2k_3^2(k_1+k_2+k_3)(-\tau)^7 + 60ik_1^2k_2^2k_3^2(k_1k_2+k_1k_2+k_2k_3)(-\tau)^8 +$$
$$+35k_1^3k_2^3k_3^3(-\tau)^9\Big)\Big|_{\text{cutoff}}^{\tau} \tag{9.29}$$

and similarly for the other contributions.
In the slow-roll limit, the bispectrum is:

$$B_\zeta^{\text{superhorizon}}(k_1,k_2,k_3) = \frac{V_0^2}{995328M_P^8\epsilon k_1^3k_2^3k_3^3}(*) \tag{9.30}$$

$$(*) = \text{cutoff}^2\Big(-2880(k_1^5+k_2^5+k_3^5) - 1728(k_1^4k_2+k_1k_2^4+k_1^4k_3+k_1k_3^4+k_2^4k_3+k_2k_3^4)+$$
$$+9216(k_1^3k_2^2+k_1^2k_2^3+k_1^3k_3^2+k_1^2k_3^3+k_2^3k_3^2+k_2^2k_3^3)+3456k_1k_2k_3(k_1k_2+k_1k_3+k_2k_3)\Big)+$$
$$\text{cutoff}^4\Big(432(k_1^6k_2+k_1k_2^6+k_1^6k_3+k_1k_3^6+k_2^6k_3+k_2k_3^6)+$$
$$+432(k_1^5k_2^2+k_1^2k_2^5+k_1^5k_3^2+k_1^2k_3^5+k_2^5k_3^2+k_2^2k_3^5)+$$
$$-1440(k_1^4k_2^3+k_1^3k_2^4+k_1^4k_3^3+k_1^3k_3^4+k_2^4k_3^3+k_2^3k_3^4)+$$
$$-432k_1k_2k_3(k_1^3k_2+k_1k_2^3+k_1^3k_3+k_1k_3^3+k_2^3k_3+k_2k_3^3)+$$
$$+4032k_1^2k_2^2k_3^2(k_1+k_2+k_3)\Big)+$$
$$\text{cutoff}^6\Big(96(k_1^6k_2^3+k_1^3k_2^6+k_1^6k_3^3+k_1^3k_3^6+k_2^6k_3^3+k_2^3k_3^6)+$$
$$-96(k_1^5k_2^4+k_1^4k_2^5+k_1^5k_3^4+k_1^4k_3^5+k_2^5k_3^4+k_2^4k_3^5)+$$
$$+144k_1k_2k_3(k_1^5k_2+k_1k_2^5+k_1^5k_3+k_1k_3^5+k_2^5k_3+k_2k_3^5)+$$
$$+144k_1^2k_2^2k_3^2(k_1^3+k_2^3+k_3^3) - 288k_1k_2k_3(k_1^3k_2^3+k_1^3k_3^3+k_2^3k_3^3)+$$
$$-960k_1^2k_2^2k_3^2(k_1^2k_2+k_1k_2^2+k_1^2k_3+k_1k_3^2+k_2^2k_3+k_2k_3^2) - 2304k_1^3k_2^3k_3^3\Big)+$$
$$\text{cutoff}^8\Big(-36k_1^2k_2^2k_3^2(k_1^4k_2+k_1k_2^4+k_1^4k_3+k_1k_3^4+k_2^4k_3+k_2k_3^4)+$$
$$+36k_1^2k_2^2k_3^2(k_1^3k_2^2+k_1^2k_2^3+k_1^3k_3^2+k_1^2k_3^3+k_2^3k_3^2+k_2^2k_3^3) - 16k_1^3k_2^3k_3^3(k_1^2+k_2^2+k_3^2)+$$
$$+144k_1^3k_2^3k_3^3(k_1k_2+k_1k_3+k_2k_3) \tag{9.31}$$

This is to be compared with Maldacena's result (5.18):

$$B_\zeta^{\text{M}}(k_1,k_2,k_3) =$$
$$-\frac{V_0^2}{288M_P^8\epsilon k_1^3k_2^3k_3^3(k_1+k_2+k_3)}\big(k_1^4+k_2^4+k_3^4-10(k_1^2k_2^2+k_1^2k_3^2+k_2^2k_3^2)-2k_1k_2k_3(k_1+k_2+k_3)\big) \tag{9.32}$$

There is not a clean value of the cutoff for which we recover this result. If we set (9.30) equal to (5.18), the solutions we obtain for the cutoff are very complicated and depend on the three momenta k_1, k_2, k_3.

One can try to study the expressions above in the equilateral limit or in the squeezed limit. Only in the squeezed limit we find a simpler expression:

$$\lim_{k_3 \ll k_1, k_2} B_\zeta^{\mathrm{M}} = \lim_{k_3 \ll k_1, k_2} B_\zeta^{\text{superhorizon}}$$
$$\frac{V_0^2}{72 M_P^8 \epsilon k_1^3 k_3^3} = \frac{V_0^2}{864 M_P^8 \epsilon k_1 k_3^3} \left(8\text{cutoff}^2 - k_1^2 \text{cutoff}^4\right) \tag{9.33}$$

which leads to cutoff $= -\sqrt{2}/k_1$ or cutoff $= -\sqrt{6}/k_1$, that is, the cutoff roughly corresponds to the conformal time when the short wavelength mode k_1 crosses the horizon. However, this information is not helpful in the general case.
Furthermore, this is only the third order approximation to the modefunctions. More correction terms arise if one continues in the series expansion.

These results seem to indicate that it is not enough to set an ultraviolet cutoff and look at the superhorizon evolution only. Taking into account the horizon crossing and properly treating the subhorizon oscillations at $\tau \to -\infty$ are probably crucial aspects to the computation.
This result is recovered in the case of generic ν. Of course the expressions are much more complicated, but then in the slow-roll limit they boil down to the ones found above.

9.2.4 Approximation on superhorizon scales: case of generic ν

The modefunctions in this case are the usual (6.30). When approximated to superhorizon scales, up to order $(-\tau)^3$, $(-\tau)^{2\nu}$ we get:

$$\theta_k(\tau) \approx c\left(-\frac{i2^\nu k^{-\nu}\Gamma(\nu)}{\pi} - \frac{i2^{-2+\nu}k^{2-\nu}(-\tau)^2\Gamma(\nu-1)}{\pi} + \frac{2^{-\nu}k^\nu(-\tau)^{2\nu}\left(1+i\cot(\pi\nu)\right)}{\Gamma(\nu+1)}\right) \tag{9.34}$$

Substituting in (9.8) and taking the imaginary part we obtain:

$$B_\zeta^{\text{superhorizon}}(k_1,k_2,k_3) = 2M_P^2\epsilon^2 A^2 (cc^*)^3 \cdot$$
$$\left[\frac{8^\nu\left(\Gamma(\nu)\right)^3}{(k_1k_2k_3)^\nu \pi^3}\left(f_1(k_1,k_2,k_3)\mathrm{Re}I_1 + f_2(k_1,k_2,k_3)\mathrm{Re}I_2 + f_3(k_1,k_2,k_3)\mathrm{Re}I_3 + f_4(k_1,k_2,k_3)\mathrm{Re}I_4\right)\right] \tag{9.35}$$

where I_i are the four integrals in conformal time and f_i are functions of the three momenta only, that can be read from (9.8).

$$B_\zeta^{\text{superhorizon}}(k_1,k_2,k_3) = \frac{e^{\frac{2C}{M_P}\sqrt{2\epsilon}}V_0^2}{M_P^8\epsilon}\Big(c_1(-\text{cutoff})^{4+\frac{4}{1-\epsilon}} + c_2(-\text{cutoff})^{2+\frac{4}{1-\epsilon}} + c_3(-\text{cutoff})^{\frac{3-\epsilon}{1-\epsilon}}$$
$$+ c_4(-\text{cutoff})^{5+\frac{2}{1-\epsilon}} + c_5(-\text{cutoff})^{3+\frac{2}{1-\epsilon}} + c_6(-\text{cutoff})^2$$
$$+ c_7(-\text{cutoff})^4 + c_8(-\text{cutoff})^6 + c_9(-\text{cutoff})^8\Big) \tag{9.36}$$

where the coefficients $c_1, \ldots, c_9$ depend on the momenta, analogous to the ones we found before, but much longer. In the slow-roll limit, taking the leading order term in the expansion $\epsilon \to 0$, we recover (9.30).

Again, this seems to indicate that the horizon crossing and a proper treatment of the highly oscillating Hankel functions when $\tau \to -\infty$ are crucial points, that cannot be overlooked by simply restricting our attention to the superhorizon evolution.

9.3 Squeezed limit

In order to simplify the integrals in (9.8), we can study the bispectrum in the squeezed limit, in which one of the three momenta is much smaller than the other two: say $k_3 \ll k_1$, k_2 and $k_1 \approx k_2$. The long wavelength mode k_3 is already out of the horizon, so we can approximate the modefunctions in the limit $k_3\tau \ll 1$. The short wavelength modes leave two Hankel functions with approximately the same argument.

The modefunctions are (6.30), reported here for comparison, and the approximated modefunctions are:

$$\theta_k(\tau) = c(-\tau)^\nu H_\nu^{(1)}(-k\tau) \qquad \theta_{k,\text{appr}}(\tau) = -\frac{i}{\pi}2^\nu c k^{-\nu}\Gamma(\nu) \tag{9.37}$$

$$\theta'_k(\tau) = -ck(-\tau)^\nu H_{\nu-1}^{(1)}(-k\tau) \qquad \theta'_{k,\text{appr}}(\tau) = \frac{i}{\pi}2^{-1+\nu} c k^{2-\nu}\Gamma(\nu-1)(-\tau) \tag{9.38}$$

At this point we substitute into (9.8) the full modefunctions for the momenta k_1 and k_2 and the approximated form on superhorizon scales for k_3. In order to compute the integrals, we need to set $k_1 = k_2$ already in the integrands.

We will need the following integrals ($k = k_1$):

$$\int x\left(H_\nu^{(2)}(kx)\right)^2 dx \tag{9.39}$$

$$\int x^2 H_\nu^{(2)}(kx) H_{\nu-1}^{(2)}(kx) dx \tag{9.40}$$

Notice that if one computes these integrals with Mathematica the results are not correct, they differ from the ones given in the literature. In particular, the problem was found with Mathematica 12.3.1.0: the problematic integral is the one containing a Bessel and a Neumann. The issue was reported to the Wolfram Support.

The first integral is known [48, 49]:

$$\int z\mathcal{C}_\nu(az)\mathcal{D}_\nu(az)dz = \frac{z^2}{4}\left(2\mathcal{C}_\nu(az)\mathcal{D}_\nu(az) - \mathcal{C}_{\nu-1}(az)\mathcal{D}_{\nu+1}(az) - \mathcal{C}_{\nu+1}(az)\mathcal{D}_{\nu-1}(az)\right) \tag{9.41}$$

where $z \in \mathbb{C}$ and $\mathcal{C}_\nu(z)$, $\mathcal{D}_\nu(z)$ are any cylinder function $J_\nu(z)$, $Y_\nu(z)$, $H_\nu^{(1)}(z)$, $H_\nu^{(2)}(z)$ or any non-trivial linear combination of them, with coefficients independent of z or of ν.
In our case:

$$\int x\left(H_\nu^{(2)}(kx)\right)^2 dx = \frac{x^2}{2}\left(\left(H_\nu^{(2)}(kx)\right)^2 - H_{\nu-1}^{(2)}(kx)H_{\nu+1}^{(2)}(kx)\right) \tag{9.42}$$

The second one can be obtained by applying the recurrence relation (A.2) and integrating by parts:

$$\mathcal{C}_{\nu-1}(z) = \frac{\nu}{z}\mathcal{C}_\nu(z) + \frac{\partial \mathcal{C}_\nu(z)}{\partial z} \tag{9.43}$$

$$\int x^2 H_\nu^{(2)}(kx)H_{\nu-1}^{(2)}(kx)dx = \frac{\nu}{k}\int xH_\nu^{(2)}(kx)H_\nu^{(2)}(kx)dx + \frac{1}{k}\int x^2 H_\nu^{(2)}(kx)\frac{\partial H_\nu^{(2)}(kx)}{\partial x}dx \tag{9.44}$$

$$\begin{aligned}
&\int x^2 H_\nu^{(2)}(kx)\frac{\partial H_\nu^{(2)}(kx)}{\partial x}dx = \\
&\qquad \int \frac{\partial}{\partial x}\left(x^2\left(H_\nu^{(2)}(kx)\right)^2\right)dx - \int 2x\left(H_\nu^{(2)}(kx)\right)^2 dx - \int x^2\frac{\partial H_\nu^{(2)}(kx)}{\partial x}H_\nu^{(2)}(kx)dx \\
&\implies \int x^2 H_\nu^{(2)}(kx)\frac{\partial H_\nu^{(2)}(kx)}{\partial x}dx = \frac{x^2}{2}\left(H_\nu^{(2)}(kx)\right)^2 - \int x\left(H_\nu^{(2)}(kx)\right)^2 dx
\end{aligned} \tag{9.45}$$

hence:

$$\int x^2 H_\nu^{(2)}(kx)H_{\nu-1}^{(2)}(kx)dx = \frac{\nu-1}{k}\int x\left(H_\nu^{(2)}(kx)\right)^2 dx + \frac{1}{k}\frac{x^2}{2}\left(H_\nu^{(2)}(kx)\right)^2 \tag{9.46}$$

First integral

The first integral in (9.8) is:

$$\int \theta^*_{k_1}(\tau')\theta^*_{k_1}(\tau')\theta^*_{k_3,\mathrm{appr}}(\tau')\left(a(\tau')\right)^2 d\tau' \tag{9.47}$$

Collecting the factor $A^2(c^*)^3$ outside:

$$I_1 = i\left(-\frac{2^\nu k_3^{-\nu}\Gamma(\nu)}{\pi}\right)\frac{(-\tau)^2}{2}\left(\left(H^{(2)}_\nu(-k_1\tau)\right)^2 - H^{(2)}_{\nu-1}(-k_1\tau)H^{(2)}_{\nu+1}(-k_1\tau)\right) \tag{9.48}$$

In the slow-roll limit, we recover the expected result:

$$I_1 \xrightarrow{\epsilon\longrightarrow 0} \frac{\sqrt{2}e^{2ik_1\tau}(2i+k_1\tau)}{k_1^3 k_3^{3/2}\pi^{3/2}\tau} \tag{9.49}$$

Second integral

The second integral:

$$\int \theta^{*\prime}_{k_1}(\tau')\theta^{*\prime}_{k_1}(\tau')\theta^*_{k_3,\mathrm{appr}}(\tau')\left(a(\tau')\right)^2 d\tau' \tag{9.50}$$

is analogous to the first one, with the substitution $\nu \longmapsto \nu - 1$.

Third integral

The third integral:

$$\int \theta^{*\prime}_{k_1}(\tau')\theta^*_{k_1}(\tau')\theta^{*\prime}_{k_3,\mathrm{appr}}(\tau')\left(a(\tau')\right)^2 d\tau' \tag{9.51}$$

gives:

$$\begin{aligned} I_3 = i\left(\frac{2^{-1+\nu}k_1 k_3^{2-\nu}\Gamma(\nu-1)}{\pi}\right)\Bigg[-\Bigg(\frac{\nu-1}{k_1}\frac{(-\tau)^2}{2}\left(\left(H^{(2)}_\nu(-k_1\tau)\right)^2 - H^{(2)}_{\nu-1}(-k_1\tau)H^{(2)}_{\nu+1}(-k_1\tau)\right)+ \\ +\frac{1}{k_1}\frac{(-\tau)^2}{2}\left(H^{(2)}_\nu(-k_1\tau)\right)^2\Bigg)\Bigg] \end{aligned} \tag{9.52}$$

which in the slow-roll limit becomes:

$$I_3 \xrightarrow{\epsilon\longrightarrow 0} \frac{e^{2ik_1\tau}\sqrt{k_3}(-3+2ik_1\tau)}{\sqrt{2}k_1^2\pi^{3/2}} \tag{9.53}$$

Substituting in (9.8), we obtain:

$$\begin{aligned} B_\zeta(k_1,k_2,k_3) =& 2M_P^2\epsilon^2 A^2 (cc^*)^3\, \mathrm{Im}\left[(\mathrm{Re}_{\mathrm{out}} + i\mathrm{Im}_{\mathrm{out}})\cdot\right. \\ &\left.(f_1(k_1,k_2,k_3)I_1 + f_2(k_1,k_2,k_3)I_2 + f_3(k_1,k_2,k_3)I_3 + f_4(k_1,k_2,k_3)I_4)\right] \end{aligned} \tag{9.54}$$

where:

$$\begin{aligned} \mathrm{Re}_{\mathrm{out}} = (-\tau)^{3\nu}\,(&J_\nu(-k_1\tau)J_\nu(-k_2\tau)J_\nu(-k_3\tau) - J_\nu(-k_1\tau)Y_\nu(-k_2\tau)Y_\nu(-k_3\tau)+ \\ &- Y_\nu(-k_1\tau)J_\nu(-k_2\tau)Y_\nu(-k_3\tau) - Y_\nu(-k_1\tau)Y_\nu(-k_2\tau)J_\nu(-k_3\tau)\,) \end{aligned} \tag{9.55}$$

$$\begin{aligned} \mathrm{Im}_{\mathrm{out}} = (-\tau)^{3\nu}\,(&J_\nu(-k_1\tau)J_\nu(-k_2\tau)Y_\nu(-k_3\tau) + J_\nu(-k_1\tau)Y_\nu(-k_2\tau)J_\nu(-k_3\tau)+ \\ &+ Y_\nu(-k_1\tau)J_\nu(-k_2\tau)Y_\nu(-k_3\tau) - Y_\nu(-k_1\tau)Y_\nu(-k_2\tau)Y_\nu(-k_3\tau)\,) \end{aligned} \tag{9.56}$$

are the real and imaginary part coming from the modefunctions outside $\theta_{k_1}(\tau)\theta_{k_2}(\tau)\theta_{k_3}(\tau)$, having collected the factor c^3 outside, and f_i are functions of the three momenta only that can be read from (9.8).

In taking the limit for $\tau \to 0$, only the imaginary part of the three modefunctions outside survives:

$$\lim_{\tau\to 0} \text{Re}_{\text{out}} = 0 \qquad\qquad \lim_{\tau\to 0} \text{Im}_{\text{out}} = \frac{8^\nu (k_1 k_2 k_3)^{-\nu}(\nu-1)^3 \left(\Gamma(\nu-1)\right)^3}{\pi^3} \tag{9.57}$$

Taking the squeezed limit $k_1 = k_2$ and $k_3/k_1 \ll 1$:

$$\boxed{B_\zeta^{\text{squeezed}}(k_1,k_2,k_3) = \frac{2^{-3+\frac{4}{1-\epsilon}} e^{\frac{2\mathrm{C}}{M_P}\sqrt{2\epsilon}}}{\pi^2} \frac{V_0^2}{M_P^8} \frac{(1-\epsilon)^3 \left(\Gamma\left(\frac{1}{2}+\frac{1}{1-\epsilon}\right)\right)^4}{(-3+\epsilon)^2\epsilon} (k_1 k_3)^{-1-\frac{2}{1-\epsilon}}} \tag{9.58}$$

In the slow-roll regime, we recover Maldacena's result [27]:

$$B_\zeta^{\text{squeezed}}(k_1,k_2,k_3) \xrightarrow{\epsilon\to 0} \frac{H_{\text{DS}}^4}{8M_P^4 k_1^3 k_3^3 \epsilon} \tag{9.59}$$

We can write down the next orders in the expansion:

$$B_\zeta^{\text{squeezed}}(k_1,k_2,k_3) \xrightarrow{\epsilon\to 0} \frac{H_{\text{DS}}^4}{8M_P^4 k_1^3 k_3^3 \epsilon} + \tag{9.60}$$

$$+ \frac{\mathrm{C} H_{\text{DS}}^4}{2\sqrt{2} M_P^5 k_1^3 k_3^3 \sqrt{\epsilon}} + \tag{9.61}$$

$$+ \frac{H_{\text{DS}}^4}{24 M_P^6 k_1^3 k_3^3} \left(12\mathrm{C}^2 - 7M_P^2 + 6M_P^2 \log\left(\frac{4}{k_1 k_3}\right) + 12 M_P^2 \psi(3/2)\right) + \tag{9.62}$$

$$+ \mathcal{O}(\sqrt{\epsilon})$$

where $\psi(z)$ is the digamma function, defined as the logarithmic derivative $\psi(z) = \dfrac{1}{\Gamma(z)}\dfrac{d\Gamma(z)}{dz}$.

9.4 The consistency relation

Maldacena in his seminal work [27] showed that there is a consistency relation between the index of the scalar power-spectrum and the three-point correlation function in the squeezed limit:

$$\boxed{\lim_{k_3\to 0} B_\zeta(k_1,k_2,k_3) = (1-n_s) P_\zeta(k_1) P_\zeta(k_3)} \tag{9.63}$$

The squeezed limit of the three-point function is suppressed like $(1-n_s)$ and vanishes for perfectly scale-invariant perturbations. A proof of this can be found in [39].

9.4.1 Sketch of the proof and meaning

In the squeezed limit, one of the wavelengths is much longer than the other two: let us choose $k_3 \ll k_1,\ k_2$ so that $k_{\text{long}} = k_3$ corresponding to the long wavelength mode and $k_{\text{short}} = k_1 \approx k_2$ corresponding to the short wavelength mode. In the squeezed limit, the three-point function is roughly a correlation of the long wavelength mode with the power-spectrum of the short wavelength mode: $\langle \zeta_{\vec{k}_1}\zeta_{\vec{k}_2}\zeta_{\vec{k}_3}\rangle \simeq \langle P_\zeta(k_1)\zeta_{\vec{k}_3}\rangle$. The reason why the long and short modes should be correlated is the following [39, 50]. The long wavelength mode will cross the horizon much earlier than the other two, therefore it will act as a perturbation of the background on which the two short modes evolve. The net effect is that the long wavelength mode changes the time t_* at which the two short wavelength modes cross the horizon by $\delta t_* = -\zeta_{\vec{k}_3}/H$.
Following [39], we evaluate:

$$\langle \zeta_{\vec{k}_1}\zeta_{\vec{k}_2}\zeta_{\vec{k}_3}\rangle \simeq \langle \left(\zeta_{\vec{k}_1}\right)^2 \zeta_{\vec{k}_3}\rangle = \langle (\zeta_{\text{short}})^2\, \zeta_{\text{long}}\rangle \tag{9.64}$$

First we calculate the power-spectrum of short fluctuations when a long mode is present $\langle(\zeta_{\rm short})^2\rangle\Big|_{\zeta_{\rm long}}$.
In real space, the background mode is homogeneous $\zeta_{\rm long}(x)=\overline{\zeta}_{\rm long}$ and it can be reabsorbed into a rescaling of the spatial coordinates $\bar{x}^i\equiv e^{\overline{\zeta}_{\rm long}}x^i$. After this rescaling, the action in the new coordinates no longer contains $\overline{\zeta}_{\rm long}$. Now, if $\overline{\zeta}_{\rm long}$ were exactly constant, computing the two-point function on top of the long wavelength perturbation would be equivalent to computing the two-point function in the "displaced" coordinates:

$$\langle\zeta_{\rm short}(\vec{x}_1)\zeta_{\rm short}(\vec{x}_2)\rangle_{\overline{\zeta}_{\rm long}}=\langle\zeta_{\rm short}(\vec{\bar{x}}_1)\zeta_{\rm short}(\vec{\bar{x}}_2)\rangle \tag{9.65}$$

If $\zeta_{\rm long}$ is slowly varying instead we can evaluate it at the middle point $\vec{x}_+\equiv\frac{1}{2}(\vec{x}_1+\vec{x}_2)$. The two-point correlation function will be:

$$\langle\zeta_{\rm short}(\vec{x}_1)\zeta_{\rm short}(\vec{x}_2)\rangle|_{\zeta_{\rm long}(x)}\simeq\langle\zeta_{\rm short}(\vec{\bar{x}}_1)\zeta_{\rm short}(\vec{\bar{x}}_2)\rangle=\xi_{\rm short}(\vec{\bar{x}}_1-\vec{\bar{x}}_2)=\xi_{\rm short}(|\vec{\bar{x}}_-|) \tag{9.66}$$

where we have defined $\vec{x}_-\equiv\vec{x}_1-\vec{x}_2$ and ξ is the two-point function, i.e. the Fourier transform of the power-spectrum:

$$\xi(\vec{x})\equiv\int\frac{d^3\vec{k}}{(2\pi)^{3/2}}P_\zeta(k)e^{i\vec{k}\cdot\vec{x}} \tag{9.67}$$

At this point we expand the coordinate rescaling as $\vec{\bar{x}}_-\simeq\vec{x}_-+\zeta_{\rm long}(\vec{x}_+)\vec{x}_-+\ldots$ and substitute in the expression above:

$$\langle\zeta_{\rm short}(\vec{x}_1)\zeta_{\rm short}(\vec{x}_2)\rangle|_{\zeta_{\rm long}(x)}\simeq\xi_{\rm short}(|\vec{x}_-|)+\zeta_{\rm long}(\vec{x}_+)\left[\vec{x}_-\cdot\nabla\xi_{\rm short}(|\vec{x}_-|)\right] \tag{9.68}$$

The three-point function is:

$$\begin{aligned}
&\langle\zeta_{\rm short}(\vec{x}_1)\zeta_{\rm short}(\vec{x}_2)\zeta_{\rm long}(\vec{x}_3)\rangle\simeq\langle\zeta_{\rm long}(\vec{x}_3)\zeta_{\rm long}(\vec{x}_+)\left[\vec{x}_-\cdot\nabla\xi_{\rm short}(|\vec{x}_-|)\right]\rangle\\
&=\int\frac{d^3\vec{k}_{\rm long}}{(2\pi)^{3/2}}\int\frac{d^3\vec{k}_+}{(2\pi)^{3/2}}\int\frac{d^3\vec{k}_{\rm short}}{(2\pi)^{3/2}}e^{i\vec{k}_{\rm long}\cdot\vec{x}_3}e^{i\vec{k}_+\cdot\vec{x}_+}\langle\zeta(\vec{k}_3)\zeta(\vec{k}_+)\rangle P_\zeta(k_{\rm short})\left[\vec{k}_{\rm short}\cdot\frac{\partial}{\partial\vec{k}_{\rm short}}\right]e^{i\vec{k}_{\rm short}\cdot\vec{x}_-}\\
&=\int\frac{d^3\vec{k}_{\rm long}d^3\vec{k}_{\rm short}}{(2\pi)^{3\cdot3/2}}e^{i\vec{k}_{\rm long}\cdot(\vec{x}_3-\vec{x}_+)}P_\zeta(k_{\rm long})P_\zeta(k_{\rm short})\left[\vec{k}_{\rm short}\cdot\frac{\partial}{\partial\vec{k}_{\rm short}}\right]e^{i\vec{k}_{\rm short}\cdot\vec{x}_-}
\end{aligned} \tag{9.69}$$

Integrating by parts:

$$\begin{aligned}
&P_\zeta(k_{\rm short})\left[\vec{k}_{\rm short}\cdot\frac{\partial}{\partial\vec{k}_{\rm short}}\right]e^{i\vec{k}_{\rm short}\cdot\vec{x}_-}=\\
&\frac{\partial}{\partial\vec{k}_{\rm short}}\cdot\left(P_\zeta(k_{\rm short})\vec{k}_{\rm short}e^{i\vec{k}_{\rm short}\cdot\vec{x}_-}\right)-e^{i\vec{k}_{\rm short}\cdot\vec{x}_-}\frac{\partial}{\partial\vec{k}_{\rm short}}\cdot\left(\vec{k}_{\rm short}P_\zeta(k_{\rm short})\right)
\end{aligned} \tag{9.70}$$

using:

$$\frac{\partial}{\partial\vec{k}_{\rm short}}\cdot\left(\vec{k}_{\rm short}P_\zeta(k_{\rm short})\right)=3P_\zeta(k_{\rm short})+k_{\rm short}\frac{dP_\zeta(k_{\rm short})}{dk_{\rm short}}=P_\zeta(k_{\rm short})\frac{d\ln\left(k^3_{\rm short}P_\zeta(k_{\rm short})\right)}{d\ln k_{\rm short}} \tag{9.71}$$

and inserting $1=\int d^3\vec{k}_3\delta^{(3)}(\vec{k}_{\rm long}+\vec{k}_3)$ we obtain:

$$\int\frac{d^3\vec{k}_{\rm long}d^3\vec{k}_{\rm short}d^3\vec{k}_3}{(2\pi)^{3\cdot3/2}}\delta^{(3)}(\vec{k}_{\rm long}+\vec{k}_3)e^{-i\vec{k}_3\cdot\vec{x}_3}e^{-i\vec{k}_{\rm long}\cdot\vec{x}_+}e^{i\vec{k}_{\rm short}\cdot\vec{x}_-}P_\zeta(k_{\rm long})P_\zeta(k_{\rm short})\frac{d\ln\left(k^3_{\rm short}P_\zeta(k_{\rm short})\right)}{d\ln k_{\rm short}} \tag{9.72}$$

In order to recover the necessary arguments of the exponentials, we let $\vec{k}_{\rm long}\equiv\vec{k}_1+\vec{k}_2$ and $\vec{k}_{\rm short}\equiv-\frac{1}{2}(\vec{k}_1-\vec{k}_2)$ so that:

$$\begin{aligned}
&\langle\zeta_{\rm short}(\vec{x}_1)\zeta_{\rm short}(\vec{x}_2)\zeta_{\rm long}(\vec{x}_3)\rangle\simeq\\
&=-\int\frac{d^3\vec{k}_1d^3\vec{k}_2d^3\vec{k}_3}{(2\pi)^{3\cdot3/2}}\delta^{(3)}(\vec{k}_1+\vec{k}_2+\vec{k}_3)e^{-i\vec{k}_1\cdot\vec{x}_1}e^{-i\vec{k}_2\cdot\vec{x}_2}e^{-i\vec{k}_3\cdot\vec{x}_3}P_\zeta(k_1)P_\zeta(k_3)\frac{d\ln\left(k_1^3P_\zeta(k_1)\right)}{d\ln k_1}
\end{aligned} \tag{9.73}$$

Fourier transforming the left hand side:

$$\lim_{k_3\to 0}\langle\zeta_{\vec{k}_1}\zeta_{\vec{k}_2}\zeta_{\vec{k}_3}\rangle = -\frac{1}{(2\pi)^{3/2}}\delta^{(3)}(\vec{k}_1+\vec{k}_2+\vec{k}_3)P_\zeta(k_1)P_\zeta(k_3)\frac{d\ln\left(k_1^3P_\zeta(k_1)\right)}{d\ln k_1}$$
$$= \frac{1}{(2\pi)^{3/2}}\delta^{(3)}(\vec{k}_1+\vec{k}_2+\vec{k}_3)(1-n_s)P_\zeta(k_1)P_\zeta(k_3) \quad (9.74)$$

This link is a very powerful one, since it applies to all single-scalar field models of inflation, regardless of the details of the potential and not necessarily in the slow-roll regime [50]. The argument only relies on the fact that the long wavelength mode remains frozen outside the horizon and does not evolve, which is true for single-scalar field models. Observing a disagreement with the consistency relation would rule out the whole class of single-scalar field models. In this sense, the consistency relation can be used as a "particle detector", in that it diagnoses extra fields during the inflationary epoch [39].

9.4.2 The consistency relation in power-law inflation

We have obtained the squeezed limit for power-law inflation in (9.58):

$$B_\zeta^{\text{squeezed}}(k_1,k_2,k_3) = \frac{2^{-3+\frac{4}{1-\epsilon}}e^{\frac{2C}{M_P}\sqrt{2\epsilon}}}{\pi^2}\frac{V_0^2}{M_P^8}\frac{(1-\epsilon)^3\left(\Gamma\left(\frac{1}{2}+\frac{1}{1-\epsilon}\right)\right)^4}{(-3+\epsilon)^2\epsilon}(k_1k_3)^{-1-\frac{2}{1-\epsilon}} \quad (9.75)$$

Recall that the power-spectrum in power-law inflation is:

$$P_\zeta(k) = \frac{4^{\frac{\epsilon}{1-\epsilon}}e^{\frac{C}{M_P}\sqrt{2\epsilon}}(1-\epsilon)^2\left(\Gamma\left(\frac{1}{2}+\frac{1}{1-\epsilon}\right)\right)^2}{\pi(3-\epsilon)\epsilon}\frac{V_0}{M_P^4}k^{-1-\frac{2}{1-\epsilon}} \quad (9.76)$$

and the scalar spectral index is:

$$n_s - 1 = -\frac{2\epsilon}{1-\epsilon} \quad (9.77)$$

If we plug these results into the consistency relation (9.63), we can verify that it is indeed satisfied.

We find for f_{NL}:

$$\boxed{f_{\text{NL}} = -\frac{5}{6}\frac{\epsilon}{1-\epsilon}} \quad (9.78)$$

This result does not come as a surprise, however the important point here is that we never made use of the slow-roll assumptions. This is a new step that has never been fully studied in the literature before. It is somehow reassuring that, even in the full model, we recover the consistency relation as we expect.

Chapter 10

A more "traditional" approach

In this chapter we perform the calculation in a "traditional" way, employing perturbation theory up to second order and using Wick's theorem to compute the three-point function. We mainly follow [22], therefore we will work in the Poisson gauge with the gauge-invariant quantity $\mathcal{R}$ defined in (4.42) and (4.45) and linked to ζ on superhorizon scales through (4.43) at linear order. Then we briefly discuss how to make contact between the two variables.

The main steps of the calculation are the following:

- write down the perturbed Einstein equations up to second order;
- introduce the gauge-invariant comoving curvature perturbation $\mathcal{R}$ to first and second order;
- express all the quantities as a function of the (first-order) gauge-invariant comoving curvature perturbation $\mathcal{R}^{(1)}$ and of its time derivative $\mathcal{R}^{(1)\prime}$;
- go to Fourier space and compute the tree-level bispectrum, using Wick's theorem to evaluate the contractions.

The first two steps have already been explored in chapter 4 and chapter 6, what is left to do is expressing all the quantities in terms of the curvature perturbation and applying Wick's theorem.
Again, we will encounter integrals of three Bessel functions or three Hankel functions, which we don't know how to solve. In this case, if we focus on superhorizon scales and set a cutoff in the integration we do get a finite result. However, as we will see, we are still probably missing a piece, since we are unable to recover the expected result in the slow-roll limit, which is our only consistency check.

10.1 Rewriting of $\mathcal{R}^{(2)}$

We recall the definitions of equations (4.42) and (4.45):

$$\mathcal{R} = \mathcal{R}^{(1)} + \frac{1}{2}\mathcal{R}^{(2)} \tag{10.1}$$

$$\mathcal{R}^{(1)} = \psi^{(1)} + \mathcal{H}\frac{\delta^{(1)}\varphi}{\varphi_0'} \tag{10.2}$$

$$\mathcal{R}^{(2)} = \left(\psi^{(2)} + \mathcal{H}\frac{\delta^{(2)}\varphi}{\varphi_0'}\right) + \frac{\left(\psi^{(1)\prime} + 2\mathcal{H}\psi^{(1)} + \mathcal{H}\frac{\delta^{(1)}\varphi'}{\varphi_0'}\right)^2}{\mathcal{H}' + 2\mathcal{H}^2 - \mathcal{H}\frac{\varphi_0''}{\varphi_0'}} - \frac{1}{3}\partial_i\omega^{(1)}\partial^i\omega^{(1)} \tag{10.3}$$

The third term in $\mathcal{R}^{(2)}$ vanishes in the Poisson gauge. Let's deal separately with the first and the second piece.

$$\mathcal{R}^{(2)} = \underbrace{\left(\psi^{(2)} + \mathcal{H}\frac{\delta^{(2)}\varphi}{\varphi_0'}\right)}_{\mathcal{R}_2^{(2)}} + \underbrace{\frac{\left(\psi^{(1)\prime} + 2\mathcal{H}\psi^{(1)} + \mathcal{H}\frac{\delta^{(1)}\varphi'}{\varphi_0'}\right)^2}{\mathcal{H}' + 2\mathcal{H}^2 - \mathcal{H}\frac{\varphi_0''}{\varphi_0'}}}_{\mathcal{R}_1^{(2)}} \tag{10.4}$$

The second piece $\mathcal{R}_1^{(2)}$ is quadratic in first order quantities. The first piece $\mathcal{R}_2^{(2)}$ is made of intrinsically second order quantities.

In $\mathcal{R}_1^{(2)}$ we can use (4.18) to express $\delta^{(1)}\varphi$ and $\delta^{(1)\prime}\varphi$ in terms of $\phi^{(1)}$ and $\phi^{(1)\prime}$, and we can use the e.o.m. for $\phi^{(1)}$ (4.25) to get rid of second time derivatives when they appear. Furthermore, we apply the second order results (4.20), (4.23) and (6.16).
Then from the definition (4.42) it follows that:

$$\phi_{\vec{k}}^{(1)} = -\frac{4\pi G\varphi_0'^2}{\mathcal{H}}\frac{1}{k^2}\mathcal{R}_{\vec{k}}^{(1)\prime} \tag{10.5}$$

$$\phi_{\vec{k}}^{(1)\prime} = \frac{4\pi G\varphi_0'^2}{\mathcal{H}}\mathcal{R}_{\vec{k}}^{(1)} + \frac{4\pi G\varphi_0'^2}{k^2}\left(1 + \frac{4\pi G\varphi_0'^2}{\mathcal{H}^2}\right)\mathcal{R}_{\vec{k}}^{(1)\prime} \tag{10.6}$$

This way we manage to express everything in terms of $\mathcal{R}^{(1)}$ and $\mathcal{R}^{(1)\prime}$ and a time integral carrying the kernel in (6.16).

Similarly in $\mathcal{R}_2^{(2)}$:

$$\begin{aligned}\mathcal{R}_{2,\vec{k}}^{(2)} =& \psi_{\vec{k}}^{(2)} + \mathcal{H}\frac{\delta^{(2)}\varphi_{\vec{k}}}{\varphi_0'} \\ =& \phi_{\vec{k}}^{(2)} + \frac{1}{k^2}\gamma_{\vec{k}} + \frac{\mathcal{H}}{4\pi G\varphi_0'^2}\left(\phi_{\vec{k}}^{(2)\prime} + \mathcal{H}\phi_{\vec{k}}^{(2)} + \frac{1}{k^2}\gamma_{\vec{k}}' - \frac{1}{k^2}\left(\alpha_{\vec{k}} - 8\pi G\beta_{\vec{k}}\right)\right)\end{aligned} \tag{10.7}$$

where α, β, γ have been introduced before in chapter 4 and are quadratic in first order quantities, therefore they are convolutions in Fourier space.
In $\mathcal{R}_2^{(2)}$ we will have:

$$\mathcal{R}_{2,\vec{k}}^{(2)} = \underbrace{\phi_{\vec{k}}^{(2)}\left(1 + \frac{\mathcal{H}^2}{\mathcal{H}^2 - \mathcal{H}'}\right) + \phi_{\vec{k}}^{(2)\prime}\frac{\mathcal{H}}{\mathcal{H}^2 - \mathcal{H}'}}_{\text{contains the time integral}} + \underbrace{\frac{1}{k^2}\left(\gamma_{\vec{k}} + \frac{\mathcal{H}}{\mathcal{H}^2 - \mathcal{H}'}\gamma_{\vec{k}}'\right) + \frac{\mathcal{H}}{\mathcal{H}^2 - \mathcal{H}'}\left(-\frac{1}{k^2}\left(\alpha_{\vec{k}} - 8\pi G\beta_{\vec{k}}\right)\right)}_{\text{quadratic in first order quantities}}$$

So at the end the whole $\mathcal{R}^{(2)}$ will be of the form:

$$\boxed{\begin{aligned}\mathcal{R}_{\vec{k}}^{(2)} = \left(1 + \frac{\mathcal{H}^2}{\mathcal{H}^2 - \mathcal{H}'} + \frac{\mathcal{H}}{\mathcal{H}^2 - \mathcal{H}'}\frac{\partial}{\partial\tau}\right)\phi_{\vec{k}}^{(2)} + \int \frac{d^3\vec{p}_1 d^3\vec{p}_2}{(2\pi)^{3/2}}\delta^{(3)}(\vec{p}_1 + \vec{p}_2 - \vec{k})\cdot \\ \left\{g_1(\tau, \vec{k}, \vec{p}_1, \vec{p}_2)\mathcal{R}_{\vec{p}_1}^{(1)}\mathcal{R}_{\vec{p}_2}^{(1)} + g_2(\tau, \vec{k}, \vec{p}_1, \vec{p}_2)\mathcal{R}_{\vec{p}_1}^{(1)}\mathcal{R}_{\vec{p}_2}^{(1)\prime}\right. \\ \left. + g_3(\tau, \vec{k}, \vec{p}_1, \vec{p}_2)\mathcal{R}_{\vec{p}_1}^{(1)\prime}\mathcal{R}_{\vec{p}_2}^{(1)} + g_4(\tau, \vec{k}, \vec{p}_1, \vec{p}_2)\mathcal{R}_{\vec{p}_1}^{(1)\prime}\mathcal{R}_{\vec{p}_2}^{(1)\prime}\right\}\end{aligned}} \tag{10.8}$$

where the functions g_i depend on time and on the momenta:

$$
\begin{aligned}
g_1(\tau,\vec{k},\vec{p}_1,\vec{p}_2) =& \frac{k^4-2k^2(p_1^2+p_2^2)+3(p_1^2-p_2^2)^2}{2pk^4}\\
g_2(\tau,\vec{k},\vec{p}_1,\vec{p}_2) =& -\frac{1}{2p(p-1)p_2^2k^4(-\tau)}\left(-9p(p_1^2-p_2^2)^2+6p(p_1^2+p_2^2)k^2-(2+3p)k^4\right)+\\
&-\frac{1}{2p(p-1)p_2^2k^4}\left(3p_2^2(p-1)^2(p_1^2-p_2^2)^2-(p-1)^2(p_1^2+3p_2^2)p_2^2k^2\right)(-\tau)\\
g_3(\tau,\vec{k},\vec{p}_1,\vec{p}_2) =& g_2(\tau,\vec{k},\vec{p}_2,\vec{p}_1)\\
g_4(\tau,\vec{k},\vec{p}_1,\vec{p}_2) =& -\frac{1}{2pp_1^2p_2^2k^4}\left(3(p_1^2-p_2^2)^2(p_1^2+p_2^2)-(3(p_1^4+p_2^4)+2p_1^2p_2^2)k^2+2(p_1^2+p_2^2)k^4\right)+\\
&+\frac{1}{2p(p-1)^2p_1^2p_2^2k^4\tau^2}\left(3(p+1)(4p-1)(p_1^2-p_2^2)^2+\right.\\
&\qquad\left.-2(p+1)(4p-1)(p_1^2+p_2^2)k^2+(3-11p+18p^2)k^4\right)+\\
&+\frac{(p-1)^2\tau^2}{2p^2}
\end{aligned}
\tag{10.9}
$$

The functions g_1 and g_4 are symmetric under exchange of the last two arguments, g_2 and g_3 are not, but when summing both terms with one time derivative we recover the symmetry, as we must.

10.2 Applying Wick's theorem

The tree-level bispectrum is:

$$
\langle \mathcal{R}_{\vec{k}_1}\mathcal{R}_{\vec{k}_2}\mathcal{R}_{\vec{k}_3}\rangle = \frac{1}{2}\langle \mathcal{R}^{(1)}_{\vec{k}_1}\mathcal{R}^{(1)}_{\vec{k}_2}\mathcal{R}^{(2)}_{\vec{k}_3}\rangle + \frac{1}{2}\langle \mathcal{R}^{(1)}_{\vec{k}_1}\mathcal{R}^{(2)}_{\vec{k}_2}\mathcal{R}^{(1)}_{\vec{k}_3}\rangle + \frac{1}{2}\langle \mathcal{R}^{(2)}_{\vec{k}_1}\mathcal{R}^{(1)}_{\vec{k}_2}\mathcal{R}^{(1)}_{\vec{k}_3}\rangle \tag{10.10}
$$

$\mathcal{R}^{(2)}$ is given in (10.8). Therefore:

$$
\boxed{
\begin{aligned}
&\langle \mathcal{R}_{\vec{k}_1}\mathcal{R}_{\vec{k}_2}\mathcal{R}_{\vec{k}_3}\rangle = \frac{1}{2}\int \frac{d^3\vec{p}_1 d^3\vec{p}_2}{(2\pi)^{3/2}}\delta^{(3)}(\vec{p}_1+\vec{p}_2-\vec{k}_3)\cdot\\
&\quad\Bigg\{\langle \mathcal{R}^{(1)}_{\vec{k}_1}\mathcal{R}^{(1)}_{\vec{k}_2}\left(1+\frac{\mathcal{H}^2}{\mathcal{H}^2-\mathcal{H}'}+\frac{\mathcal{H}}{\mathcal{H}^2-\mathcal{H}'}\frac{\partial}{\partial\tau}\right)\phi^{(2)}_{\vec{k}_3}\rangle\\
&\quad+g_1(\tau,\vec{k}_3,\vec{p}_1,\vec{p}_2)\langle \mathcal{R}^{(1)}_{\vec{k}_1}\mathcal{R}^{(1)}_{\vec{k}_2}\mathcal{R}^{(1)}_{\vec{p}_1}\mathcal{R}^{(1)}_{\vec{p}_2}\rangle + g_2(\tau,\vec{k}_3,\vec{p}_1,\vec{p}_2)\langle \mathcal{R}^{(1)}_{\vec{k}_1}\mathcal{R}^{(1)}_{\vec{k}_2}\mathcal{R}^{(1)}_{\vec{p}_1}\mathcal{R}^{(1)\prime}_{\vec{p}_2}\rangle\\
&\quad+g_3(\tau,\vec{k}_3,\vec{p}_1,\vec{p}_2)\langle \mathcal{R}^{(1)}_{\vec{k}_1}\mathcal{R}^{(1)}_{\vec{k}_2}\mathcal{R}^{(1)\prime}_{\vec{p}_1}\mathcal{R}^{(1)}_{\vec{p}_2}\rangle + g_4(\tau,\vec{k}_3,\vec{p}_1,\vec{p}_2)\langle \mathcal{R}^{(1)}_{\vec{k}_1}\mathcal{R}^{(1)}_{\vec{k}_2}\mathcal{R}^{(1)\prime}_{\vec{p}_1}\mathcal{R}^{(1)\prime}_{\vec{p}_2}\rangle\Bigg\}\\
&\quad+\vec{k}_2\longleftrightarrow\vec{k}_3+\vec{k}_1\longleftrightarrow\vec{k}_3
\end{aligned}
}
\tag{10.11}
$$

We have written schematically the last two pieces, but actually it is not enough to switch the two momenta: there are some complex conjugates to take care of, and sometimes $\tau \longleftrightarrow \eta$.

We quantize as:

$$
\hat{\mathcal{R}}^{(1)}(\vec{x},\tau) = \int \frac{d^3\vec{k}}{(2\pi)^{3/2}}\left[\theta_{\vec{k}}(\tau)\hat{a}_{\vec{k}}+\theta^*_{-\vec{k}}(\tau)\hat{a}^\dagger_{-\vec{k}}\right]e^{i\vec{k}\cdot\vec{x}} \tag{10.12}
$$

with the usual modefunctions (6.30):

$$
\theta_k(\tau) = c(-\tau)^\nu H^{(1)}_\nu(-k\tau) \qquad \alpha = \frac{1+p}{2(p-1)} \qquad \nu = \frac{3p-1}{2(p-1)} \qquad \alpha = \nu - 1 \tag{10.13}
$$

When performing the contractions, we will find pieces like:

$$\begin{aligned}
\langle\hat{\mathcal{R}}^{(1)}_{\vec{q}_1}(\tau_1)\hat{\mathcal{R}}^{(1)}_{\vec{q}_2}(\tau_2)\rangle &= \theta_{q_1}(\tau_1)\theta^{*}_{q_1}(\tau_2)\delta^{(3)}(\vec{q}_1+\vec{q}_2)\equiv G_{\mathcal{R}\mathcal{R}}(q_1;\tau_1,\tau_2)\delta^{(3)}(\vec{q}_1+\vec{q}_2)\\
\langle\hat{\mathcal{R}}^{(1)}_{\vec{q}_1}(\tau_1)\hat{\mathcal{R}}^{(1)\prime}_{\vec{q}_2}(\tau_2)\rangle &= \theta_{q_1}(\tau_1)\theta^{*\prime}_{q_1}(\tau_2)\delta^{(3)}(\vec{q}_1+\vec{q}_2)\equiv G_{\mathcal{R}\mathcal{R}'}(q_1;\tau_1,\tau_2)\delta^{(3)}(\vec{q}_1+\vec{q}_2)\\
\langle\hat{\mathcal{R}}^{(1)\prime}_{\vec{q}_1}(\tau_1)\hat{\mathcal{R}}^{(1)}_{\vec{q}_2}(\tau_2)\rangle &= \theta'_{q_1}(\tau_1)\theta^{*}_{q_1}(\tau_2)\delta^{(3)}(\vec{q}_1+\vec{q}_2)\equiv G_{\mathcal{R}'\mathcal{R}}(q_1;\tau_1,\tau_2)\delta^{(3)}(\vec{q}_1+\vec{q}_2)\\
\langle\hat{\mathcal{R}}^{(1)\prime}_{\vec{q}_1}(\tau_1)\hat{\mathcal{R}}^{(1)\prime}_{\vec{q}_2}(\tau_2)\rangle &= \theta'_{q_1}(\tau_1)\theta^{*\prime}_{q_1}(\tau_2)\delta^{(3)}(\vec{q}_1+\vec{q}_2)\equiv G_{\mathcal{R}'\mathcal{R}'}(q_1;\tau_1,\tau_2)\delta^{(3)}(\vec{q}_1+\vec{q}_2)
\end{aligned} \tag{10.14}$$

10.3 Time-integrated piece

We focus first on the piece containing the time integral over the source, carried by $\phi^{(2)}$. Recall from equation (6.16):

$$\begin{aligned}
\phi^{(2)}_{\vec{k}}(\tau) &= 2^{\alpha}\left((1-p)\tau\right)^{\alpha}\left[b_J(k)J_\alpha(-k\tau)+b_Y(k)Y_\alpha(-k\tau)\right]\\
&+\frac{\pi}{4i}(-\tau)^{\alpha}\int_{\tau_i}^{\tau}d\eta(-\eta)^{1-\alpha}\left[H^{(1)}_\alpha(-k\eta)H^{(2)}_\alpha(-k\tau)-H^{(1)}_\alpha(-k\tau)H^{(2)}_\alpha(-k\eta)\right]S_{\vec{k}}(\eta)
\end{aligned} \tag{10.15}$$

The contribution from the homogeneus solution can be set to zero with the choice of the initial condition. Let's consider the inhomogeneous piece.

The source term can be rewritten in terms of $\mathcal{R}^{(1)}$ and $\mathcal{R}^{(1)\prime}$, as shown before. Schematically:

$$\begin{aligned}
S_{\vec{k}}(\eta)=&\mathcal{S}_1(\eta,\vec{k},\vec{p}_1,\vec{p}_2)\mathcal{R}^{(1)}_{\vec{p}_1}(\eta)\mathcal{R}^{(1)}_{\vec{p}_2}(\eta)+\mathcal{S}_2(\eta,\vec{k},\vec{p}_1,\vec{p}_2)\mathcal{R}^{(1)}_{\vec{p}_1}(\eta)\mathcal{R}^{(1)\prime}_{\vec{p}_2}(\eta)+\\
&\mathcal{S}_3(\eta,\vec{k},\vec{p}_1,\vec{p}_2)\mathcal{R}^{(1)\prime}_{\vec{p}_1}(\eta)\mathcal{R}^{(1)}_{\vec{p}_2}(\eta)+\mathcal{S}_4(\eta,\vec{k},\vec{p}_1,\vec{p}_2)\mathcal{R}^{(1)\prime}_{\vec{p}_1}(\eta)\mathcal{R}^{(1)\prime}_{\vec{p}_2}(\eta)
\end{aligned} \tag{10.16}$$

For example, if we consider the first contribution in (10.11) where the second order piece is associated to $\vec{k}_3$:

$$\begin{aligned}
&\langle\mathcal{R}^{(1)}_{\vec{k}_1}(\tau)\mathcal{R}^{(1)}_{\vec{k}_2}(\tau)\left(1+p+(p-1)(-\tau)\frac{\partial}{\partial\tau}\right)\phi^{(2)}_{\vec{k}_3}(\tau)\rangle=\\
&=\int\frac{d^3\vec{p}_1d^3\vec{p}_2}{(2\pi)^{3/2}}\delta^{(3)}(\vec{p}_1+\vec{p}_2-\vec{k}_3)\left(1+p+(p-1)(-\tau)\frac{\partial}{\partial\tau}\right)\Bigg\{\frac{\pi}{4i}(-\tau)^{\alpha}\cdot\\
&\quad\int_{\tau_i}^{\tau}d\eta(-\eta)^{1-\alpha}\left[H^{(1)}_\alpha(-k_3\eta)H^{(2)}_\alpha(-k_3\tau)-H^{(1)}_\alpha(-k_3\tau)H^{(2)}_\alpha(-k_3\eta)\right]\cdot\\
&\quad\Big(\mathcal{S}_1(\eta,\vec{k}_3,\vec{p}_1,\vec{p}_2)\langle\mathcal{R}^{(1)}_{\vec{k}_1}(\tau)\mathcal{R}^{(1)}_{\vec{k}_2}(\tau)\mathcal{R}^{(1)}_{\vec{p}_1}(\eta)\mathcal{R}^{(1)}_{\vec{p}_2}(\eta)\rangle+\\
&\quad\mathcal{S}_2(\eta,\vec{k}_3,\vec{p}_1,\vec{p}_2)\langle\mathcal{R}^{(1)}_{\vec{k}_1}(\tau)\mathcal{R}^{(1)}_{\vec{k}_2}(\tau)\mathcal{R}^{(1)}_{\vec{p}_1}(\eta)\mathcal{R}^{(1)\prime}_{\vec{p}_2}(\eta)\rangle+\\
&\quad\mathcal{S}_3(\eta,\vec{k}_3,\vec{p}_1,\vec{p}_2)\langle\mathcal{R}^{(1)}_{\vec{k}_1}(\tau)\mathcal{R}^{(1)}_{\vec{k}_2}(\tau)\mathcal{R}^{(1)\prime}_{\vec{p}_1}(\eta)\mathcal{R}^{(1)}_{\vec{p}_2}(\eta)\rangle+\\
&\quad\mathcal{S}_4(\eta,\vec{k}_3,\vec{p}_1,\vec{p}_2)\langle\mathcal{R}^{(1)}_{\vec{k}_1}(\tau)\mathcal{R}^{(1)}_{\vec{k}_2}(\tau)\mathcal{R}^{(1)\prime}_{\vec{p}_1}(\eta)\mathcal{R}^{(1)\prime}_{\vec{p}_2}(\eta)\rangle\Big)\Bigg\}
\end{aligned} \tag{10.17}$$

$$\begin{aligned}
&=\int\frac{d^3\vec{p}_1d^3\vec{p}_2}{(2\pi)^{3/2}}\delta^{(3)}(\vec{p}_1+\vec{p}_2-\vec{k}_3)\frac{\pi}{4i}\Bigg\{(-\tau)^{\alpha}\int_{\tau_i}^{\tau}d\eta(-\eta)^{1-\alpha}\cdot\\
&\quad(p-1)(-k_3\tau)\left(H^{(1)}_\alpha(-k_3\eta)H^{(2)}_{\alpha+1}(-k_3\tau)-H^{(1)}_{\alpha+1}(-k_3\tau)H^{(2)}_\alpha(-k_3\eta)\right)\cdot\\
&\quad\Big(\mathcal{S}_1(\eta,\vec{k}_3,\vec{p}_1,\vec{p}_2)\langle\mathcal{R}^{(1)}_{\vec{k}_1}(\tau)\mathcal{R}^{(1)}_{\vec{k}_2}(\tau)\mathcal{R}^{(1)}_{\vec{p}_1}(\eta)\mathcal{R}^{(1)}_{\vec{p}_2}(\eta)\rangle+\\
&\quad\mathcal{S}_2(\eta,\vec{k}_3,\vec{p}_1,\vec{p}_2)\langle\mathcal{R}^{(1)}_{\vec{k}_1}(\tau)\mathcal{R}^{(1)}_{\vec{k}_2}(\tau)\mathcal{R}^{(1)}_{\vec{p}_1}(\eta)\mathcal{R}^{(1)\prime}_{\vec{p}_2}(\eta)\rangle+\\
&\quad\mathcal{S}_3(\eta,\vec{k}_3,\vec{p}_1,\vec{p}_2)\langle\mathcal{R}^{(1)}_{\vec{k}_1}(\tau)\mathcal{R}^{(1)}_{\vec{k}_2}(\tau)\mathcal{R}^{(1)\prime}_{\vec{p}_1}(\eta)\mathcal{R}^{(1)}_{\vec{p}_2}(\eta)\rangle+\\
&\quad\mathcal{S}_4(\eta,\vec{k}_3,\vec{p}_1,\vec{p}_2)\langle\mathcal{R}^{(1)}_{\vec{k}_1}(\tau)\mathcal{R}^{(1)}_{\vec{k}_2}(\tau)\mathcal{R}^{(1)\prime}_{\vec{p}_1}(\eta)\mathcal{R}^{(1)\prime}_{\vec{p}_2}(\eta)\rangle\Big)\Bigg\}
\end{aligned} \tag{10.18}$$

where in the last step we have taken care of the time derivative.

Now we perform the contractions by applying Wick's theorem. We only keep connected pieces, i.e. the terms proportional to $\delta^{(3)}(\vec{k}_1+\vec{k}_2)$ will be discarded.
The parenthesis containing the vacuum expectation values gives:

$$\begin{aligned}(\dots) =&\delta^{(3)}(\vec{k}_1+\vec{k}_2)\delta^{(3)}(\vec{p}_1+\vec{p}_2)\Big(\mathcal{S}_1 G_{\mathcal{RR}}(k_1;\tau,\tau)G_{\mathcal{RR}}(p_1;\eta,\eta)+\mathcal{S}_2 G_{\mathcal{RR}}(k_1;\tau,\tau)G_{\mathcal{RR}'}(p_1;\eta,\eta)+\\ &\mathcal{S}_3 G_{\mathcal{RR}}(k_1;\tau,\tau)G_{\mathcal{R}'\mathcal{R}}(p_1;\eta,\eta)+\mathcal{S}_4 G_{\mathcal{RR}}(k_1;\tau,\tau)G_{\mathcal{R}'\mathcal{R}'}(p_1;\eta,\eta)\Big)+\\ &\delta^{(3)}(\vec{k}_1+\vec{p}_1)\delta^{(3)}(\vec{k}_2+\vec{p}_2)\Big(\mathcal{S}_1 G_{\mathcal{RR}}(k_1;\tau,\eta)G_{\mathcal{RR}}(k_2;\tau,\eta)+\mathcal{S}_2 G_{\mathcal{RR}}(k_1;\tau,\eta)G_{\mathcal{RR}'}(k_2;\tau,\eta)+\\ &\mathcal{S}_3 G_{\mathcal{RR}'}(k_1;\tau,\eta)G_{\mathcal{RR}}(k_2;\tau,\eta)+\mathcal{S}_4 G_{\mathcal{RR}'}(k_1;\tau,\eta)G_{\mathcal{RR}'}(k_2;\tau,\eta)\Big)+\\ &\delta^{(3)}(\vec{k}_1+\vec{p}_2)\delta^{(3)}(\vec{k}_2+\vec{p}_1)\Big(\mathcal{S}_1 G_{\mathcal{RR}}(k_1;\tau,\eta)G_{\mathcal{RR}}(k_2;\tau,\eta)+\mathcal{S}_2 G_{\mathcal{RR}'}(k_1;\tau,\eta)G_{\mathcal{RR}}(k_2;\tau,\eta)+\\ &\mathcal{S}_3 G_{\mathcal{RR}}(k_1;\tau,\eta)G_{\mathcal{RR}'}(k_2;\tau,\eta)+\mathcal{S}_4 G_{\mathcal{RR}'}(k_1;\tau,\eta)G_{\mathcal{RR}'}(k_2;\tau,\eta)\Big)\end{aligned} \tag{10.19}$$

When integrating over $\vec{p}_1$ and $\vec{p}_2$, the net result is a factor 2, thanks to the Dirac deltas. In fact $\mathcal{S}_1$ and $\mathcal{S}_4$ are symmetric under the exchange of the last two arguments, so they give straightforwardly two equal terms; $\mathcal{S}_2$ and $\mathcal{S}_3$ are not symmetric, but the sum of the two terms is, so when adding the pieces from both terms we find pairs of equal objects.

Finally:

$$\boxed{\begin{aligned}&\langle\mathcal{R}^{(1)}_{k_1}(\tau)\mathcal{R}^{(1)}_{k_2}(\tau)\left(1+p+(p-1)(-\tau)\frac{\partial}{\partial\tau}\right)\phi^{(2)}_{\vec{k}_3}(\tau)\rangle=\\ &\frac{1}{(2\pi)^{3/2}}\delta^{(3)}(\vec{k}_1+\vec{k}_2+\vec{k}_3)\frac{\pi}{2i}\Bigg\{(-\tau)^{\alpha}\int_{\tau_i}^{\tau}d\eta(-\eta)^{1-\alpha}\cdot\\ &(p-1)(-k_3\tau)\left(H^{(1)}_{\alpha}(-k_3\eta)H^{(2)}_{\alpha+1}(-k_3\tau)-H^{(1)}_{\alpha+1}(-k_3\tau)H^{(2)}_{\alpha}(-k_3\eta)\right)\cdot\\ &\Big(\mathcal{S}_1(\eta,\vec{k}_3,\vec{k}_1,\vec{k}_2)\theta_{k_1}(\tau)\theta_{k_2}(\tau)\theta^*_{k_1}(\eta)\theta^*_{k_2}(\eta)+\\ &\mathcal{S}_2(\eta,\vec{k}_3,\vec{k}_1,\vec{k}_2)\theta_{k_1}(\tau)\theta_{k_2}(\tau)\theta^*_{k_1}(\eta)\theta^{*\prime}_{k_2}(\eta)+\\ &\mathcal{S}_3(\eta,\vec{k}_3,\vec{k}_1,\vec{k}_2)\theta_{k_1}(\tau)\theta_{k_2}(\tau)\theta^{*\prime}_{k_1}(\eta)\theta^*_{k_2}(\eta)+\\ &\mathcal{S}_4(\eta,\vec{k}_3,\vec{k}_1,\vec{k}_2)\theta_{k_1}(\tau)\theta_{k_2}(\tau)\theta^{*\prime}_{k_1}(\eta)\theta^{*\prime}_{k_2}(\eta)\Big)\Bigg\}\end{aligned}} \tag{10.20}$$

and then I will have the terms $\vec{k}_2\longleftrightarrow\vec{k}_3$ and $\vec{k}_1\longleftrightarrow\vec{k}_3$.

10.3.1 Parametrization of the source term

We rewrote the source as in (10.16), by explicitly writing α, β, γ and their derivatives all in terms of $\mathcal{R}^{(1)}$ and $\mathcal{R}^{(1)\prime}$. Following the suggestion in [51], we rewrite everything in terms of the maginudes of the momenta, getting rid of scalar products thanks to the Dirac delta, which enforces $\vec{k}_1+\vec{k}_2+\vec{k}_3=0$. The normalization of the scale factor (6.5) has been used.

$$\mathcal{S}_1(\tau,\vec{k},\vec{p}_1,\vec{p}_2)= \tag{10.21}$$

$$\begin{aligned}&-\frac{1}{2p}\frac{1}{k^4}\left(3(p_1^2-p_2^2)^2(p_1^2+p_2^2)+(-6p_1^4-6p_2^4+4p_1^2p_2^2)k^2+3(p_1^2+p_2^2)k^4\right)+\\ &\frac{1}{\tau^2}\left[\frac{1}{(p-1)^2p}\frac{1}{k^4}\left(3(4p-1)(p_1^2-p_2^2)^2-2(4p-1)(p_1^2+p_2^2)k^2+(3+2p)k^4\right)\right]\end{aligned} \tag{10.22}$$

$$\begin{aligned}
&\mathcal{S}_2(\tau,\vec{k},\vec{p}_1,\vec{p}_2) = \\
&\quad\frac{1}{(-\tau)}\Bigg[-\frac{1}{2p(p-1)}\frac{1}{p_2^2k^4}\Big(3(p_1^2-p_2^2)^2(p_1^2+p_2^2+3pp_2^2)+ \\
&\qquad -2(3p_1^4+2(1+3p)p_2^4-p_1^2p_2^2)k^2+(3p_1^2+(1+3p)p_2^2)k^4\Big)\Bigg]+ \\
&\quad\frac{1}{(-\tau)^3}\Bigg[\frac{1}{2p(p-1)^3}\frac{1}{p_2^2k^4}\Big(3(-2+p+13p^2)(p_1^2-p_2^2)^2+ \\
&\qquad -2(-2+p+13p^2)(p_1^2+p_2^2)k^2+(6+p(-17+31p))k^4\Big)\Bigg]
\end{aligned}\tag{10.23}$$

$\mathcal{S}_2$ and $\mathcal{S}_3$ are the same up to the exchange of $\vec{p}_1 \longleftrightarrow \vec{p}_2$:

$$\mathcal{S}_3(\tau,\vec{k},\vec{p}_1,\vec{p}_2) = \mathcal{S}_2(\tau,\vec{k},\vec{p}_2,\vec{p}_1)$$

$$\begin{aligned}
&\mathcal{S}_4(\tau,\vec{k},\vec{p}_1,\vec{p}_2) = \\
&\quad-\frac{1}{p}\frac{1}{k^4}\Big(-3(p_1^2-p_2^2)^2+2(p_1^2+p_2^2)k^2+k^4\Big)+ \\
&\quad\frac{1}{\tau^2}\Bigg[\frac{1}{2p(p-1)^2}\frac{1}{p_1^2p_2^2k^4}\Big(3(1-8p)(p_1^2-p_2^2)^2(p_1^2+p_2^2)+ \\
&\qquad +2(13p(p_1^4+p_2^4)+2(-2+3p)p_1^2p_2^2)k^2-(3+14p)(p_1^2+p_2^2)k^4+4pk^6\Big)\Bigg]+ \\
&\quad\frac{1}{\tau^4}\Bigg[\frac{2}{p(p-1)^4}\frac{1}{p_1^2p_2^2k^4}\Big(3p(1+p)(-2+5p)(p_1^2-p_2^2)^2+ \\
&\qquad -2p(1+p)(-2+5p)(p_1^2+p_2^2)k^2+(1+3p-24p^2+30p^3)k^4\Big)\Bigg]
\end{aligned}\tag{10.24}$$

To compute the integrals over conformal time, it is convenient to single out the powers of time:

$$\begin{aligned}
\mathcal{S}_1 &\longrightarrow \frac{1}{\tau^2}\mathcal{S}_{1,2}+\mathcal{S}_{1,0} \\
\mathcal{S}_2 &\longrightarrow \frac{1}{(-\tau)^3}\mathcal{S}_{2,3}+\frac{1}{(-\tau)}\mathcal{S}_{2,1} \\
\mathcal{S}_3 &\longrightarrow \frac{1}{(-\tau)^3}\mathcal{S}_{3,3}+\frac{1}{(-\tau)}\mathcal{S}_{3,1} \\
\mathcal{S}_4 &\longrightarrow \frac{1}{\tau^4}\mathcal{S}_{4,4}+\frac{1}{\tau^2}\mathcal{S}_{4,2}+\mathcal{S}_{4,0}
\end{aligned}\tag{10.25}$$

where the $\mathcal{S}_{i,j}$ are functions of $\vec{k}$, $\vec{p}_1$, $\vec{p}_2$ only. Again, $\mathcal{S}_{1,j}$ and $\mathcal{S}_{4,j}$ are symmetric under the exchange $\vec{k}_1 \longleftrightarrow \vec{k}_2$ while $\mathcal{S}_{2,j}$ and $\mathcal{S}_{3,j}$ are not.

10.4 Non-integrated piece

The contribution from the remaining part of the three-point function, the one in (10.11) that does not carry the integration over time, is:

$$\langle \mathcal{R}_{\vec{k}_1}\mathcal{R}_{\vec{k}_2}\mathcal{R}_{\vec{k}_3}\rangle\Big|_{\text{non-integrated piece}} = \frac{1}{2}\int \frac{d^3\vec{p}_1 d^3\vec{p}_2}{(2\pi)^{3/2}}\delta^{(3)}(\vec{p}_1+\vec{p}_2-\vec{k}_3)\cdot$$
$$\Big\{g_1(\tau,\vec{k}_3,\vec{p}_1,\vec{p}_2)\langle \mathcal{R}^{(1)}_{\vec{k}_1}\mathcal{R}^{(1)}_{\vec{k}_2}\mathcal{R}^{(1)}_{\vec{p}_1}\mathcal{R}^{(1)}_{\vec{p}_2}\rangle + g_2(\tau,\vec{k}_3,\vec{p}_1,\vec{p}_2)\langle \mathcal{R}^{(1)}_{\vec{k}_1}\mathcal{R}^{(1)}_{\vec{k}_2}\mathcal{R}^{(1)}_{\vec{p}_1}\mathcal{R}^{(1)\prime}_{\vec{p}_2}\rangle$$
$$+ g_3(\tau,\vec{k}_3,\vec{p}_1,\vec{p}_2)\langle \mathcal{R}^{(1)}_{\vec{k}_1}\mathcal{R}^{(1)}_{\vec{k}_2}\mathcal{R}^{(1)\prime}_{\vec{p}_1}\mathcal{R}^{(1)}_{\vec{p}_2}\rangle + g_4(\tau,\vec{k}_3,\vec{p}_1,\vec{p}_2)\langle \mathcal{R}^{(1)}_{\vec{k}_1}\mathcal{R}^{(1)\prime}_{\vec{k}_2}\mathcal{R}^{(1)\prime}_{\vec{p}_1}\mathcal{R}^{(1)}_{\vec{p}_2}\rangle\Big\}$$
$$+\vec{k}_2 \longleftrightarrow \vec{k}_3 + \vec{k}_1 \longleftrightarrow \vec{k}_3$$

As before, applying Wick's theorem and integrating over $\vec{p}_1$, $\vec{p}_2$:

$$\begin{aligned}\frac{1}{(2\pi)^{3/2}}\delta^{(3)}(\vec{k}_1+\vec{k}_2+\vec{k}_3)\Big\{&g_1(\tau,\vec{k}_3,\vec{k}_1,\vec{k}_2)\theta_{k_1}(\tau)\theta_{k_2}(\tau)\theta^*_{k_1}(\tau)\theta^*_{k_2}(\tau)+\\
&g_2(\tau,\vec{k}_3,\vec{k}_1,\vec{k}_2)\theta_{k_1}(\tau)\theta_{k_2}(\tau)\theta^*_{k_1}(\tau)\theta^{*\prime}_{k_2}(\tau)+\\
&g_3(\tau,\vec{k}_3,\vec{k}_1,\vec{k}_2)\theta_{k_1}(\tau)\theta_{k_2}(\tau)\theta^{*\prime}_{k_1}(\tau)\theta^*_{k_2}(\tau)+\\
&g_4(\tau,\vec{k}_3,\vec{k}_1,\vec{k}_2)\theta_{k_1}(\tau)\theta_{k_2}(\tau)\theta^{*\prime}_{k_1}(\tau)\theta^{*\prime}_{k_2}(\tau)\Big\}\\
+\vec{k}_2 \longleftrightarrow \vec{k}_3 + \vec{k}_1 \longleftrightarrow \vec{k}_3&\end{aligned} \tag{10.26}$$

The functions g_i have been given in (10.9).

10.5 Full bispectrum

We should now put together the time-integrated and the non-integrated pieces. Schematically:

$$\begin{aligned}&\langle \mathcal{R}_{\vec{k}_1}\mathcal{R}_{\vec{k}_2}\mathcal{R}_{\vec{k}_3}\rangle\\
&= \frac{1}{(2\pi)^{3/2}}\delta^{(3)}(\vec{k}_1+\vec{k}_2+\vec{k}_3)\Bigg\{i\frac{\pi}{2}(cc^*)^2 k_3(p-1)(-\tau)^{-4+3\nu}H^{(1)}_\nu(-k_1\tau)H^{(1)}(-k_2\tau)\cdot\\
&\int_{\tau_i}^{\tau_f} d\eta(-\eta)^{2+\nu}\Big(H^{(1)}_\nu(-k_3\tau)H^{(2)}_{\nu-1}(-k_3\eta) - H^{(1)}_{\nu-1}(-k_3\eta)H^{(2)}_\nu(-k_3\tau)\Big)\cdot\\
&\quad\Big\{\Big((-\tau)^4\mathcal{S}_{1,0}(\vec{k}_3,\vec{k}_1,\vec{k}_2)+(-\tau)^2\mathcal{S}_{1,2}(\vec{k}_3,\vec{k}_1,\vec{k}_2)\Big)H^{(2)}_\nu(-k_1\eta)H^{(2)}_\nu(-k_2\eta)+\\
&\quad\Big(-k_2(-\tau)^3\mathcal{S}_{2,1}(\vec{k}_3,\vec{k}_1,\vec{k}_2)-k_2(-\tau)\mathcal{S}_{2,3}(\vec{k}_3,\vec{k}_1,\vec{k}_2)\Big)H^{(2)}_\nu(-k_1\eta)H^{(2)}_{\nu-1}(-k_2\eta)+\\
&\quad\Big(-k_1(-\tau)^3\mathcal{S}_{3,1}(\vec{k}_3,\vec{k}_1,\vec{k}_2)-k_1(-\tau)\mathcal{S}_{3,3}(\vec{k}_3,\vec{k}_1,\vec{k}_2)\Big)H^{(2)}_{\nu-1}(-k_1\eta)H^{(2)}_\nu(-k_2\eta)+\\
&\quad\Big(k_1k_2(-\tau)^4\mathcal{S}_{4,0}(\vec{k}_3,\vec{k}_1,\vec{k}_2)+k_1k_2(-\tau)^2\mathcal{S}_{4,2}(\vec{k}_3,\vec{k}_1,\vec{k}_2)+\\
&\qquad+k_1k_2\mathcal{S}_{4,4}(\vec{k}_3,\vec{k}_1,\vec{k}_2)\Big)H^{(2)}_{\nu-1}(-k_1\eta)H^{(2)}_{\nu-1}(-k_2\eta)\Big\}+\\
&g_1(\tau,\vec{k}_3,\vec{k}_1,\vec{k}_2)\theta_{k_1}(\tau)\theta_{k_2}(\tau)\theta^*_{k_1}(\tau)\theta^*_{k_2}(\tau)+g_2(\tau,\vec{k}_3,\vec{k}_1,\vec{k}_2)\theta_{k_1}(\tau)\theta_{k_2}(\tau)\theta^*_{k_1}(\tau)\theta^{*\prime}_{k_2}(\tau)+\\
&g_3(\tau,\vec{k}_3,\vec{k}_1,\vec{k}_2)\theta_{k_1}(\tau)\theta_{k_2}(\tau)\theta^{*\prime}_{k_1}(\tau)\theta^*_{k_2}(\tau)+g_4(\tau,\vec{k}_3,\vec{k}_1,\vec{k}_2)\theta_{k_1}(\tau)\theta_{k_2}(\tau)\theta^{*\prime}_{k_1}(\tau)\theta^{*\prime}_{k_2}(\tau)\Bigg\}\\
&+\vec{k}_2 \longleftrightarrow \vec{k}_3 + \vec{k}_1 \longleftrightarrow \vec{k}_3\end{aligned} \tag{10.27}$$

As before, we need to integrate three Hankel functions times some power of conformal time. One can try to set a cutoff and approximate to superhorizon scales, as attempted before in the in-in formalism framework. The calculation is reported in Appendix B.

The final result of this calculation is not yet ready to be compared with the in-in formalism approach: there are some additional contribution, due to the different definitions of the gauge-invariant variables ζ and $\mathcal{R}$.

10.6 Comparison between the two approaches

The variable ζ as defined by Maldacena in the gauge (8.4) is equivalent to $\mathcal{R}$ at the linear level and on superhorizon scales. We refer to [28] for a discussion about the different conventions used in the literature, however at the linear level the definitions of $\mathcal{R}$ and of ζ all agree, up to a sign. But, when we go to second order, things change. Maldacena [27] defines the variable through an exponential, Acquaviva *et al.* [22] use a different variable.

Let us first consider these two definitions:

$$e^{2\zeta_M} = 1 + 2\zeta_M + 2\zeta_M^2 + \mathcal{O}(\zeta^3) \qquad\qquad 1 + \zeta^{(1)} + \frac{1}{2}\zeta^{(2)} + \mathcal{O}(\zeta^3) \tag{10.28}$$

Comparing the two, up to second order we can write the following relation:

$$\zeta_M \simeq \zeta^{(1)} + \frac{1}{2}\zeta^{(2)} - \left(\zeta^{(1)}\right)^2 \tag{10.29}$$

The bispectra are related as:

$$\langle \zeta_{M,\vec{k}_1}\zeta_{M,\vec{k}_2}\zeta_{M,\vec{k}_3}\rangle = \frac{1}{2}\langle \zeta^{(1)}_{\vec{k}_1}\zeta^{(1)}_{\vec{k}_2}\zeta^{(2)}_{\vec{k}_3}\rangle + 2 \text{ perm.} - \langle \zeta^{(1)}_{\vec{k}_1}\zeta^{(1)}_{\vec{k}_2}\left(\zeta^{(1)}\right)^2_{\vec{k}_3}\rangle + 2 \text{ perm.} \tag{10.30}$$

so there is an additional contribution.

Acquaviva *et al.* worked in terms of the gauge-invariant variable $\mathcal{R}$. As pointed out in [52], in the uniform field or comoving gauge where $\delta\varphi = 0$ we have:

$$\zeta_M = \mathcal{R}_A^{(1)} + \left(\mathcal{R}_A^{(1)}\right)^2 + \frac{1}{2}\mathcal{R}_A^{(2)} - \frac{1}{2}\frac{\left(\mathcal{R}_A^{(1)\prime} + 2\mathcal{H}\mathcal{R}_A^{(1)}\right)^2}{\mathcal{H}' + 2\mathcal{H}^2 - \mathcal{H}\frac{\varphi_0''}{\varphi_0'}} \tag{10.31}$$

the last correction term comes from the fact that $\mathcal{R}_A^{(2)}$ is not the curvature perturbation defined on comoving hypersurfaces, as one can verify by setting $\delta\varphi = 0$ in the definition, and fails to be conserved on large scales.

Therefore:

$$\langle \zeta_M\zeta_M\zeta_M\rangle = \frac{1}{2}\langle \mathcal{R}_A^{(1)}\mathcal{R}_A^{(1)}\mathcal{R}_A^{(2)}\rangle + \langle \mathcal{R}_A^{(1)}\mathcal{R}_A^{(1)}\left(\mathcal{R}_A^{(1)}\right)^2\rangle - \frac{1}{2}\langle \mathcal{R}_A^{(1)}\mathcal{R}_A^{(1)}\frac{\left(\mathcal{R}_A^{(1)\prime} + 2\mathcal{H}\mathcal{R}_A^{(1)}\right)^2}{\mathcal{H}' + 2\mathcal{H}^2 - \mathcal{H}\frac{\varphi_0''}{\varphi_0'}}\rangle + 2 \text{ perm.} \tag{10.32}$$

One can check that, even taking care of these additional contributions, the result shown in the Appendix (B.31) still does not match the slow-roll limit (5.19): the coefficients of the momenta are different. This could be due to the integration procedure: as we have seen before, setting a cutoff and only looking at superhorizon scales may be an intrinsically flawed procedure. This is a delicate point and it is worthy of further investigation.

Chapter 11

Climbing scalars

We now turn to the second part of this work, devoted to the analysis of a particular model for the onset of inflation. The final goal will be to have a prediction for non-Gaussianity in this class of models, here we will only present the first part of this project. We will study numerically the power-spectrum for one of these models and discuss the expectations for the next steps.

11.1 Starting point: CMB anomalies

One of the anomalies in the CMB is the lack of power at large angular scales: with respect to ΛCDM, there is a lack of power in the two-point correlation function of temperature anisotropies for angles larger than $\sim 60°$, with a typical 2 to 3σ significance. This was already noticed by COBE and later confirmed by WMAP and Planck, see [53] and references therein.
The CMB temperature power-spectrum is shown in Figure 11.1, the region we are interested in is the low-ℓ region, corresponding to the largest angular scales. They correspond to the first wavelengths that exited the horizon during the inflationary epoch[1].

This anomaly can be explained as statistical fluctuation, but only if one accepts to be living in a very particular realization of the ΛCDM model. We cannot blame systematics because different experiments confirmed the effect. Furthermore, we cannot ascribe the effect to residual foreground emission, because this should increase the power rather than reduce it, and the significance of the anomaly grows when extending the Galactic mask which is a very conservative choice [53].

For completeness, we mention that there are two main possibilities in suppressing the low ℓ amplitudes [3]:

- play with physics of the inflationary phase in the early Universe, in particular choose kinetic-dominated initial conditions at the onset of inflation. The key point is the existence of a stage

[1]Let's make contact between the wavenumber k and the angular scale ℓ. In the flat sky approximation, if $D_{\rm LS}$ is the comoving distance to the last scattering surface, a comoving length $l_{\rm com}$ at last scattering subtends an angle on the sky:

$$\theta = \frac{l_{\rm com}}{D_{\rm LS}} \tag{11.1}$$

This is to be calibrated on the sound horizon, with Planck results [54]:

$$\theta_s = \frac{r_s}{d_A(z_s)} \qquad r_s = 144.71 \pm 0.60 \text{ Mpc}, \ \theta_s = (1.04131 \pm 0.00062) \times 10^{-2} \tag{11.2}$$

Using $l_{\rm com} \sim \frac{\pi}{k}$ and $\theta \sim \frac{\pi}{\ell}$, we obtain:

$$\ell \sim k d_A \tag{11.3}$$

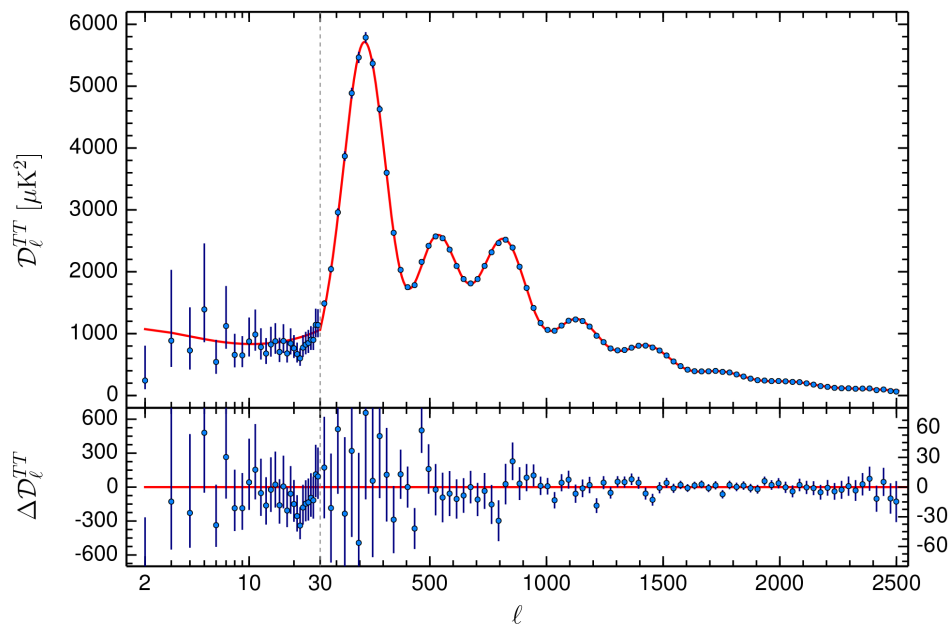

Figure 11.1: Planck 2015 CMB power-spectrum of temperature fluctuations, compared with the base ΛCDM fit, and residuals. From [55].

during which the velocity of the scalar field is not negligible, either before or during the observed 65 e-folds, so the usual slow-roll approach breaks down in that regime;

- attribute the suppression to late Universe physics, under the influence of an effective cosmological constant. This would relate the suppression of CMB anisotropy power at horizon scales $\sim H^{-1}$ to the smallness of the cosmological constant, which becomes dominant precisely at times $\sim H^{-1}$. In this scenario, late time acceleration and low power on largest scales seem two unrelated problems are linked in a "why now?" problem.

Of course in the following we will focus on the first one.

The primordial power-spectrum is usually parametrized in terms of an amplitude A_s and a tilt $n_s - 1$ as:

$$\mathcal{P}_\zeta(k) = A_s \left(\frac{k}{k_*}\right)^{n_s-1} \tag{11.4}$$

where k_* is a pivot scale. As we have already mentioned, Planck measures [31]:

$$A_s = \left(2.101^{+0.031}_{-0.034}\right) \times 10^{-9} \qquad n_s = 0.9649 \pm 0.0042 \qquad \text{at } 68\%,\ k_* = 0.05\ \text{Mpc}^{-1} \tag{11.5}$$

Lack of power at large angular scales is a typical manifestation of early departures from slow-roll, which follow naturally the emergence from an initial singularity. When this happens, the power-spectrum approaches a limiting behaviour in the infrared [53, 56, 57]:

$$\boxed{\mathcal{P}_\zeta(k) = A_s \frac{k^3}{(k^2 + \Delta^2)^{2-\frac{n_s}{2}}}} \tag{11.6}$$

where Δ is a new physical scale that enters into play and controls the transition from large-scale depression to the usual $n_s - 1$ tilt. The new scale Δ could be around 10^{-4} Mpc^{-1}.

Comparison is shown in Figure 11.2, where 11.2a is the case of a perfect scale invariance.

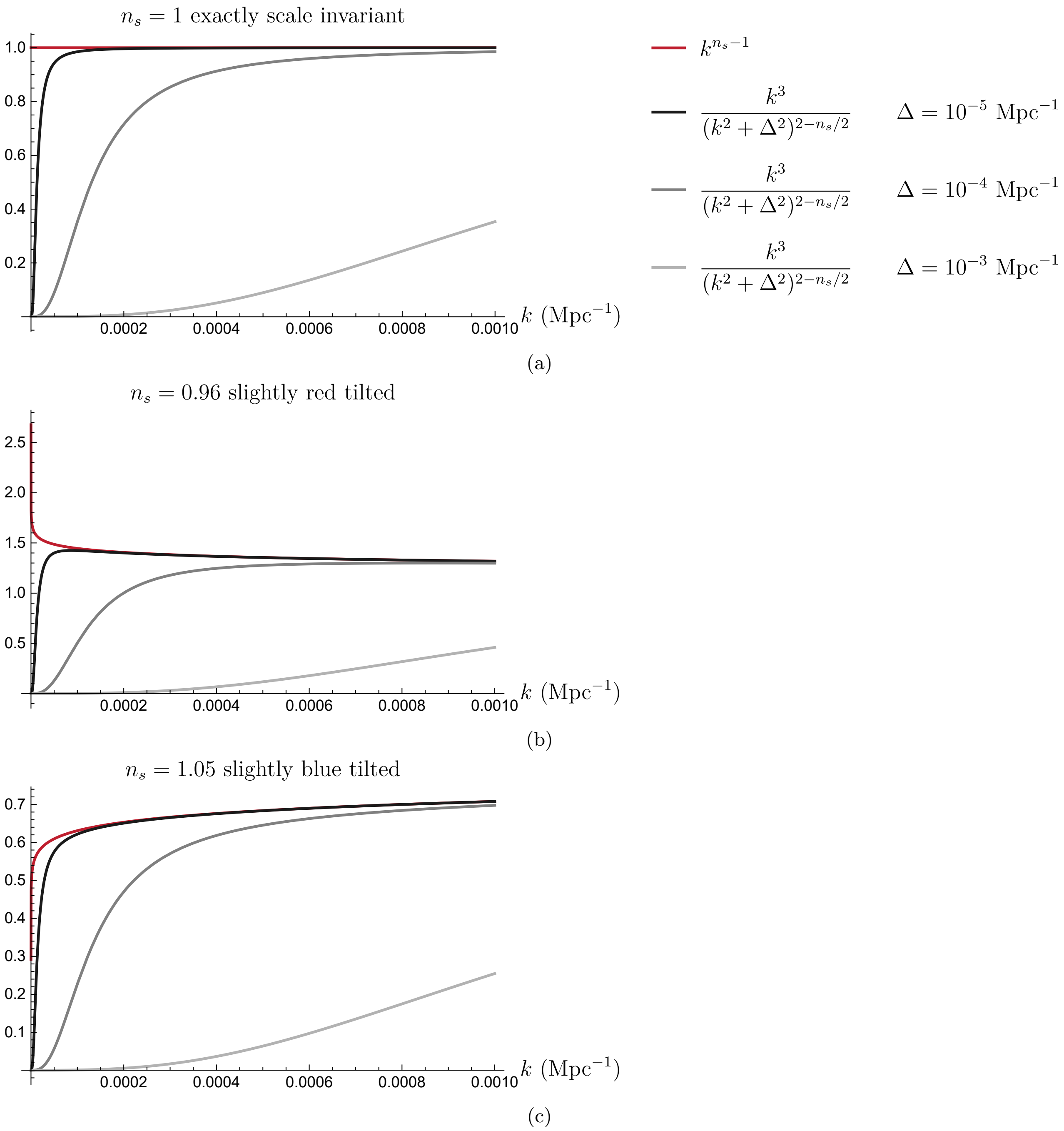

Figure 11.2: Comparison between the usual power law power-spectrum and the modified one.

11.2 Climbing scalars

A fascinating way to obtain a power-spectrum like (11.6) relies on the phenomenon of "climbing scalars". These arise in String Theory in a supersymmetry breaking scenario, which leaves behind a leading exponential potential for a ubiquitous scalar degree of freedom, the dilaton ϕ, playing here the role of the inflaton. Under certain conditions on the exponent, the scalar can be compelled to emerge from the Big Bang while climbing up an exponential potential, then bounce back and slowly roll down, thus injecting an inflationary phase. This happens for certain "critical" value of the exponent [1,2] and beyond, and String Theory gives a sharp prediction for the exponent of the potential. Remarkably, the transition occurs precisely at the value that is characteristic of orientifold models with "brane supersymmetry breaking". In this fashion, in their early Cosmology there is an upper bound for the value of $g_s = e^{\phi}$, which is also the coupling constant of String Theory.

In String Theory, one has to deal with a perturbation theory involving two parameters: the string coupling constant g_s, and the ratio between the string characteristic scale and the curvature radius of the background geometry l_s/R. Recall that $l_s = \sqrt{\alpha'}$, where the string tension is defined as $1/2\pi\alpha'$. There may be issues with the expansion in l_s/R, especially towards the initial singularity where α' corrections are in principle large, but the perturbative expansion in g_s is well under control thanks to the climbing mechanism.

There are other reasons why these kind of models are interesting.
Naively, one could ask why the inflaton should be bound to slowly roll, when in the Early Universe everything is moving "fast". The climbing scalar models provide a natural mechanism to reach inflation, starting from kinetic-dominated initial conditions, and to give inflation its initial impetus: the scalar slows down while climbing, and if the key top-down exponential is supplemented by another mild term, inflation can start in the ensuing descent.
In this fashion, these models motivate a new class of phenomena where inflation begins off the attractor. Numerical solutions show [2] that it is far less efficient to inflate off the attractor than on it, but nonetheless it happens, and as the scalar looses its energy due to cosmic friction a slow roll is attained.
Finally, the claim behind these models is that we may be observing, on the largest scales, something other than inflation, maybe a pre-inflationary phase. This would imply that inflation did not last much longer than the approximately 60 e-folds needed to solve the horizon and flatness problems. As we have already mentioned, this is connected to one of the most challenging issues arising in the EFT approach to inflation, the "η-problem".

We will now follow [1, 2] to illustrate the climbing phenomenon in the simplest model, consisting in two exponential potentials. See also [58] and the class of integrable models in [59], which contain analytic solutions of toy models that display clearly the transition from fast-roll to slow-roll via the climbing. There are many other ways to achieve the climbing, since it is a universal phenomenon that presents itself whenever the potential grows as $e^{\gamma\phi}$, with $\gamma > \gamma_c$, in an asymptotic region. Hence, if the Starobinsky model is complemented by one such potential, climbing along it is inevitable, and the ensuing descent combines slow-roll with the final oscillations in the well that end inflation. In this fashion, one can provide a good fits to the CMB data [56], compatibly with small values of the tensor-to-scalar ratio.

11.3 A simple model

Consider the class of low energy, four-dimensional actions for a single scalar field coupled to gravity:

$$S = \int d^4x\sqrt{-g}\left\{M_P^2\frac{R}{2} - \frac{1}{2}(\partial\varphi)^2 - V(\varphi) + ...\right\} \tag{11.7}$$

We focus on spatially flat cosmology, for which the standard Friedmann-Lemaître-Robetrson Walker metric reads:

$$ds^2 = -dt^2 + a^2(t)d\vec{x}\cdot d\vec{x} \tag{11.8}$$

It will be useful to generalize this metric, considering a wider class:

$$ds^2 = -e^{2\mathcal{B}(x)}dx^2 + e^{2A(x)}d\vec{x}\cdot d\vec{x} \tag{11.9}$$

which involves a "gauge function" $\mathcal{B}$, and the scale factor has been written as $a = e^A$. The "parametric time" x and the actual cosmic time t measured by comoving observers are related through the function $\mathcal{B}$:

$$dt = \pm e^{\mathcal{B}(x)}dx \tag{11.10}$$

We will work with dimensionless variables:

$$dx = \frac{\sqrt{3V}}{M_P}dt \qquad \chi = \frac{1}{M_P}\sqrt{\frac{3}{2}}\varphi \qquad A = \frac{\mathcal{A}}{3} \tag{11.11}$$

Making the gauge choice:

$$V e^{2\mathcal{B}} = V_0 \tag{11.12}$$

the Friedmann equation and the Klein-Gordon equation become:

$$\frac{d\mathcal{A}}{dx} = \sqrt{1 + \left(\frac{d\chi}{dx}\right)^2} \tag{11.13}$$

$$\frac{d^2\chi}{dx^2} + \frac{d\chi}{dx}\sqrt{1 + \left(\frac{d\chi}{dx}\right)^2} + \left[1 + \left(\frac{d\chi}{dx}\right)^2\right] \frac{1}{2V}\frac{\partial V}{\partial \chi} = 0 \tag{11.14}$$

A simple model that can experience the climbing is:

$$V = V_0 \left(e^{\sqrt{6}\varphi/M_P} + e^{\sqrt{6}\gamma\varphi/M_P}\right) = V_0 \left(e^{2\chi} + e^{2\gamma\chi}\right) \qquad 0 < \gamma < 1 \tag{11.15}$$

Here the first contribution is the "hard" exponential from String Theory, left behind by brane supersymmetry breaking. The scalar is forced to emerge from the initial singularity while climbing up the mild part of the potential, the second term, until it bounces against the String Theory wall, reverts its motion and rolls back. The second term alone would give rise to Lucchin-Matarrese power-law inflation [4], it is a "phenomenological" term that needs to be added in order for the scalar to drive inflation at late times if $\gamma < 1/\sqrt{3}$. The initial climbing and reversal phases are the ones that can leave imprints on the largest angular scales and cause the suppression (11.6).
The dynamics is determined by a single parameter, characterizing to which extent the scalar field feels the impact with the steep portion of the potential.

11.3.1 Analytic solutions for the single exponential

Analytic solutions can be obtained for the class of single exponential potentials:

$$V = V_0 e^{2\gamma\chi} \tag{11.16}$$

Equations (11.13) and (11.14) become:

$$\left(\frac{d\mathcal{A}}{dx}\right)^2 - \left(\frac{d\chi}{dx}\right)^2 = 1 \tag{11.17}$$

$$\frac{d^2\chi}{dx^2} + \frac{d\chi}{dx}\sqrt{1 + \left(\frac{d\chi}{dx}\right)^2} + \gamma\left[1 + \left(\frac{d\chi}{dx}\right)^2\right] = 0 \tag{11.18}$$

Notice that the equation for χ is effectively of first order. Furthermore, up to a field redefinition $\chi \mapsto -\chi$, we can restrict ourselves to positive values of γ.

Equation (11.18) has an interesting analogy: it resembles the motion of a Newtonian particle in a viscous medium, subject to a constant force [1]. The equation of motion is:

$$m\dot{v}(t) + bv(t) = f \qquad\qquad v(t) = (v_0 - v_l)e^{-\frac{bt}{m}} + v_l \tag{11.19}$$

where $v_l = f/b$ is the limiting speed. As long as b is finite, there are two branches of solutions, depending on whether the initial velocity v_0 is larger or smaller than v_l. As $b \to 0$, the upper branch disappears.
In our case too there are two branches of cosmological solutions if $\gamma < 1$, the climbing solution being the branch that corresponds to $v_0 < v_l$. When we reach the "critical" value $\gamma = 1$, the descending branch ceases to exist and only the climbing one is left.

We can solve the system (11.17)-(11.18) via the substitution:

$$\frac{d\mathcal{A}}{dx} = \cosh f \qquad\qquad \frac{d\chi}{dx} = \sinh f \tag{11.20}$$

Case $0 < \gamma < 1$

There are two classes of solutions:

$$\left.\frac{d\chi}{dx}\right|_c = \frac{1}{2}\left[\sqrt{\frac{1-\gamma}{1+\gamma}}\coth\left(\frac{x}{2}\sqrt{1-\gamma^2}\right) - \sqrt{\frac{1+\gamma}{1-\gamma}}\tanh\left(\frac{x}{2}\sqrt{1-\gamma^2}\right)\right] \tag{11.21}$$

$$\left.\frac{d\chi}{dx}\right|_d = \frac{1}{2}\left[\sqrt{\frac{1-\gamma}{1+\gamma}}\tanh\left(\frac{x}{2}\sqrt{1-\gamma^2}\right) - \sqrt{\frac{1+\gamma}{1-\gamma}}\coth\left(\frac{x}{2}\sqrt{1-\gamma^2}\right)\right] \tag{11.22}$$

which, recalling that $\coth x - \text{csch} x = \tanh(x/2)$, can also be rewritten as:

$$\left.\frac{d\chi}{dx}\right|_c = -\frac{1}{\sqrt{1-\gamma^2}}\left[\gamma\coth\left(x\sqrt{1-\gamma^2}\right) - \text{csch}\left(x\sqrt{1-\gamma^2}\right)\right] \tag{11.23}$$

$$\left.\frac{d\chi}{dx}\right|_d = -\frac{1}{\sqrt{1-\gamma^2}}\left[\gamma\coth\left(x\sqrt{1-\gamma^2}\right) + \text{csch}\left(x\sqrt{1-\gamma^2}\right)\right] \tag{11.24}$$

Equation (11.21) describes a scalar field that emerges from the initial singularity *climbing up* the exponential potential, then reverts its motion and eventually climbs down, while (11.22) describes a field that emerges *climbing down* or descending. Both are shown in Figure 11.3. The system possesses a double $\mathbb{Z}_2$ symmetry, it is left unchanged by the simultaneous transformation $\chi \mapsto -\chi$ and $\gamma \mapsto -\gamma$. This maps the two solutions into each other. The climbing solutions (11.21) initially climb up, then revert their motion and go down. The stationary point depends on the value of γ: the larger it is, the sooner in parametric time the solution reverses its motion. In our mechanical analogy, the climbing solution would correspond to the branch $v_0 < v_l$.

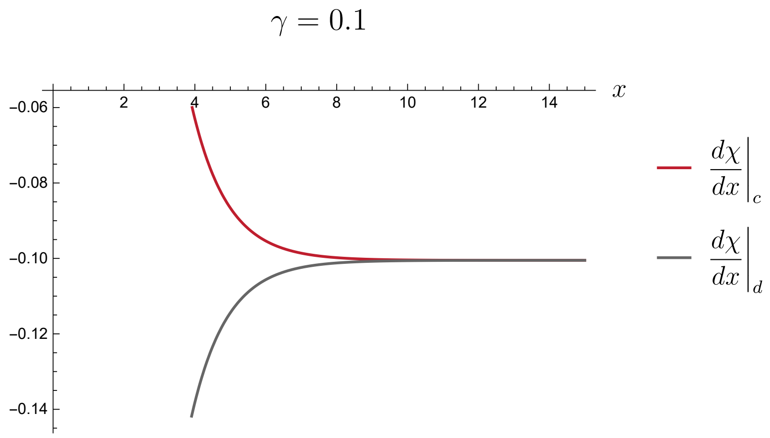

Figure 11.3: The climbing and descending solutions (11.21) and (11.22). Notice the analogy with the Newtonian system. Both solution converge asymptotically to the limiting speed.

Close to the initial singularity:

$$\frac{d\chi}{dx} \sim \pm\frac{1}{(1\pm\gamma)x} \tag{11.25}$$

but in terms of cosmic time the dependence on γ disappears and the dynamics is initially dominated by the kinetic terms:

$$\frac{d\chi}{dt} \sim \pm\frac{1}{t} \tag{11.26}$$

In particular, we will focus on the climbing solution, for which the scale factor is given by:

$$\frac{d\mathcal{A}}{dx} = \frac{1}{2}\left[\sqrt{\frac{1-\gamma}{1+\gamma}}\coth\left(\frac{x}{2}\sqrt{1-\gamma^2}\right) + \sqrt{\frac{1+\gamma}{1-\gamma}}\tanh\left(\frac{x}{2}\sqrt{1-\gamma^2}\right)\right] \tag{11.27}$$

The corresponding solutions are:

$$\chi(x) = \chi_0 + \frac{1}{1+\gamma}\log \sinh\left(\frac{x}{2}\sqrt{1-\gamma^2}\right) - \frac{1}{1-\gamma}\log \cosh\left(\frac{x}{2}\sqrt{1-\gamma^2}\right) \tag{11.28}$$

$$\mathcal{A}(x) = \mathcal{A}_0 + \frac{1}{1+\gamma}\log \sinh\left(\frac{x}{2}\sqrt{1-\gamma^2}\right) + \frac{1}{1-\gamma}\log \cosh\left(\frac{x}{2}\sqrt{1-\gamma^2}\right) \tag{11.29}$$

Notice that the integration constant $\mathcal{A}_0$ can be set to zero up to a rescaling of the spatial coordinates. Instead, the integration constant χ_0 does play an important role in dynamics. The solution is shown in Figure 11.4.

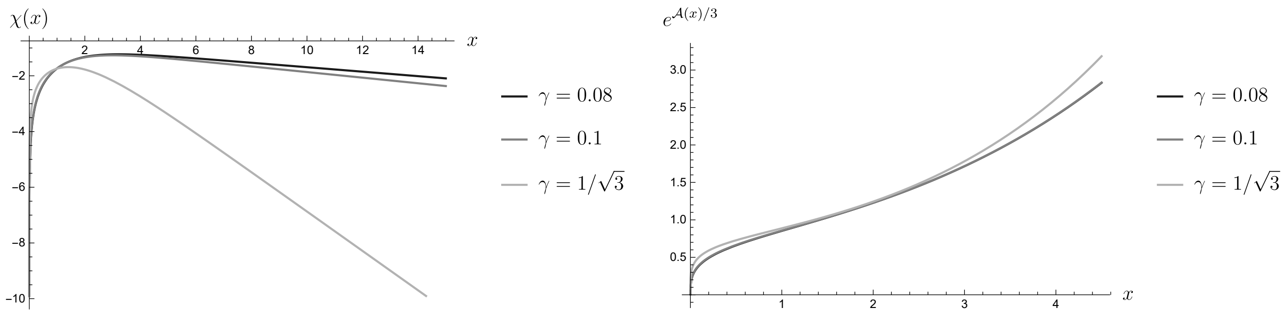

(a) (b)

Figure 11.4: Climbing solution for different values of γ, the field $\chi(x)$ on the left and the scale factor $a(x)$ on the right. The initial value has been set to $\chi_0 = -1$.

In [56] the behaviour of the solutions (11.29), (11.28) close to the initial singularity $x \to 0$ was studied.

$$\chi(x) \overset{x\to 0}{\sim} \chi_0 + \frac{1}{1+\gamma}\log\left(\frac{x}{2}\sqrt{1-\gamma^2}\right) \tag{11.30}$$

$$\mathcal{A}(x) \overset{x\to 0}{\sim} a_0 + \frac{1}{1+\gamma}\log\left(\frac{x}{2}\sqrt{1-\gamma^2}\right) \tag{11.31}$$

This approximation holds very well also in the case of the double exponential potential: in fact, the first phase is mostly sensitive to the mild portion of the potential, the one depending on $e^{2\gamma\chi}$.
The climbing phase ends at a turning point whose location, sensitive to χ_0, determines to which extent the scalar feels the first, "hard" exponential while reverting to a descending phase. Eventually, if $\gamma < 1/\sqrt{3}$, the Universe will attain an accelerated expansion, again largely under the spell of the mild exponential alone.

Lucchin-Matarrese attractor

For $0 < \gamma < 1$, there is a special exact solution: the Lucchin-Matarrese attractor [4]. Both classes of solution eventually approach in parametric time a *limiting speed*:

$$\frac{d\chi}{dx} = -\frac{\gamma}{\sqrt{1-\gamma^2}} \qquad\qquad \frac{d\mathcal{A}}{dx} = \frac{1}{\sqrt{1-\gamma^2}} \tag{11.32}$$

We can derive this limiting speed by requiring $\frac{d\chi}{dx}$ =const.

In cosmic time:

$$\chi(t) = -\frac{1}{\gamma}\log\left(\frac{\gamma^2}{\sqrt{1-\gamma^2}}\frac{\sqrt{3V_0}}{M_P}t\right) \tag{11.33}$$

$$a(t) = e^{\frac{\chi_0}{3\gamma}}\left(\frac{\sqrt{3V_0}}{M_P}\frac{\gamma^2}{\sqrt{1-\gamma^2}}\right)^{1/3\gamma^2} t^{1/3\gamma^2} \tag{11.34}$$

This is indeed power-law inflation $a(t) \propto t^p$ with $p = 1/3\gamma^2$ as in [15].

In conformal time:

$$\tau - \tau_0 = -\frac{M_P e^{-\gamma\chi_0}}{\sqrt{V_0}} \frac{\sqrt{3(1-\gamma^2)}}{1-3\gamma^2} e^{-\frac{1-3\gamma^2}{\sqrt{1-\gamma^2}}x} \tag{11.35}$$

Recall that τ is negative, according to our convention. The behaviour $\tau(x)$ is displayed in Figure 11.5.

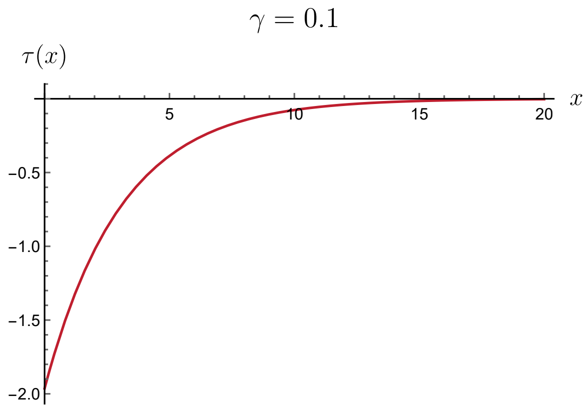

Figure 11.5: Conformal time as a function of parametric time, for the attractor solution. As before $\gamma = 0.1$, $\chi_0 = -1$ and $V_0 = M_P = 1$.

The corresponding expressions for the field and the scale factor are:

$$\chi(\tau) = \frac{\chi_0}{1-3\gamma^2} + \frac{3\gamma}{1-3\gamma^2} \log\left(\sqrt{\frac{V_0}{3M_P^2}} \frac{1-3\gamma^2}{\sqrt{1-\gamma^2}}(-\tau)\right) \tag{11.36}$$

$$a(\tau) = e^{-\frac{\gamma\chi_0}{1-3\gamma^2}} \left(\sqrt{\frac{3M_P^2}{V_0}} \frac{\sqrt{1-\gamma^2}}{1-3\gamma^2}\right)^{\frac{1}{1-3\gamma^2}} (-\tau)^{-\frac{1}{1-3\gamma^2}} \tag{11.37}$$

that is, we recover (2.32) for the field, and the scale factor has the correct behaviour $a(\tau) \propto (-\tau)^{\frac{p}{1-p}}$.

The limiting speed and the Lucchin-Matarrese attractor cease to exist when $\gamma \to 1^-$, in which case the initial climbing phase of the second solution tends to shrink more and more towards the origin and disappear. A single class of solutions remains, describing a climbing scalar.

About the scale factor normalization

Following [13], the definition of the scale factor should be, more rigorously:

$$a(t) = a_* \left[1 + \frac{H_*(t-t_*)}{p}\right]^p \tag{11.38}$$

since this returns exactly de Sitter in the $p \to \infty$ limit. In conformal time:

$$\tau = \int \frac{dt}{a(t)}$$

$$\tau - \tau_* = -\frac{p}{a_* H_*(p-1)} \left(1 + \frac{H_*(t-t_*)}{p}\right)^{1-p}$$

$$a(\tau) = a_* \left[\frac{a_* H_*(1-p)(\tau - \tau_*)}{p}\right]^{\frac{p}{1-p}} \tag{11.39}$$

What is a_*? Another way to fix the normalization is via the background equation of motion for the field, with $a(\tau) = A(-\tau)^{\frac{p}{1-p}}$:

$$\varphi_0'' + 2\mathcal{H}\varphi_0' + a^2 \frac{\partial V}{\partial \varphi} = 0 \tag{11.40}$$

This way we find, as before:

$$A = \left(e^{-\gamma\chi_0} \sqrt{\frac{3M_P^2}{V_0}} \frac{\sqrt{1-\gamma^2}}{1-3\gamma^2} \right)^{\frac{1}{1-3\gamma^2}} \tag{11.41}$$

Its limit for $\gamma \to 0$ is the inverse of the would-be de Sitter Hubble parameter, as expected:

$$\lim_{\gamma \to 0} A(-\tau)^{\frac{p}{1-p}} = -\frac{1}{\tau}\sqrt{\frac{3M_P^2}{V_0}} \equiv -\frac{1}{H_{\rm DS}\tau} \tag{11.42}$$

We can rewrite A in a more convenient way, getting rid of the exponent, if we collect the constants in the expression for the field, reintroducing C as in (2.32):

$$\varphi_0(\tau) = M_P \sqrt{\frac{2}{3}} \frac{3\gamma}{1-3\gamma^2} \log(-\tau) + \mathrm{C} \tag{11.43}$$

with:

$$\mathrm{C} \equiv M_P \sqrt{\frac{2}{3}} \frac{\chi_0}{1-3\gamma^2} + M_P \sqrt{\frac{2}{3}} \frac{3\gamma}{1-3\gamma^2} \log\left(\sqrt{\frac{V_0}{3M_P^2}} \frac{1-3\gamma^2}{\sqrt{1-\gamma^2}} \right) \tag{11.44}$$

The equation of motion gives:

$$A = e^{-\frac{\mathrm{C}\gamma}{M_P}\sqrt{\frac{3}{2}}} \sqrt{\frac{3M_P^2}{V_0}} \frac{\sqrt{1-\gamma^2}}{1-3\gamma^2} \tag{11.45}$$

Case $\gamma = 1$

The critical solution has a simpler form:

$$\left.\frac{d\chi}{dx}\right|_{\gamma=1} = \frac{1}{2}\left[\frac{1}{x} - x\right] \tag{11.46}$$

This is also the limit of the climbing solution in the case $\gamma < 1$ as γ approaches 1 from below, while the descending solution becomes singular.

Case $\gamma > 1$

In the "overcritical" region, only one climbing solution survives:

$$\left.\frac{d\chi}{dx}\right|_{\gamma>1} = \frac{1}{2}\left[\sqrt{\frac{\gamma-1}{\gamma+1}} \cot\left(\frac{x}{2}\sqrt{\gamma^2-1}\right) - \sqrt{\frac{\gamma+1}{\gamma-1}} \tan\left(\frac{x}{2}\sqrt{\gamma^2-1}\right)\right] \tag{11.47}$$

Near the initial singularity:

$$\left.\frac{d\chi}{dx}\right|_{\gamma>1} \sim \frac{1}{(1+\gamma)x} \tag{11.48}$$

This time though the parametric time x only lives in a finite interval:

$$0 < x < \frac{\pi}{\sqrt{\gamma^2-1}} \tag{11.49}$$

The sharp change of the solutions at the critical value $\gamma = 1$ reminds of a phase transition. Recall that for $0 < \gamma < 1$ the $\mathbb{Z}_2$ transformations discussed above map the two branches of solutions into each other, while for $\gamma > 1$ a single solution exist and that is mapped into itself, so the symmetry is somehow recovered.

Chapter 12

Focus on a particular model

12.1 Two-exponential potential

A particularly interesting class of potentials is [59]:

$$\boxed{\mathcal{V} = \lambda \left(e^{2\gamma\chi} + e^{\frac{2}{\gamma}\chi} \right)} \tag{12.1}$$

with $\lambda > 0$ and $0 < \gamma < 1$ so that the first term is a mild exponential while the second is a steep one. For $\gamma < 1/\sqrt{3}$, the first term can drive an inflationary phase. The slopes of the two exponentials are connected: the steeper the first one, the milder the second one. This model is interesting because it offers relatively simple analytic solutions, at the price of linking the two slopes, which is anyway not a big limitation.

We now follow [59] and briefly go through the main steps of their derivation.
We consider again the slight generalization of the FLRW metric given in (11.9):

$$ds^2 = -e^{2\mathcal{B}(x)} dx^2 + e^{2A(x)} d\vec{x} \cdot d\vec{x} \tag{12.2}$$

where the parametric time x is linked to the cosmic time t through:

$$dt = \pm e^{\mathcal{B}(x)} dx \tag{12.3}$$

The sign can be chosen in order to recover the desired cosmology, as will be clear later.

We work with the dimensionless variables:

$$dx = \frac{\sqrt{3V}}{M_P} dt \qquad \chi = \frac{1}{M_P}\sqrt{\frac{3}{2}}\varphi \qquad A = \frac{\mathcal{A}}{3} \qquad \mathcal{V} = \frac{1}{M_P^2}\frac{3}{2}V \tag{12.4}$$

The equations of motion for $(\mathcal{A}, \chi)$ follow from the Lagrangian:

$$\mathcal{L} = e^{\mathcal{A}-\mathcal{B}} \left[-\frac{1}{2}\left(\frac{d\mathcal{A}}{dx}\right)^2 + \frac{1}{2}\left(\frac{d\chi}{dx}\right)^2 - e^{2\mathcal{B}}\mathcal{V}(\chi) \right] \tag{12.5}$$

For the potential (12.1) a convenient gauge choice is:

$$\mathcal{B} = \mathcal{A} \tag{12.6}$$

which brings to:

$$\mathcal{L} = \frac{1}{2}\left(\left(\frac{d\chi}{dx}\right)^2 - \left(\frac{d\mathcal{A}}{dx}\right)^2 \right) - e^{2\mathcal{A}}\lambda\left(e^{2\gamma\chi} + e^{\frac{2}{\gamma}\chi} \right) \tag{12.7}$$

The first part of the Lagrangian is "Lorentz invariant", which suggest to perform the analogous of a "Lorentz boost":

$$\widehat{\mathcal{A}} = \frac{1}{\sqrt{1-\gamma^2}}\left(\mathcal{A} + \gamma\chi\right) \tag{12.8}$$

$$\widehat{\chi} = \frac{1}{\sqrt{1-\gamma^2}}\left(\chi + \gamma\mathcal{A}\right) \tag{12.9}$$

Now the Lagrangian has a separable form:

$$\mathcal{L} = \frac{1}{2}\left(\left(\frac{d\widehat{\chi}}{dx}\right)^2 - \left(\frac{d\widehat{\mathcal{A}}}{dx}\right)^2\right) - \lambda e^{2\sqrt{1-\gamma^2}\widehat{\mathcal{A}}} - \lambda e^{\frac{2}{\gamma}\sqrt{1-\gamma^2}\widehat{\chi}} \tag{12.10}$$

and the resulting equations of motion for $\widehat{\mathcal{A}}$ and $\widehat{\chi}$ are independent and they have the form of energy conservation relations:

$$\left(\frac{d\widehat{\mathcal{A}}}{dx}\right)^2 = 2\lambda\left(e^{2\widehat{\mathcal{A}}\sqrt{1-\gamma^2}} + e^{2\widehat{\mathcal{A}}_0\sqrt{1-\gamma^2}}\right) \tag{12.11}$$

$$\left(\frac{d\widehat{\chi}}{dx}\right)^2 = 2\lambda\left(e^{2\widehat{\chi}_0\sqrt{\frac{1}{\gamma^2}-1}} - e^{2\widehat{\chi}\sqrt{\frac{1}{\gamma^2}-1}}\right) \tag{12.12}$$

Notice that $\widehat{\chi}$ cannot proceed arbitrarily along the steep exponential, but it is always bound to be less than $\widehat{\chi}_0$, which is a manifestation of the climbing phenomenon.

The Hamiltonian constraint gives the relation between the two integration constants:

$$\widehat{\mathcal{A}}_0 = \frac{1}{\gamma}\widehat{\chi}_0 \tag{12.13}$$

Defining:

$$\omega^2 \equiv 2\lambda e^{2\widehat{\mathcal{A}}_0\sqrt{1-\gamma^2}}\left(\frac{1}{\gamma^2} - 1\right) = 2\lambda\frac{1-\gamma^2}{\gamma^2}e^{2\mathcal{A}_0} \tag{12.14}$$

the solutions for the scale factor and for the field are:

$$e^{\mathcal{A}} = e^{\mathcal{A}_0}\frac{\left[\cosh\left(\omega(x-x_0)\right)\right]^{\frac{\gamma^2}{1-\gamma^2}}}{\left[\sinh\left(\omega\gamma x\right)\right]^{\frac{1}{1-\gamma^2}}} \tag{12.15}$$

$$e^{\chi} = e^{\chi_0}\frac{\left[\sinh\left(\omega\gamma x\right)\right]^{\frac{\gamma}{1-\gamma^2}}}{\left[\cosh\left(\omega(x-x_0)\right)\right]^{\frac{\gamma}{1-\gamma^2}}} \tag{12.16}$$

The parameter x_0 is the one characterizing the evolution of the field and, in particular, how hard will the impact with the steep exponential be.

The relation between parametric time and cosmic time is given by (12.3) with the gauge choice (12.6):

$$dt = \pm e^{\mathcal{A}}dx = \pm e^{\frac{\widehat{\mathcal{A}} - \gamma\widehat{\chi}}{\sqrt{1-\gamma^2}}}dx \tag{12.17}$$

which in our case gives:

$$dt = \pm e^{\mathcal{A}_0}\frac{\left[\cosh\left(\omega(x-x_0)\right)\right]^{\frac{\gamma^2}{1-\gamma^2}}}{\left[\sinh\left(\omega\gamma x\right)\right]^{\frac{1}{1-\gamma^2}}}dx \tag{12.18}$$

There is an important remark to be made here. In order for the scale factor to describe an expanding Universe, we should choose the minus sign. Large positive values of x translate into early cosmological

epochs close to the initial singularity, while on the contrary small values of x translate into large values of t.
This counter-intuitive relation will actually become useful when dealing with the problem numerically: we will integrate in x from zero up to some value in parametric time, therefore larger upper extremum of integration means we are looking further away in the past in cosmic time.

In conformal time:

$$d\tau = -e^{\frac{2}{3}\mathcal{A}(x)}dx \tag{12.19}$$

In Figures 12.2, 12.1 we show the behaviour of the scale factor and of the field (12.15), (12.16) respectively. The plots are to be read from right to left: large parametric time corresponds to early epochs, close to the initial singularity, then the field bounces against the steep portion of the potential, reverts its motion and injects an inflationary phase. This system of coordinates kind of "compresses" the inflationary phase close to $x \to 0$.
The parameter γ is fixed a defines the model, the parameters $(\mathcal{A}_0, x_0)$ we are free to play with.

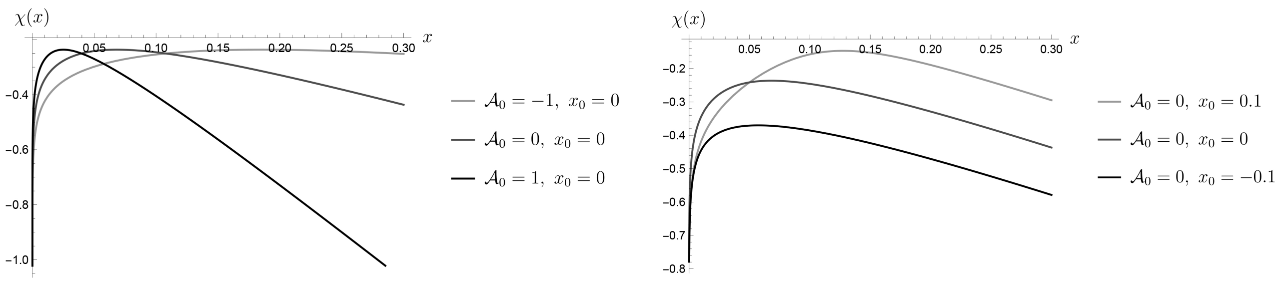

(a) Behaviour of the field, varying $\mathcal{A}_0$.

(b) Behaviour of the field, varying x_0.

Figure 12.1

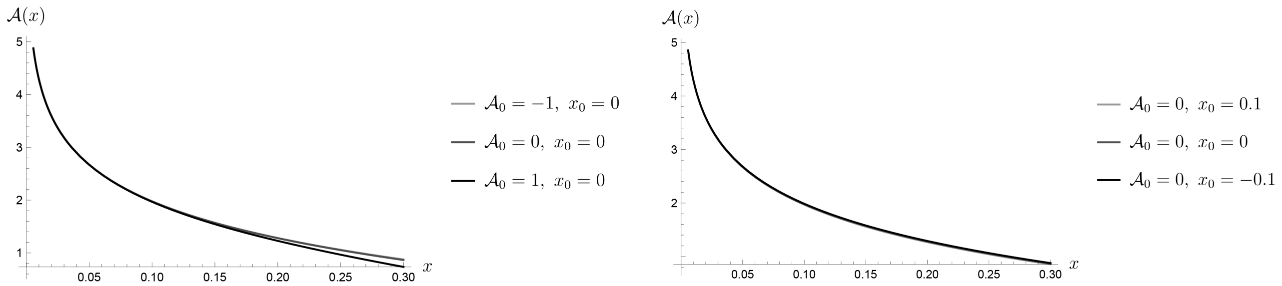

(a) Behaviour of $\mathcal{A}(x)$, varying $\mathcal{A}_0$.

(b) Behaviour of $\mathcal{A}(x)$, varying x_0.

Figure 12.2

The impact of the scalar field impinging on the steep part of the potential is characterized both by $\mathcal{A}_0$ and x_0.
As can be seen in Figure 12.1a, decreasing $\mathcal{A}_0$ smooths the reversal of the field motion and simultaneously shifts it to larger parametric time, or earlier cosmological epochs. Moreover, it affects the "velocity" of the field in parametric time towards the initial singularity. As we will show, the asymptotic behaviour of the derivative only depends on the parameter $\mathcal{A}_0$ and not on x_0:

$$\frac{d\chi(x)}{dx} \xrightarrow{x \gg 1} -\sqrt{2\lambda}e^{\mathcal{A}_0}\sqrt{\frac{1-\gamma}{1+\gamma}} \tag{12.20}$$

Similarly, also increasing x_0 shifts the maximum of the field towards larger x. However, the most important effect in changing x_0 is that it affects the height of the maximum along the vertical axis, as can be seen in Figure 12.1b. Increasing x_0 brings the peak higher, while varying $\mathcal{A}_0$ does not affect the height.

Schematically, $\mathcal{A}_0$ determines how drastic the impact of the field with the potential barrier will be, x_0 tells us how high the field gets to climb before reverting its motion and rolling down. The effect of the two parameters is quite intertwined and the actual parametric time at which the reversal happens depends on both of them.

A warning is in order. The dependence of our expressions (12.15), (12.16) on the parameters $(\mathcal{A}_0, x_0)$ is quite complicated, it goes through hyperbolic sines and cosines. Therefore one cannot vary the parameters arbitrarily: there is a certain range in which the effect on the dynamics is more evident. See Figure 12.3. In particular, regarding x_0, notice that the changes can be appreciated only inside a small range of values, roughly $[-0.1, 0.1]$, then there is a stabilization.

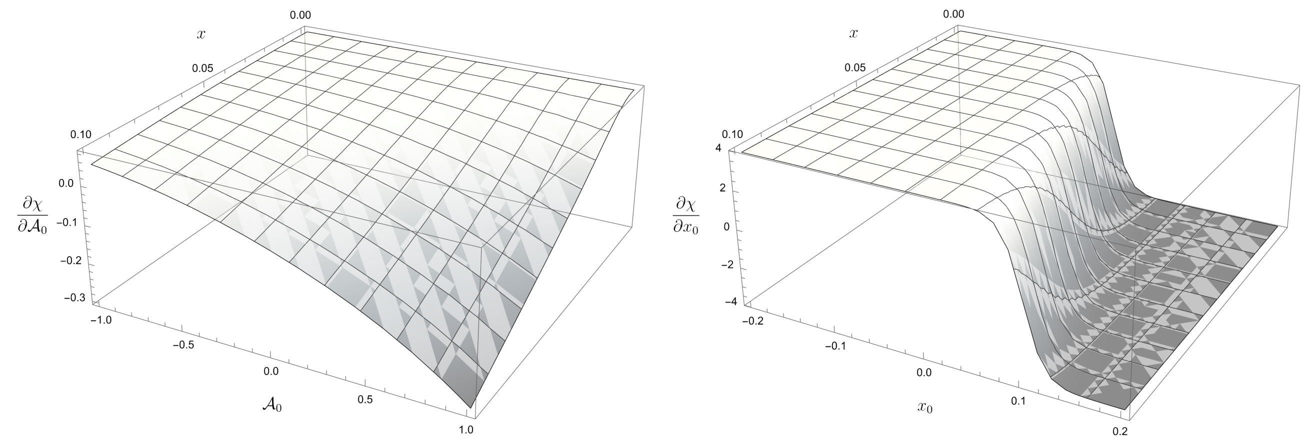

(a) Behaviour of the field, varying $\mathcal{A}_0$. (b) Behaviour of the field, varying x_0.

Figure 12.3

12.2 Asymptotic behaviours

Since the full expressions can be complicated to deal with, it will be useful to study the asymptotic behaviours of the scale factor and of the field.

12.2.1 Late cosmological epochs (small x)

Small parametric time x corresponds to late cosmological epochs, therefore we expect the system to have reached the Lucchin-Matarrese attractor in this regime. Expanding (12.15) and (12.16) for small x we find:

$$e^{\mathcal{A}} \xrightarrow{x \ll 1} e^{\mathcal{A}_0} \left(\cosh(x_0\omega)\right)^{\frac{\gamma^2}{1-\gamma^2}} (\gamma\omega)^{-\frac{1}{1-\gamma^2}} x^{-\frac{1}{1-\gamma^2}} \tag{12.21}$$

$$e^{\chi} \xrightarrow{x \ll 1} e^{\chi_0} \left(\cosh(x_0\omega)\right)^{-\frac{\gamma}{1-\gamma^2}} (\gamma\omega)^{\frac{\gamma}{1-\gamma^2}} x^{\frac{\gamma}{1-\gamma^2}} \tag{12.22}$$

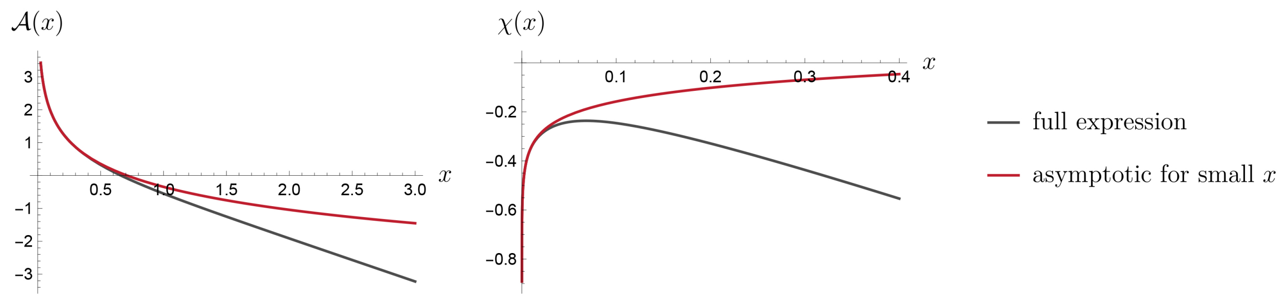

Figure 12.4: Full expression and Lucchin-Matarrese attractor, for $\mathcal{A}_0 = 0$ and $x_0 = 0$. Notice the different scale on the x axis.

Using (12.19), the change of variable in this regime becomes:

$$\tau \simeq -\mathrm{K}x^{1-\frac{2}{3(1-\gamma^2)}} \tag{12.23}$$

$$\mathrm{K} \equiv (2\lambda)^{-\frac{1}{3(1-\gamma^2)}} e^{-\frac{2\gamma^2}{3(1-\gamma^2)}\mathcal{A}_0} \frac{3}{1-3\gamma^2} \left(1-\gamma^2\right)^{1-\frac{1}{3(1-\gamma^2)}} \left(\cosh\left(\sqrt{2\lambda}e^{\mathcal{A}_0}x_0\frac{\sqrt{1-\gamma^2}}{\gamma}\right)\right)^{\frac{2\gamma^2}{3(1-\gamma^2)}} \tag{12.24}$$

As a consistency check, we can substitute $x \sim (-\tau)^{1+\frac{2}{1-3\gamma^2}}$ into (12.21) and (12.21). We obtain that $a(\tau) \propto (-\tau)^{\frac{3}{-1+3\gamma^2}}$ and $\varphi(\tau) \propto \log(-\tau)$, which are the expressions for power-law inflation [59].

12.2.2 Early cosmological epochs (large x)

Close to the initial singularity, the systems experiencing the climbing all show a universal behaviour. The Mukhanov-Sasaki potential $W_s = \frac{z''}{z}$ in (8.9) has the asymptotic form:

$$W_s \xrightarrow{\tau\to-\infty} -\frac{1}{4(\tau-\tau_0)^2} \tag{12.25}$$

where τ_0 marks the initial singularity [2, 56]. It would be like solving the Mukhanov-Sasaki equation with $\nu = 0$, as a matter of fact the solutions in this regime are of the type $H_0^{(1)}(-k\tau)$.

In order to find asymptotic expressions for the scale factor and for the field, we look at their derivatives. The derivative of $\mathcal{A}(x)$ approaches a constant value:

$$\frac{d\mathcal{A}(x)}{dx} \xrightarrow{x\to\infty} -\sqrt{2\lambda}e^{\mathcal{A}_0}\sqrt{\frac{1-\gamma}{1+\gamma}} \tag{12.26}$$

The constant of integration can be fixed by looking at the full expression for $\mathcal{A}(x)$ and keeping only the most relevant exponentials in the hyperbolic functions.

$$\mathcal{A}(x) \simeq \mathcal{A}_0 + \log 2 - \sqrt{2\lambda}e^{\mathcal{A}_0}\sqrt{\frac{1-\gamma}{1+\gamma}}\,(x - x\gamma + x_0\gamma) \tag{12.27}$$

Similarly for the field:

$$\chi(x) \simeq -\frac{\sqrt{2\lambda}e^{\mathcal{A}_0}}{\sqrt{1-\gamma^2}}\,(x(1-\gamma) - x_0) \tag{12.28}$$

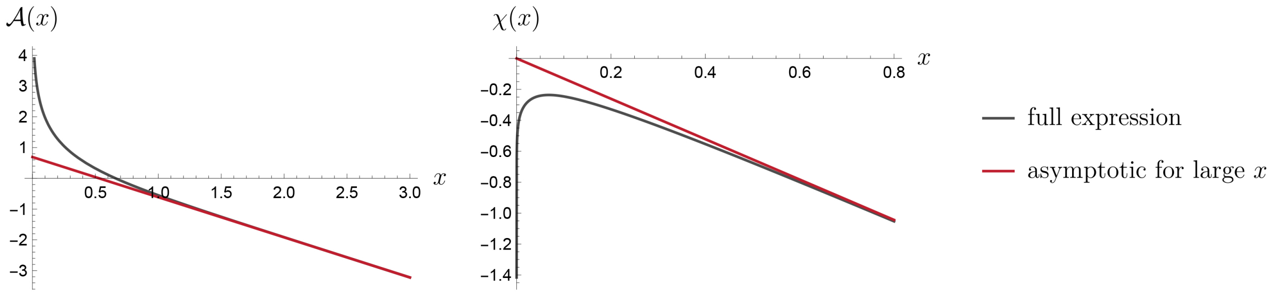

Figure 12.5: Full expression and asymptotic behaviour at early epochs, for $\mathcal{A}_0 = 0$ and $x_0 = 0$.

The change of variable in this limit becomes:

$$\tau = \frac{3}{2^{1/3}\sqrt{2\lambda}}\sqrt{\frac{1+\gamma}{1-\gamma}}\exp\left\{-\frac{\mathcal{A}_0}{3} - \frac{2\sqrt{2\lambda}e^{\mathcal{A}_0}\,(x(1-\gamma)+x_0\gamma)}{3\sqrt{1-\gamma^2}}\right\} \tag{12.29}$$

12.3 Perturbations

The equation of motion for ζ in conformal time is:

$$\zeta_k'' + 2\frac{z'}{z}\zeta_k' + k^2\zeta_k = 0 \tag{12.30}$$

In terms of parametric time, we obtain:

$$dt = -e^{\mathcal{A}}dx \qquad \frac{d}{d\tau} = -e^{-\frac{2\mathcal{A}}{3}}\frac{d}{dx} \qquad \frac{d^2}{d\tau^2} = e^{-\frac{4\mathcal{A}}{3}}\left(-\frac{2}{3}\frac{d\mathcal{A}}{dx}\frac{d}{dx} + \frac{d^2}{dx^2}\right) \tag{12.31}$$

$$\frac{d^2\zeta_k}{dx^2} + 2\left(\frac{\frac{d^2\chi}{dx^2}}{\frac{d\chi}{dx}} - \frac{\frac{d^2\mathcal{A}}{dx^2}}{\frac{d\mathcal{A}}{dx}}\right)\frac{d\zeta_k}{dx} + e^{\frac{4\mathcal{A}}{3}}k^2\zeta_k = 0 \tag{12.32}$$

The quantity in parenthesis multiplying the first derivative term is:

$$\frac{\frac{d^2\chi}{dx^2}}{\frac{d\chi}{dx}} - \frac{\frac{d^2\mathcal{A}}{dx^2}}{\frac{d\mathcal{A}}{dx}} = \frac{\frac{d}{dx}\left(\frac{\frac{d\chi}{dx}}{\frac{d\mathcal{A}}{dx}}\right)}{\frac{\frac{d\chi}{dx}}{\frac{d\mathcal{A}}{dx}}} \tag{12.33}$$

This equation is difficult to solve numerically, due to singularities that arise when $x \to 0$ and spoil the numerical integration. We need to rephrase the problem in terms of a more convenient variable.

Previously, we introduced the Mukhanov-Sasaki variable as $v = z\mathcal{R}$ in order to get rid of the first derivative term and obtain an equation resembling an harmonic oscillator. In a similar fashion we can define[1]:

$$\tilde{z} \equiv \frac{\frac{d\chi}{dx}}{\frac{d\mathcal{A}}{dx}} \qquad \tilde{z}\zeta \equiv \tilde{v} \tag{12.34}$$

$$\boxed{\frac{d^2\tilde{v}}{dx^2} + \left(e^{\frac{4\mathcal{A}}{3}}k^2 - \frac{\frac{d^2\tilde{z}}{dx^2}}{\tilde{z}}\right)\tilde{v} = 0} \tag{12.35}$$

At late epochs, corresponding to $x \to 0$, we recover the well-known power-law inflation solution. Furthermore $\tilde{z} \xrightarrow{x\to 0} -\gamma$ which gives $\tilde{v} \simeq -\gamma\zeta$.

Equation (12.35) is the one we have to solve numerically.

12.3.1 Mukanov-Sasaki potential and a consistency check

As pointed out in [2] and later works on the subject, all the relevant information is contained in the Mukhanov-Sasaki potential $W_s = \frac{z''}{z}$, see equation (8.9). The Mukhanov-Sasaki potential reaches the limiting behaviour on the Lucchin-Matarrese attractor:

$$W_s \xrightarrow{\tau\to 0} \frac{\nu^2 - \frac{1}{4}}{\tau^2} \tag{12.36}$$

while towards the initial singularity τ_0 it approaches:

$$W_s \xrightarrow{\tau\to\tau_0} -\frac{1}{4}\frac{1}{(\tau-\tau_0)^2} \tag{12.37}$$

These asymptotic behaviours indicate that at some point W_s is bound to cross the horizontal axis. Moreover, this generic structure of the Mukhanov-Sasaki potential is universal to all the systems that experience the climbing.

As a consistency check, we have computed $z = \sqrt{6}M_P e^{\mathcal{A}/3}\frac{d\chi}{dx}\left(\frac{d\mathcal{A}}{dx}\right)^{-1}$ and the Mukhanov-Sasaki potential for large x, close to the initial singularity, and we recover indeed the universal behaviour.

The potential W_s is displayed in Figure 12.6 for two sets of parameters. The dashed lines represent the asymptotic behaviour at early times.

[1] To make contact with the notation of [2], $z = \sqrt{6}M_P a\tilde{z}$ and $\tilde{v} = \frac{1}{\sqrt{6}M_P}Q$. Our $\tilde{v}$ is, aside from an irrelevant constant, the rescaled Mukhanov-Sasaki variable Q.

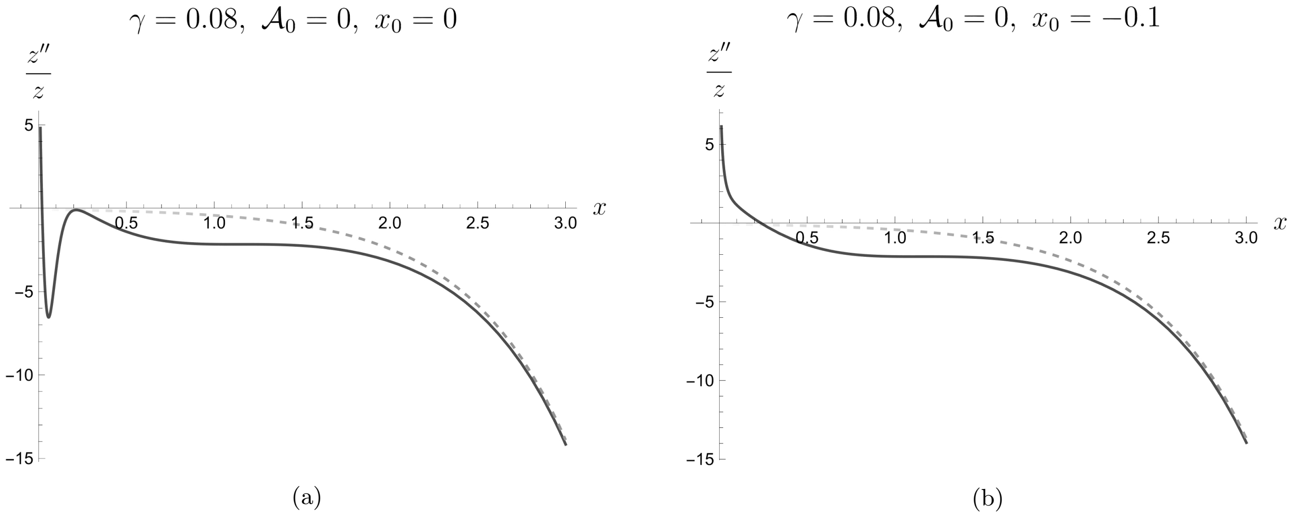

Figure 12.6

12.3.2 Bunch-Davies initial conditions

In order to solve the second order differential equation (12.35) we need to impose initial conditions. We know that, when the modes are deep inside the horizon, the modefunctions v_k must be asymptotically the Minkowski ones:

$$v_k(\tau) \sim \frac{1}{\sqrt{2k}} e^{-ik\tau} \tag{12.38}$$

Then we can fix $\tilde{v}_k$ by rescaling $\tilde{v}_k = \frac{v_k}{\sqrt{6}M_P a}$.

A way to approach the problem is to solve the e.o.m. (8.9) with the asymptotic form of $\frac{z''}{z}$ given in (12.37). We find the familiar result, with $\nu = 0$:

$$v_k(\tau) = \sqrt{-\tau}\left[c_1(k)H_0^{(1)}(-k\tau) + c_2(k)H_0^{(2)}(-k\tau)\right] \tag{12.39}$$

and imposing the Bunch-Davies prescription $c_2 = 0$ and $c_1 = \frac{\sqrt{2}}{\pi}$.
Using (12.29) to change variable and rescaling to get $\tilde{v}_k$ we finally obtain:

$$\begin{aligned}\tilde{v}_k^{\mathrm{BD}}(x) =& \frac{1}{4M_P} i e^{-\frac{1}{2}\mathcal{A}_0}\sqrt{\pi}\left(\frac{1}{2\lambda}\frac{1+\gamma}{1-\gamma}\right)^{1/4} \cdot \\ & H_0^{(1)}\left(-k\frac{3}{2^{1/3}\sqrt{2\lambda}}\sqrt{\frac{1+\gamma}{1-\gamma}}\right)\exp\left\{-\frac{\mathcal{A}_0}{3} - \frac{2}{3}\frac{\sqrt{2\lambda}e^{\mathcal{A}_0}\left(x(1-\gamma)+x_0\gamma\right)}{3\sqrt{1-\gamma^2}}\right\}\end{aligned} \tag{12.40}$$

One can check that using the e.o.m. for $\tilde{v}_k$ (12.35) and the asymptotic behaviour of the scale factor and the field (12.27), (12.28) we obtain the same result. In that case, we would find the following equation:

$$\frac{d^2\tilde{v}_k}{dx^2} + be^{dx}\tilde{v}_k = 0 \tag{12.41}$$

$$b \equiv k^2 2^{4/3} e^{4\mathcal{A}_0/3} e^{-\frac{4}{3}\frac{\sqrt{2\lambda}e^{\mathcal{A}_0}\gamma}{\sqrt{1-\gamma^2}}x_0} \qquad d \equiv -\frac{4}{3}\sqrt{2\lambda}e^{\mathcal{A}_0}\sqrt{\frac{1-\gamma}{1+\gamma}} \tag{12.42}$$

The solutions are Hankel functions of index 0 and argument $\dfrac{2\sqrt{be^{dx}}}{d}$, as found above.

12.4 Numerical solution

Equation (12.35) has been solved numerically, with Mathematica 12.3.1.0.
The command `ParametricNDSolve` was used, to find a solution $\tilde{v}_k(x)$ with k as parameter. Schematically:

```
parSol[γ_?NumericQ,A0_?NumericQ,x0_?NumericQ, λ_?NumericQ,
xi_?NumericQ,xf_?NumericQ,xic_?NumericQ] := ParametricNDSolve[
eq,vtilde(xic) == vtildeBD(xic), vtilde'(xic) == vtildeBD'(xic),
vtilde,{x,xi,xf},k,WorkingPrecision->MachinePrecision
```

This is done for a given range of wavenumbers from $k_{\mathrm{min}} \sim 10^{-2}$ to $k_{\mathrm{max}} \sim 10^{2}$. The integration is carried out from xi to xf, the Bunch-Davies initial conditions (12.40) are imposed at a time xic.

Ideally, one would like to integrate up to $x = 0$, but since there are divergencies this cannot be done: the final time of integration is chosen to be as small as possible, to ensure that all the wavelengths of interest are well outside the horizon by then.
The time xic at which we impose the Bunch-Davies initial conditions needs some care. It has to be very large, to make sure that we are still on the climbing phase. As a matter of fact, the whole point of the climbing phenomenon is that the field cannot emerge from the initial singularity while descending, it can only climb up the potential; but if we look at later times, we may see it either climbing or descending already, depending on the free parameters. Therefore we need to set initial conditions as early as possible. This is a delicate point and can lead to artifacts in the final results, like oscillations that are clearly not physical.

To compute the power-spectrum, we should evaluate $\frac{k^3}{2\pi^2}\frac{1}{(\tilde{z}(x))^2}\tilde{v}_k(x)\tilde{v_k^*}(x)$ at the end of inflation $x = 0$. Again, we cannot go numerically at $x = 0$ therefore we have to set with choosing a x_{PS} as small as possible. The crucial point is that we must evaluate the power-spectra at a time much later than the freeze-out time of the last mode of interest k_{max} [60]. Since xi has been chosen this way, it can also be used to evaluate the power-spectrum.

```
mySol = parSol[γsol,A0sol,x0sol,λsol,xisol,xfsol,xicsol]

curlyPnumeric[k_] := Module[
  {vtilde=vtilde[k]/.mySol},
  k^3/(2π^2) 1/(ztilde[x])^2 (vtilde[x]/.mySol)Conjugate[vtilde[x]/.mySol]
  /.{γ->γsol,A0->A0sol}/.x->xPS
]
```

To be compared with the power-spectrum computed on the Lucchin-Matarrese attractor, power-law inflation. Both power-spectra were Planck normalized at $k = 100$, so that we have well reached the attractor.

Three cases are studied in the following. Figure 12.7 displays the behaviour of the field for three sets of parameters, Figure 12.9 shows the corresponding power-spectra $\mathcal{P}_k(k)$.

We recover the main qualitative features of the power-spectrum in the presence of a climbing scalar, studied in [2, 56]:

- a suppression of the power-spectrum for low-k with respect to the attractor;
- a pre-inflationary peak, that may be displaced from the attractor.

The meaning of the peak is the following. During the pre-inflationary kinetic dominated phase of the climbing, the power-spectrum is suppressed Then, as the field starts to slow down against the hard exponential, the power-spectrum goes up. When the field reverts its motion and rolls down, it initially accelerates again, which tricks the power-spectrum into another suppressed phase. Eventually, the expansion of the Universe takes over and the field slows down, approaching the attractor: the power-spectrum reaches the k^{n_s-1} behaviour.

According to the analysis in [56], the peak is an overshoot which can present itself when the actual Mukhanov-Sasaki potential W_s happens to emerge from the horizontal axis more steeply than the

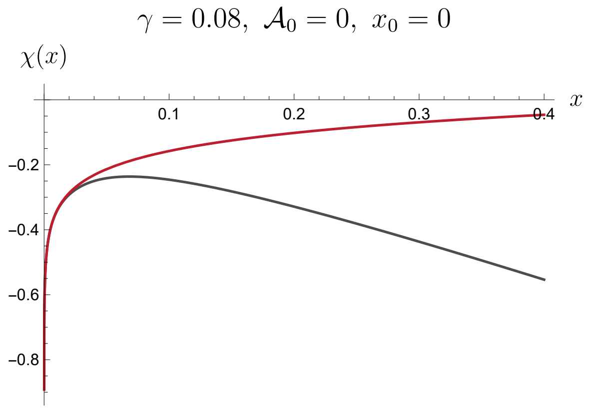

(a)

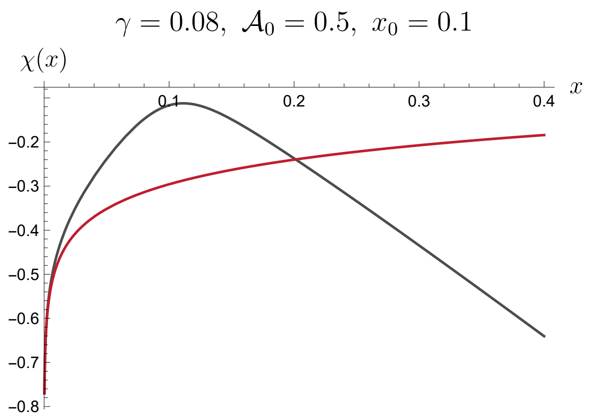

(b)

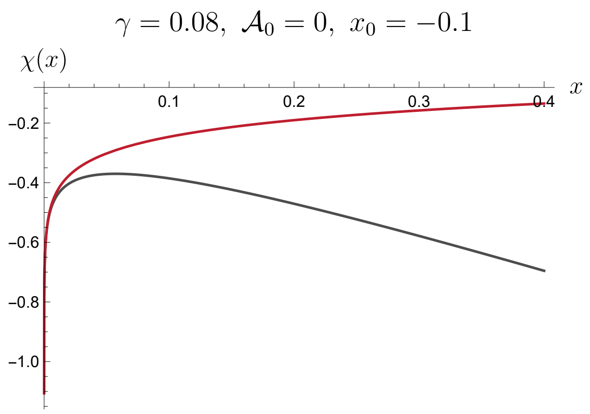

(c)

Figure 12.7

attractor curve. This is always the case for the three potentials displayed in Figure 12.8, and indeed we do see the peak in all the power-spectra in Figure 12.9.
The characteristics of the peak depend on the nature of the impact against the potential barrier. If the field strongly bounces against the steep portion of the potential, and climbs higher up the potential barrier, then the peak moves towards lower k and further away from the attractor.

The first power-spectrum in Figure 12.9 shows a mild bounce against the potential barrier, there is a peak and then we soon reach the attractor. The other two cases show a more drastic scattering, for which the peak moves towards lower values of k: in the second case the field climbs much higher than

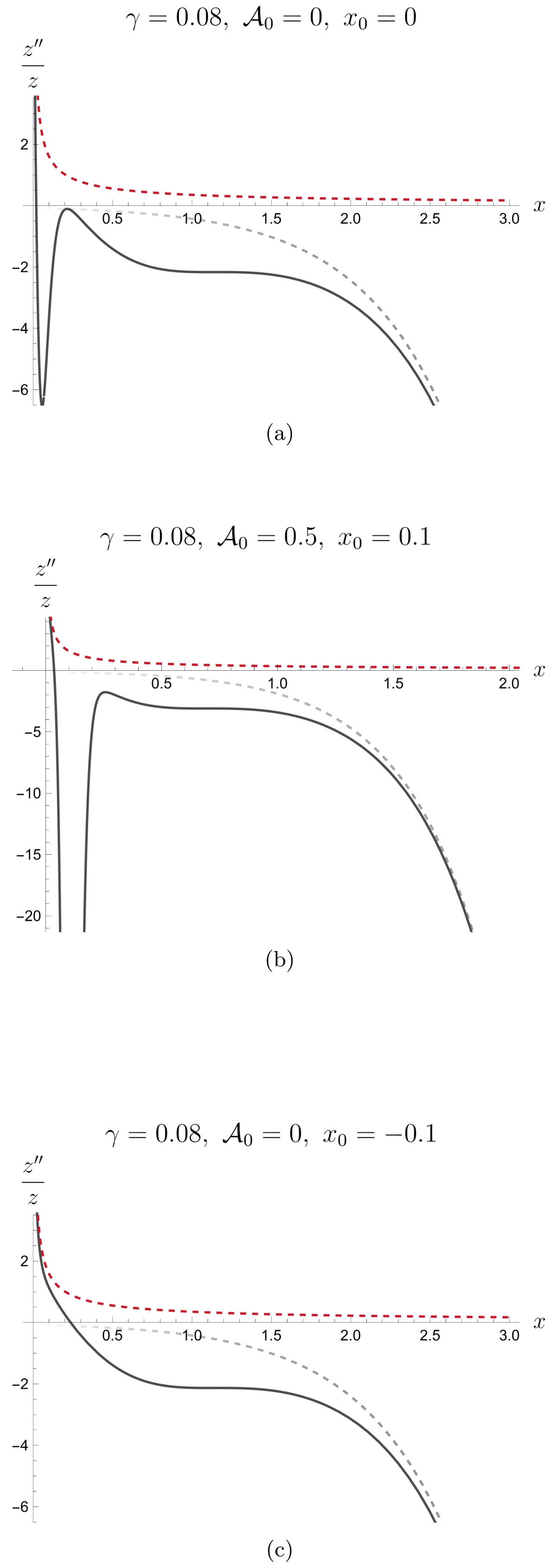

Figure 12.8: Full Mukhanov-Sasaki potential, compared to the asymptotic behaviours (dashed): in red the Lucchin-Matarrese attractor, in gray the asymptotic behaviour close to the initial singularity.

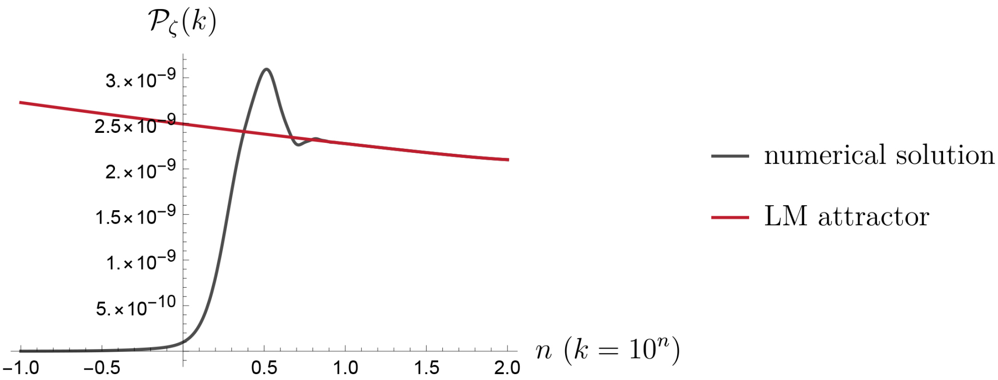

(a)

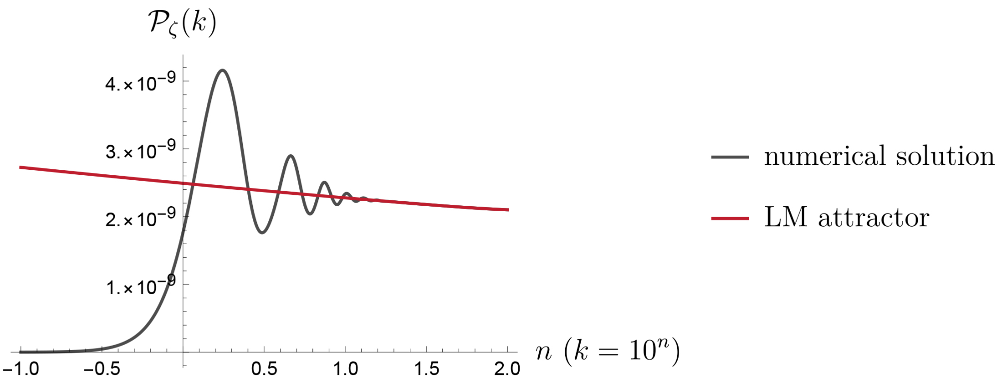

(b)

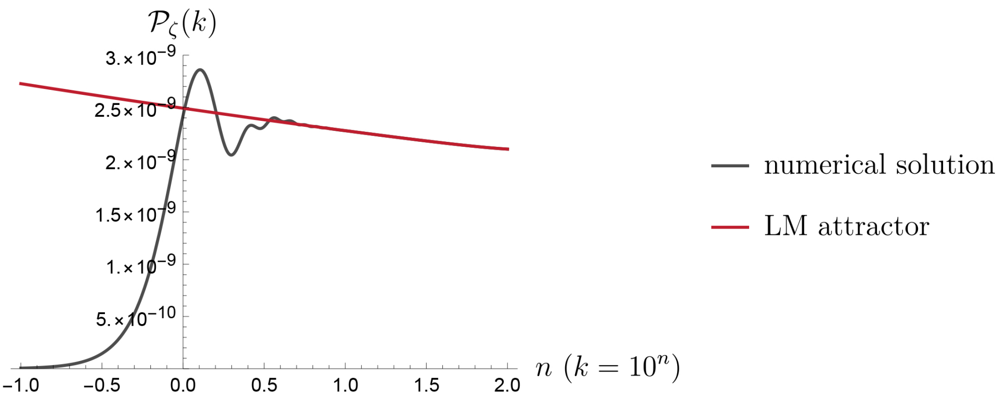

(c)

Figure 12.9

the attractor solution (see the corresponding plot in Figure 12.7), in the third case it does not and the peak in the power-spectrum is less pronounced.

Previous numerical studies like the one in [56] have shown that the pre-inflationary peak can actually move even further from the attractor than what we observe here. This is probably due to the very nature of this specific model we are studying: the two exponents are linked. If we look at the mild potential $e^{2\gamma\chi}$ and fit $\gamma \simeq 0.08$ to the CMB data, then the steep portion of the potential $e^{\frac{2}{\gamma}\chi}$ becomes really steep. We basically have a vertical wall and, even playing with the parameters $(\mathcal{A}_0, x_0)$, the scalar field cannot climb arbitrarily high. In other words, we have little variability in the dynamics. However, we still manage to observe in the power-spectrum the features that are peculiar to the climbing phenomena.

Chapter 13

Future prospects

13.1 Next steps

The final goal of this work will be having a prediction for f_{NL} in the class of models that experience the climbing phenomenon, for which Lucchin-Matarrese power-law inflation is the attractor solution. The next step will be a numerical study of the bispectra in this type of models. It may be that the particular two-exponential potential with exponents γ and $\frac{1}{\gamma}$ is not the best suited one for this study, for two main reasons: because the change of coordinates to parametric time compresses the inflationary phase very close to $x = 0$, and because the steepness of the "hard" exponential strongly limits the dynamics of the field. One could abandon the idea to have analytic expressions for the scale factor and the field, and write a more generic code that deals with everything numerically.

Roughly, we expect primordial non-Gaussianity to be enhanced due to the suppression in the power-spectrum at low-ℓ. We can do a back-of-the-envelope calculation, based on Maldacena's consistency relation (9.63).
In single-field inflation, we expect that:

$$\lim_{k_3 \to 0} B_\zeta(k_1, k_2, k_3) = (1 - n_s) P_\zeta(k_1) P_\zeta(k_3) \tag{13.1}$$

where $n_s - 1$ is the logarithmic derivative of the dimensionless power-spectrum associated with the short wavelength mode k_1.
If we parametrize the infrared suppression in the power-spectrum as in equation (11.6), then:

$$\begin{aligned} n_s(k) - 1 &= \frac{d}{d\mathrm{log}k} \mathrm{log}\left(A_s \frac{k^3}{(k^2 + \Delta^2)^{2-\frac{n_s}{2}}} \right) \\ &= 3 - (4 - n_s) \frac{k^2}{k^2 + \Delta^2} \end{aligned} \tag{13.2}$$

Therefore the consistency relation becomes:

$$\lim_{k_3 \to 0} B_\zeta(k_1, k_2, k_3) = 4\pi^4 A_s^4 k_{\mathrm{short}}^{n_s - 4} \left(k_{\mathrm{long}}^2 + \Delta^2\right)^{-3+\frac{n_s}{2}} \left(k_{\mathrm{long}}^2 (1 - n_s) - 3\Delta^2\right) \tag{13.3}$$

to be compared with the standard case $n_s(k) = n_s$ and $\Delta = 0$:

$$\lim_{k_3 \to 0} B_\zeta(k_1, k_2, k_3) = 4\pi^4 A_s^4 \left(k_{\mathrm{long}} k_{\mathrm{short}}\right)^{n_s - 4} (n_s - 1) \tag{13.4}$$

There are two competing effects here. On the one hand n_s changes as a consequence of the low-k suppression, and we expect this to enhance the bispectrum. On the other hand, though, $B_\zeta \propto P_\zeta^2$ and one of them, the power-spectrum associated to the long wavelength mode, is suppressed.

From the point of view of $f_{\rm NL}$:

$$f_{\rm NL} = -\frac{5}{12}\left(1 - n_s(k)\right) \tag{13.5}$$

where the last equality is nothing but the consistency relation, which we expect to recover since we are looking at a single field model. Indeed, both sides give:

$$\boxed{f_{\rm NL} = \frac{5}{12}\frac{k_3^2(n_s-1)+2\Delta^2}{k_3^2+\Delta^2}} \tag{13.6}$$

where k_3 is the long wavelength mode, $k_3 \ll k_1,\ k_2$. The form of the power-spectrum (11.6) and in particular the appearance of the new scale Δ bring about a scale dependence in the non-Gaussianity parameter. Furthermore, $f_{\rm NL}$ changes sign: it approaches $\frac{5}{4}$ as $k_3 \to 0$, but for k_3 large enough it approaches the usual expression $-\frac{5}{12}(1-n_s)$ which is negative, with the scalar spectral index we observe. A plot is shown in Figure 13.1a. The scalar spectral index n_s has been fixed to the Planck fit (5.23) $n_s = 0.9649 \pm 0.0042$, for the new scale Δ we use the result of [58]:

$$\Delta = (0.351 \pm 0.114) \times 10^{-3}\ \text{Mpc}^{-1} \qquad\qquad \text{at 99.4\% C.L.} \tag{13.7}$$

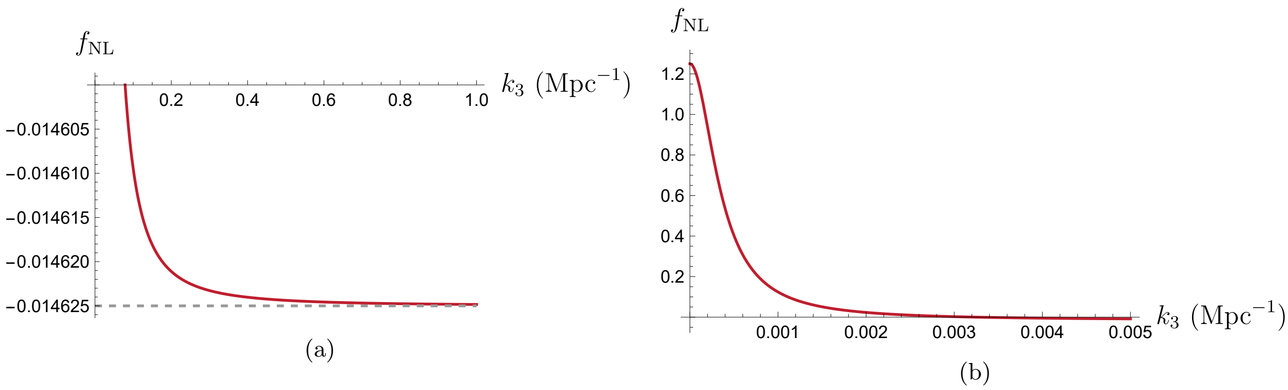

Figure 13.1: Plot of the non-Gaussianity parameter (13.6). The standard result $-\frac{5}{12}(1-n_s)$ is dashed, for comparison. An enlarged view of the low-k region is provided in Figure 13.1b, where we can appreciate that $f_{\rm NL}$ changes sign at a scale of about $\sim 10\Delta$ for this value of n_s.

For completeness, in Figure 13.2 we also display the plot accounting for the errors on the parameters n_s and Δ.

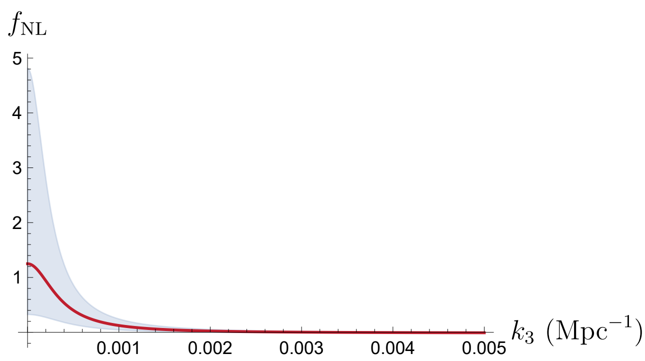

Figure 13.2

This is a first, rough expectation. However, the third order action (8.10) is much more complicated and rich, and contains many vertices. This contribution we have just computed is only one among the possible terms, maybe not even the most important one.
Only the full calculation will tell us whether this rough prediction captures the underlying physics. This needs to be studied numerically.

13.2 Future observational prospects

Having detailed predictions for $f_{\rm NL}$ is a key point for our understanding of inflation. In the following decade, a lot of new data will be available, both on the CMB and on the large-scale structure sides, that will help us discriminate among different scenarios. Large-angle CMB anisotropies have been able to constrain the bispectrum amplitude in various momentum configurations with a sensitivity of $\Delta f_{\rm NL} \gtrsim \mathcal{O}(10)$. Upcoming galaxy surveys aim at $\Delta f_{\rm NL} \sim \mathcal{O}(1)$, a theoretical thresholds that marks the separation between fundamentally different mechanisms for inflation.

13.2.1 Cosmic Microwave Background

As we have already mentioned, CMB experiments have an intrinsic limitation at low ℓ given by cosmic variance [33] while at high ℓ they are limited by Silk damping. The state-of-the-art Planck 2018 results for $f_{\rm NL}$ are already close to this fundamental limit [30]: more experiments will come, but there is not much room for improvement on constraining non-Gaussianity from the CMB alone. We briefly present some forecasts for the future missions CORE and LiteBIRD.

LiteBIRD (Lite satellite for the study of B-mode polarization and Inflation from cosmic background Radiation Detection) and CORE (Cosmic Origins Explorer) are both fourth-generation full-sky, microwave band satellites, after COBE, WMAP and Planck.

LiteBIRD was selected as "Large Mission" by the Japanese space agency JAXA [61], launch is planned for 2028. It will be the first mission fully devoted to the CMB polarization, with the primary goal of detecting primordial gravitational waves through the B-mode polarization of the CMB. It will cover the frequency range 34-448 GHz with a typical angular resolution of 30 arcmin at 100 GHz (compare with Planck's resolution of 33-5 arcmin).

CORE was proposed to ESA [62]. It aims to map the polarization to detect primordial gravitational waves from inflation, probe neutrino masses, constrain shape and amplitude of primordial non-Gaussianity, map the galactic polarized dust emission and the galactic magnetic field. CORE will map the sky in temperature and polarization in the frequency range 60-600 GHz, with angular resolution of 5 arcmin at 200 GHz.

Forecasts on the non-Gaussianity parameters for these missions are shown in Table 13.1. LiteCORE-80, LiteCORE-120, LiteCORE-150 are three configurations with varying angular resolution, thanks to a larger telescope of 80 cm, 120 cm, 150 cm respectively. CORE-M5 or MiniCORE is a possible downscoped version, with a 80 cm telescope, covering the reduced 100-600 GHz frequency range. All the CORE configurations assume $\ell_{\rm max} = 3000$, except for LiteCORE-80 which has $\ell_{\rm max} = 2400$, while the much lower resolution LiteBIRD has $\ell_{\rm max} = 1350$.
For comparison, the Planck 2018 results are shown [30]. The last column is an ideal full-sky and noiseless experiment with $\ell_{\rm max} = 3000$.

	LiteCORE-80	LiteCORE-120	CORE-M5	LiteBIRD	Planck 2018	ideal
T local	4.5	3.7	3.6	9.4	5.6	2.7
T equilat	65	59	58	92	66	46
T orthog	31	27	26	58	36	20
E local	5.4	4.5	4.2	11	28	2.4
E equilat	51	46	45	76	161	31
E orthog	24	21	20	42	86	13
T+E local	2.7	2.2	2.1	5.6	5.1	1.4
T+E equilat	25	22	21	40	47	15
T+E orthog	12	10.0	9.6	23	23	6.7

Table 13.1: Forecasts from [62] for the 1σ error bars on $f_{\rm NL}$ for the standard shapes local, equilateral, orthogonal. The results from Planck are not forecasts, they are real measured error bars [30].

Compared to Planck, the CORE configurations provide just a modest improvement in temperature-only (as expected since Planck already is nearly cosmic variance limited in temperature), but a very significant improvement in polarization-only, for a final improvement in full T+E of about a factor of 2. Because of its lower resolution, LiteBIRD performs significantly worse, with final T+E error bars comparable to the current ones from Planck.

However, this is still not enough. The crucial threshold lays at $f_{\rm NL} = 1$, because observing $f_{\rm NL} > 1$ would rule out single-field models of inflation. This threshold lays below cosmic variance.

We briefly mention an alternative probe from the CMB that could be promising: spectral distortion anisotropies [63].
Spectral distortions are created by processes that drive matter and radiation out of thermal equilibrium, after thermalization becomes inefficient at redshift $z \lesssim 2 \times 10^6$ (energy-releasing mechanisms that heat the baryonic matter, or inject photons or other electromagnetically interacting particles). The distorsions are caused by energy exchange between electrons and photons through Compton scattering. They are usually characterized as y-type distortions and μ-type (or chemical potential): the former probes the thermal history during recombination and reionization, the latter forms at earlier epochs and directly probes events in the pre-recombination era.
Spectral distorsions can be used to probe local-type primordial non-Gaussianity at small scales. In fact, non-Gaussian couplings between short and long wavelength modes create inhomogeneities in the amplitude of the small-scale power, which in turn lead to an anisotropic spectral distortion that correlate with tracers of the long wavelength modes. Cross correlations of T and E with μ-distorsions anisotropies would probe the squeezed configuration of the bispectrum, thus offering an interesting way to complement other probes. The measurement of $\mu - T$ cross correlation will set the first upper bound on $f_{\rm NL}^{\rm local}$ on small scales, $k \approx 740$ Mpc^{-1}.

13.2.2 Large-scale structure

While the CMB is mostly linear physics, large-scale structure is highly nonlinear and much more complicated.
The galaxy/halo bias is expected to depend on $f_{\rm NL}$, in the following way. Galaxies are biased tracers of the underlying dark matter distribution, much like observing lights on Earth at night would not faithfully reveal the distribution of the land beneath. Roughly:

$$\text{bias} \equiv \frac{\text{clustering of galaxies}}{\text{clustering of dark matter}} = \frac{\left(\frac{\delta\rho}{\rho}\right)_{\text{halos}}}{\left(\frac{\delta\rho}{\rho}\right)_{\text{DM}}} \tag{13.8}$$

The theory predicts the density fluctuations for dark matter, while observations probe halos and galaxies. If we parametrize $\delta_g(k,z) = b\delta_{\rm DM}(k,z)$ then the power-spectra are related through:

$$P_g(k,z) = b^2 P_{\rm DM}(k,z) \tag{13.9}$$

The bias function can be scale-dependent, and this is where non-Gaussianity enters into play. In the seminal works [64, 65] it was shown that:

$$b(k) = b_{\rm G} + f_{\rm NL}\frac{\text{const}}{k^2} \tag{13.10}$$

Let's parametrize the Bardeen gravitational potential Φ as:

$$\Phi_{\rm NG}(x) = \phi(x) + f_{\rm NL}\left(\phi^2(x) - \langle\phi^2\rangle\right) \tag{13.11}$$

where ϕ is a Gaussian field. Within this sign convention, positive $f_{\rm NL}$ leads to overdense region being more evolved and producing more clusters than their Gaussian counterparts, while on the contrary negative $f_{\rm NL}$ will produce deeper voids and leave overdense regions less evolved [65]. In other words, large value of $f_{\rm NL}^{\rm local}$ implies larger amplitudes in the 2-point clustering of galaxies at large separations than expected in the standard ΛCDM paradigm [66].

The contribution to the bias induced by primordial non-Gaussianity is amplified at large scales. Therefore the clustering of large-scale structure objects offers a way to measure the non-linear parameter $f_{\rm NL}$ which is complementary to the CMB.

Studies of the galaxy bispectrum indicate that an accuracy in determining local $f_{\rm NL}$ of order $\sigma_{f_{\rm NL}} \sim$ few is achievable. Not only can this provide independent constraints on scales smaller than those probed by CMB, but also the constraints can be comparable to, if not better than, those from CMB. The best limit one can achieve from an all-sky survey up to redshift ~ 5 should reach $f_{\rm NL}^{\rm local} \sim 0.2$ and $f_{\rm NL}^{\rm equil} \sim 2$, an order of magnitude better than the best limits achievable by CMB [67].

Constraints from present surveys are not competitive with Planck, or at most comparable, depending on the shape. Different combinations of probes have been studied, see for example [66, 68]. Current results favour positive $f_{\rm NL}^{\rm local}$, but do not rule out $f_{\rm NL}^{\rm local} = 0$.

Improvements are expected in the near future.
The near-infrared spectroscopic and photometric galaxy survey Euclid [69], through the combination of lensing, galaxy clustering and clusters, can constrain $\Delta f_{\rm NL} \sim 2$: this is competitive and possibly superior to future CMB experiments.
The first all-sky spectral survey SPHEREx is expected to be sensitive to $|f_{\rm NL}^{\rm local}| \sim 1$ with an error $\sigma_{f_{\rm NL}} = 0.87$ [70]: it will provide a bound on $f_{\rm NL}^{\rm local}$ that will be even ~ 6 better than the corresponding expected constraint from the Euclid spectroscopic sample, and a similar factor with respect to the current CMB-based bound.
The spectroscopic surveys of SKA (Square Kilometer Array) will be able to constrain the non-Gaussianity parameter down to $\sigma_{f_{\rm NL}} = 1.54$ for the full survey [71].

13.3 Conclusions

In this thesis work we have focused on computing the bispectrum of primordial curvature perturbations in power-law inflation [4]. An analytic expression in the squeezed regime $k_3 \ll k_1,\ k_2$ has been derived, without the usual slow-roll assumption:

$$B_\zeta^{\rm squeezed}(k_1,k_2,k_3) = \frac{2^{-3+\frac{4}{1-\epsilon}} e^{\frac{2C}{M_P}\sqrt{2\epsilon}}}{\pi^2} \frac{V_0^2}{M_P^8} \frac{(1-\epsilon)^3 \left(\Gamma\left(\frac{1}{2}+\frac{1}{1-\epsilon}\right)\right)^4}{(-3+\epsilon)^2\epsilon} (k_1 k_3)^{-1-\frac{2}{1-\epsilon}} \tag{13.12}$$

We have verified that Maldacena's consistency relation [27] is verified for the full model, whereas in the literature so far it has been studied in the slow-roll regime only.
It would be desirable to have an analytic expression of the equilateral bispectrum as well, since the squeezed and equilateral configurations are the most important ones when confronting models with observations. However, as we have seen, the integrals are difficult to deal with analytically and the equilateral case will probably have to be studied numerically.

Furthermore, we have discussed a class of models, motivated by the phenomenon of climbing scalars in String Theory, that may lead to a suppressed power-spectrum at low ℓ [1, 2]. Power-law inflation is the attractor solution at late times for these models. The power-spectrum for a particular model has been studied numerically: the qualitative features we observe are well-known and peculiar to the systems experiencing the climbing, however the power-spectrum for this specific potential had never been presented before.
The next step will be to extend the analysis to the bispectrum, and compare the results with the behaviour on the attractor.

Having neat predictions for primordial non-Gaussianity is of crucial importance. Future observational prospects are bright: the upcoming missions, especially on the large-scale structure side, are likely to measure $f_{\rm NL}$ down to a fundamental threshold, that will shed light on the very nature of the mechanism of inflation.

Chapter 14

Acknowledgements

I wish to thank all my supervisors, for their support and insights, and Prof. Marco Peloso for his suggestions. They taught me to have faith that the final view is worth the climb.
I thank my family, my parents and my sister, and my grandma who loves chatting with me about the Universe. A special thanks to Luca, who patiently listened to all of my doubts and could probably defend this work together with me.

Appendix A

Useful expressions

A.1 Bessel and Hankel functions

We refer to [49] and [48] for the following list of properties of the Bessel and Hankel functions.

The Hankel functions are defined as:

$$H_\nu^{(1)}(z) = J_\nu(z) + iY_\nu(z) \qquad H_\nu^{(2)}(z) = J_\nu(z) - iY_\nu(z) \tag{A.1}$$

Let $\mathcal{C}_\nu(z)$ denote $J_\nu(z)$, $Y_\nu(z)$, $H_\nu^{(1)}(z)$, $H_\nu^{(2)}(z)$, or any non-trivial linear combination of these functions, the coefficients in which are independent of z and ν. The following recurrence relations hold:

$$\mathcal{C}_{\nu-1}(z) + \mathcal{C}_{\nu+1}(z) = \frac{2\nu}{z}\mathcal{C}_\nu(z) \tag{A.2a}$$

$$\mathcal{C}_{\nu-1}(z) - \mathcal{C}_{\nu+1}(z) = 2\frac{\partial \mathcal{C}_\nu(z)}{\partial z} \tag{A.2b}$$

The Bessel and Neumann functions have the following asymptotic behaviour for small arguments:

$$J_\nu(z) \xrightarrow{z\to 0} \frac{1}{\Gamma(\nu+1)}\left(\frac{z}{2}\right)^\nu \qquad 0 < z < \sqrt{\nu+1} \tag{A.3}$$

$$Y_\nu(z) \xrightarrow{z\to 0} -\frac{1}{\pi}\Gamma(\nu)\left(\frac{z}{2}\right)^{-\nu} \qquad \mathrm{Re}\nu > 0 \text{ or } \nu = -\frac{1}{2}, -\frac{3}{2}, -\frac{5}{2}, \dots \tag{A.4}$$

Asymptotically for large argument:

$$\begin{aligned} H_\nu^{(1)}(x) &\sim \sqrt{\frac{2}{\pi x}} e^{i\left(x - \nu\frac{\pi}{2} - \frac{\pi}{4}\right)} \\ H_\nu^{(2)}(x) &\sim \sqrt{\frac{2}{\pi x}} e^{-i\left(x - \nu\frac{\pi}{2} - \frac{\pi}{4}\right)} \end{aligned} \tag{A.5}$$

For small arguments, the Hankel functions have the following asymptotic behaviour:

$$\begin{aligned} H_\nu^{(1)}(z) &\xrightarrow{z\to 0} -\frac{i}{\pi}\Gamma(\nu)\left(\frac{z}{2}\right)^{-\nu} \qquad \mathrm{Re}\nu > 0 \\ H_\nu^{(2)}(z) &\xrightarrow{z\to 0} \frac{i}{\pi}\Gamma(\nu)\left(\frac{z}{2}\right)^{-\nu} \qquad \mathrm{Re}\nu > 0 \end{aligned} \tag{A.6}$$

There are explicit expressions for Hankel functions of certain indices. For $\nu = 3/2$:

$$H_{3/2}^{(1)}(z) = -i\sqrt{\frac{2}{\pi}} z^{-3/2}(1 + iz)e^{-iz} \tag{A.7}$$

A.2 Exponential integral

$$\int_{-\infty(1-i\epsilon)}^{\tau_e} d\tau \frac{e^{ik_T\tau}}{\tau} = -E_1(ik_T\tau_e) \tag{A.8}$$

Where the exponential integral is defined as:

$$\mathrm{Ei}(x) = \int_{-\infty}^{x} \frac{e^t}{t} dt = -\int_{-x}^{\infty} \frac{e^-t}{t} dt \qquad x \in \mathbb{R} \tag{A.9}$$

$$E_1(z) = \int_{z}^{\infty} \frac{e^{-t}}{t} dt \qquad z \in \mathbb{C},\ |\arg(z)| < \pi \tag{A.10}$$

For $x > 0$:

$$-E_1(x) = \mathrm{Ei}(-x) \tag{A.11}$$

For $z \in \mathbb{R}$ or $\mathbb{C}$ off the negative real axis:

$$E_1(z) = -\gamma - \log z - \sum_{k=1}^{\infty} \frac{(-z)^k}{k \cdot k!} \tag{A.12}$$

where γ is the Euler-Mascheroni constant $\gamma \approx 0.577$.

Appendix B

A first attempt to deal with the traditional calculation

As an attempt to deal with the integrals of three Hankel functions appearing in (10.11), we try to approximate the functions on superhorizon scales and set a cutoff in the integration. We deal with the time-integrated piece (10.20) and the remaining non-integrated piece separately, then we put them together.

B.1 Approximation on superhorizon scales: time-integrated piece

For small arguments, the Hankel functions have the asymptotic behaviour (A.5):

$$H_\nu^{(1)}(z) \xrightarrow{z \longrightarrow 0} -\frac{i}{\pi}\Gamma(\nu)\left(\frac{z}{2}\right)^{-\nu} \qquad \mathrm{Re}\nu > 0 \tag{B.1}$$

and $H_\nu^{(2)}(z) = \left(H_\nu^{(1)}(z)\right)^*$.

We want to compute (10.20) and the corresponding contributions from the other two momenta:

$$\begin{aligned}
&\frac{1}{(2\pi)^{3/2}}\delta^{(3)}(\vec{k}_1+\vec{k}_2+\vec{k}_3)\frac{\pi}{2i}\Bigg\{(-\tau)^\alpha \theta_{k_1}(\tau)\theta_{k_2}(\tau)\int_{\tau_i}^{\tau} d\eta(-\eta)^{1-\alpha}\cdot \\
&(p-1)(-k_3\tau)\left(H_\alpha^{(1)}(-k_3\eta)H_{\alpha+1}^{(2)}(-k_3\tau) - H_{\alpha+1}^{(1)}(-k_3\tau)H_\alpha^{(2)}(-k_3\eta)\right)\cdot \\
&\quad\Big(\mathcal{S}_1(\eta,\vec{k}_3,\vec{k}_1,\vec{k}_2)\theta^*_{k_1}(\eta)\theta^*_{k_2}(\eta) + \mathcal{S}_2(\eta,\vec{k}_3,\vec{k}_1,\vec{k}_2)\theta^*_{k_1}(\eta)\theta^{*\prime}_{k_2}(\eta) + \\
&\quad\mathcal{S}_3(\eta,\vec{k}_3,\vec{k}_1,\vec{k}_2)\theta^{*\prime}_{k_1}(\eta)\theta^*_{k_2}(\eta) + \mathcal{S}_4(\eta,\vec{k}_3,\vec{k}_1,\vec{k}_2)\theta^{*\prime}_{k_1}(\eta)\theta^{*\prime}_{k_2}(\eta)\Big)\Bigg\} \\
&+\vec{k}_2 \longleftrightarrow \vec{k}_3 + \vec{k}_1 \longleftrightarrow \vec{k}_3
\end{aligned} \tag{B.2}$$

From (6.30) we have:

$$\theta_k(\tau) = c(-\tau)^\nu H_\nu^{(1)}(-k\tau) \qquad\qquad \theta'_k(\tau) = -ck(-\tau)^\nu H_{\nu-1}^{(1)}(-k\tau)$$

and recall that $\alpha = \nu - 1$.

The time integrals to be computed are:

$$\begin{aligned}
&H^{(2)}_{\alpha+1}(-k_3\tau)\int_{\tau_i}^{\tau} d\eta(-\eta)^{1-\alpha}H^{(1)}_{\alpha}(-k_3\eta)\cdot \\
&\quad\Big(\mathcal{S}_1(\eta,\vec{k}_3,\vec{k}_1,\vec{k}_2)\theta^*_{k_1}(\eta)\theta^*_{k_2}(\eta)+\mathcal{S}_2(\eta,\vec{k}_3,\vec{k}_1,\vec{k}_2)\theta^*_{k_1}(\eta)\theta^{*\prime}_{k_2}(\eta)+ \\
&\quad\mathcal{S}_3(\eta,\vec{k}_3,\vec{k}_1,\vec{k}_2)\theta^{*\prime}_{k_1}(\eta)\theta^*_{k_2}(\eta)+\mathcal{S}_4(\eta,\vec{k}_3,\vec{k}_1,\vec{k}_2)\theta^{*\prime}_{k_1}(\eta)\theta^{*\prime}_{k_2}(\eta)\Big) \\
&-H^{(1)}_{\alpha+1}(-k_3\tau)\int_{\tau_i}^{\tau} d\eta(-\eta)^{1-\alpha}H^{(2)}_{\alpha}(-k_3\eta)\cdot \\
&\quad\Big(\mathcal{S}_1(\eta,\vec{k}_3,\vec{k}_1,\vec{k}_2)\theta^*_{k_1}(\eta)\theta^*_{k_2}(\eta)+\mathcal{S}_2(\eta,\vec{k}_3,\vec{k}_1,\vec{k}_2)\theta^*_{k_1}(\eta)\theta^{*\prime}_{k_2}(\eta)+ \\
&\quad\mathcal{S}_3(\eta,\vec{k}_3,\vec{k}_1,\vec{k}_2)\theta^{*\prime}_{k_1}(\eta)\theta^*_{k_2}(\eta)+\mathcal{S}_4(\eta,\vec{k}_3,\vec{k}_1,\vec{k}_2)\theta^{*\prime}_{k_1}(\eta)\theta^{*\prime}_{k_2}(\eta)\Big) \\
&\equiv H^{(2)}_{\alpha+1}(-k_3\tau)I_1-H^{(1)}_{\alpha+1}(-k_3\tau)I_2
\end{aligned} \tag{B.3}$$

$$\begin{aligned}
I_1=&\int_{\tau_i}^{\tau} d\eta(-\eta)^{1-\alpha}H^{(1)}_{\alpha}(-k_3\eta)\cdot \\
&\Bigg[\left(\mathcal{S}_{1,0}(\vec{k}_3,\vec{k}_1,\vec{k}_2)+\frac{1}{(-\eta)^2}\mathcal{S}_{1,2}(\vec{k}_3,\vec{k}_1,\vec{k}_2)\right)\theta^*_{k_1}(\eta)\theta^*_{k_2}(\eta)+ \\
&\left(\frac{1}{(-\tau)}\mathcal{S}_{2,1}(\vec{k}_3,\vec{k}_1,\vec{k}_2)+\frac{1}{(-\tau)^3}\mathcal{S}_{2,3}(\vec{k}_3,\vec{k}_1,\vec{k}_2)\right)\theta^*_{k_1}(\eta)\theta^{*\prime}_{k_2}(\eta)+ \\
&\left(\frac{1}{(-\tau)}\mathcal{S}_{3,1}(\vec{k}_3,\vec{k}_1,\vec{k}_2)+\frac{1}{(-\tau)^3}\mathcal{S}_{3,3}(\vec{k}_3,\vec{k}_1,\vec{k}_2)\right)\theta^{*\prime}_{k_1}(\eta)\theta^*_{k_2}(\eta)+ \\
&\left(\mathcal{S}_{4,0}(\vec{k}_3,\vec{k}_1,\vec{k}_2)+\frac{1}{(-\tau)^2}\mathcal{S}_{4,2}(\vec{k}_3,\vec{k}_1,\vec{k}_2)+\frac{1}{(-\tau)^4}\mathcal{S}_{4,4}(\vec{k}_3,\vec{k}_1,\vec{k}_2)\right)\theta^{*\prime}_{k_1}(\eta)\theta^{*\prime}_{k_2}(\eta)\Big)\Bigg]
\end{aligned} \tag{B.4}$$

$$\begin{aligned}
I_2=&\int_{\tau_i}^{\tau} d\eta(-\eta)^{1-\alpha}H^{(2)}_{\alpha}(-k_3\eta)\cdot \\
&\Bigg[\left(\mathcal{S}_{1,0}(\vec{k}_3,\vec{k}_1,\vec{k}_2)+\frac{1}{(-\eta)^2}\mathcal{S}_{1,2}(\vec{k}_3,\vec{k}_1,\vec{k}_2)\right)\theta^*_{k_1}(\eta)\theta^*_{k_2}(\eta)+ \\
&\left(\frac{1}{(-\tau)}\mathcal{S}_{2,1}(\vec{k}_3,\vec{k}_1,\vec{k}_2)+\frac{1}{(-\tau)^3}\mathcal{S}_{2,3}(\vec{k}_3,\vec{k}_1,\vec{k}_2)\right)\theta^*_{k_1}(\eta)\theta^{*\prime}_{k_2}(\eta)+ \\
&\left(\frac{1}{(-\tau)}\mathcal{S}_{3,1}(\vec{k}_3,\vec{k}_1,\vec{k}_2)+\frac{1}{(-\tau)^3}\mathcal{S}_{3,3}(\vec{k}_3,\vec{k}_1,\vec{k}_2)\right)\theta^{*\prime}_{k_1}(\eta)\theta^*_{k_2}(\eta)+ \\
&\left(\mathcal{S}_{4,0}(\vec{k}_3,\vec{k}_1,\vec{k}_2)+\frac{1}{(-\tau)^2}\mathcal{S}_{4,2}(\vec{k}_3,\vec{k}_1,\vec{k}_2)+\frac{1}{(-\tau)^4}\mathcal{S}_{4,4}(\vec{k}_3,\vec{k}_1,\vec{k}_2)\right)\theta^{*\prime}_{k_1}(\eta)\theta^{*\prime}_{k_2}(\eta)\Big)\Bigg]
\end{aligned} \tag{B.5}$$

The first piece, proportional to $\mathcal{S}_1$, is:

$$\begin{aligned}
I_{1,1}=&c^*c^*\mathcal{S}_{1,0}\int_{\tau_i}^{\tau} d\eta(-\eta)^{2+\nu}H^{(1)}_{\nu-1}(-k_3\eta)H^{(2)}_{\nu}(-k_1\eta)H^{(2)}_{\nu}(-k_2\eta)+ \\
&c^*c^*\mathcal{S}_{1,2}\int_{\tau_i}^{\tau} d\eta(-\eta)^{\nu}H^{(1)}_{\nu-1}(-k_3\eta)H^{(2)}_{\nu}(-k_1\eta)H^{(2)}_{\nu}(-k_2\eta) \\
\simeq&c^*c^*\frac{i}{\pi^3}(\nu-1)^2\left(\Gamma(\nu-1)\right)^3 2^{3\nu-1}\frac{k_3}{(k_1k_2k_3)^{\nu}}\cdot \\
&\left(\mathcal{S}_{1,0}\int_{\tau_i}^{\tau} d\eta(-\eta)^{3-2\nu}+\mathcal{S}_{1,2}\int_{\tau_i}^{\tau} d\eta(-\eta)^{1-2\nu}\right)
\end{aligned} \tag{B.6}$$

$$\begin{aligned}
I_{2,1} =& c^* c^* \mathcal{S}_{1,0} \int_{\tau_i}^{\tau} d\eta (-\eta)^{2+\nu} H_{\nu-1}^{(2)}(-k_3\eta) H_{\nu}^{(2)}(-k_1\eta) H_{\nu}^{(2)}(-k_2\eta) + \\
& c^* c^* \mathcal{S}_{1,2} \int_{\tau_i}^{\tau} d\eta (-\eta)^{\nu} H_{\nu-1}^{(2)}(-k_3\eta) H_{\nu}^{(2)}(-k_1\eta) H_{\nu}^{(2)}(-k_2\eta) \\
\simeq & - c^* c^* \frac{i}{\pi^3} (\nu-1)^2 (\Gamma(\nu-1))^3 \, 2^{3\nu-1} \frac{k_3}{(k_1 k_2 k_3)^{\nu}} \cdot \\
& \left(\mathcal{S}_{1,0} \int_{\tau_i}^{\tau} d\eta (-\eta)^{3-2\nu} + \mathcal{S}_{1,2} \int_{\tau_i}^{\tau} d\eta (-\eta)^{1-2\nu} \right)
\end{aligned} \tag{B.7}$$

Set:

$$-\eta \equiv x \tag{B.8}$$

$$\begin{aligned}
I_{1,1} =& (c^*)^2 \frac{i}{\pi^3} (\nu-1)^2 (\Gamma(\nu-1))^3 \, 2^{3\nu-1} \frac{k_3}{(k_1 k_2 k_3)^{\nu}} \cdot \\
& \left(-\mathcal{S}_{1,0} \frac{1}{4-2\nu} x^{4-2\nu} \Big|_{x_i}^{x_f} - \mathcal{S}_{1,2} \frac{1}{2-2\nu} x^{2-2\nu} \Big|_{x_i}^{x_f} \right) \qquad \text{if } \nu \neq 2, \, \nu \neq 1 \\
I_{2,1} =& - I_{1,1}
\end{aligned} \tag{B.9}$$

In a similar fashion, we compute all the other integrals. The second piece, proportional to $\mathcal{S}_2$, is:

$$\begin{aligned}
I_{1,2} =& c^* c^* (-k_2) \mathcal{S}_{2,1} \int_{\tau_i}^{\tau} d\eta (-\eta)^{1+\nu} H_{\nu-1}^{(1)}(-k_3\eta) H_{\nu}^{(2)}(-k_1\eta) H_{\nu-1}^{(2)}(-k_2\eta) + \\
& c^* c^* (-k_2) \mathcal{S}_{2,3} \int_{\tau_i}^{\tau} d\eta (-\eta)^{-1+\nu} H_{\nu-1}^{(1)}(-k_3\eta) H_{\nu}^{(2)}(-k_1\eta) H_{\nu-1}^{(2)}(-k_2\eta) + \\
\simeq & - c^* c^* \left(\frac{i}{\pi} \right)^3 (\nu-1) (\Gamma(\nu-1))^3 \, 2^{3\nu-2} \frac{(-k_2^2 k_3)}{(k_1 k_2 k_3)^{\nu}} \cdot \\
& \left(\mathcal{S}_{2,1} \int_{\tau_i}^{\tau} d\eta (-\eta)^{3-2\nu} + \mathcal{S}_{2,3} \int_{\tau_i}^{\tau} d\eta (-\eta)^{1-2\nu} \right) \\
=& - (c^*)^2 \frac{i}{\pi^3} (\nu-1) (\Gamma(\nu-1))^3 \, 2^{3\nu-2} \frac{k_2^2 k_3}{(k_1 k_2 k_3)^{\nu}} \cdot \\
& \left(-\mathcal{S}_{2,1} \frac{1}{4-2\nu} x^{4-2\nu} \Big|_{x_i}^{x_f} - \mathcal{S}_{2,3} \frac{1}{2-2\nu} x^{2-2\nu} \Big|_{x_i}^{x_f} \right) \qquad \text{if } \nu \neq 2, \, \nu \neq 1 \\
I_{2,2} =& - I_{1,2}
\end{aligned} \tag{B.10}$$

The third piece, proportional to $\mathcal{S}_3$, is like the previous one, but with $\vec{k}_1 \longleftrightarrow \vec{k}_2$. Recall that $\mathcal{S}_{2,i}(\vec{k}_3, \vec{k}_2, \vec{k}_1) = \mathcal{S}_{3,i}(\vec{k}_3, \vec{k}_1, \vec{k}_2)$.

$$\begin{aligned}
I_{1,3} =& - (c^*)^2 \frac{i}{\pi^3} (\nu-1) (\Gamma(\nu-1))^3 \, 2^{3\nu-2} \frac{k_1^2 k_3}{(k_1 k_2 k_3)^{\nu}} \cdot \\
& \left(-\mathcal{S}_{3,1} \frac{1}{4-2\nu} x^{4-2\nu} \Big|_{x_i}^{x_f} - \mathcal{S}_{3,3} \frac{1}{2-2\nu} x^{2-2\nu} \Big|_{x_i}^{x_f} \right) \qquad \text{if } \nu \neq 2, \, \nu \neq 1 \\
I_{2,3} =& - I_{1,3}
\end{aligned} \tag{B.11}$$

And the fourth piece, proportional to $\mathcal{S}_4$, is:

$$\begin{aligned}
I_{1,4} =& c^* c^* \int_{\tau_i}^{\tau} d\eta (-\eta)^{2-\nu} (-\eta)^{2\nu} H^{(1)}_{\nu-1}(-k_3\eta) H^{(2)}_{\nu-1(-k_1\eta)} H^{(2)}_{\nu-1}(-k_2\eta)(k_1k_2)\cdot \\
& \left(\mathcal{S}_{4,0}(\vec{k}_3,\vec{k}_1,\vec{k}_2) + \frac{1}{(-\tau)^2}\mathcal{S}_{4,2}(\vec{k}_3,\vec{k}_1,\vec{k}_2) + \frac{1}{(-\tau)^4}\mathcal{S}_{4,4}(\vec{k}_3,\vec{k}_1,\vec{k}_2)\right) \\
\simeq& - c^* c^* \left(\frac{i}{\pi}\right)^3 (\Gamma(\nu-1))^3\, 2^{3\nu-3} \frac{k_1^2k_2^2k_3}{(k_1k_2k_3)^\nu}\cdot \\
& \left(\mathcal{S}_{4,0}\int_{\tau_i}^{\tau} d\eta(-\eta)^{5-2\nu} + \mathcal{S}_{4,2}\int_{\tau_i}^{\tau} d\eta(-\eta)^{3-2\nu} + \mathcal{S}_{4,4}\int_{\tau_i}^{\tau} d\eta(-\eta)^{1-2\nu}\right) \\
=& c^* c^* \frac{i}{\pi^3} (\Gamma(\nu-1))^3\, 2^{3\nu-3} \frac{k_1^2k_2^2k_3}{(k_1k_2k_3)^\nu}\cdot \\
& \left(-\mathcal{S}_{4,0}\frac{1}{6-2\nu}x^{6-2\nu}\Big|_{x_i}^{xf} - \mathcal{S}_{4,2}\frac{1}{4-2\nu}x^{4-2\nu}\Big|_{x_i}^{xf} - \mathcal{S}_{4,4}\frac{1}{2-2\nu}x^{2-2\nu}\Big|_{x_i}^{xf}\right) \\
& \text{if } \nu \neq 3,\ \nu \neq 2,\ \nu \neq 1 \\
I_{2,4} =& - I_{1,4}
\end{aligned} \tag{B.12}$$

In performing the integrals, we assumed $\nu \neq 1, 2, 3$. For sure $\nu > 3/2$, and it asymptotically reaches $3/2$ in the de Sitter limit $p \to \infty$. In terms of the exponent of the potential γ, $\nu = 2$ implies $\gamma = 1/3$ and $\nu = 3$ implies $\gamma = 1/\sqrt{5}$. These values are both much larger than the one found in [56]: they found $\gamma \approx 0.08$ in order to fit the large-k behaviour of the observed power-spectrum, with scalar spectral index $n_s \approx 0.96$. Hence we should not be worried about these conditions.

Now we put the four pieces together:

$$\begin{aligned}
I_1 =& I_{1,1} + I_{1,2} + I_{1,3} + I_{1,4} \\
\simeq& (c^*)^2 \frac{i2^{3\nu-4}}{\pi^3} (\Gamma(\nu-1))^3 \frac{k_3}{(k_1k_2k_3)^\nu}\cdot \\
& \left\{ x^{2-2\nu}\Big|_{x_i}^{xf} \left(4(\nu-1)\mathcal{S}_{1,2} - 2k_2^2\mathcal{S}_{2,3} - 2k_1^2\mathcal{S}_{3,3} + \frac{1}{\nu-1}k_1^2k_2^2\mathcal{S}_{4,4}\right) + \right. \\
& x^{4-2\nu}\Big|_{x_i}^{xf} \left(4\frac{(\nu-1)^2}{\nu-2}\mathcal{S}_{1,0} - 2\frac{\nu-1}{\nu-2}k_2^2\mathcal{S}_{2,1} - 2\frac{\nu-1}{\nu-2}k_1^2\mathcal{S}_{3,1} + \frac{1}{\nu-2}k_1^2k_2^2\mathcal{S}_{4,2}\right) + \\
& \left. x^{6-2\nu}\Big|_{x_i}^{xf} \left(\frac{1}{\nu-3}k_1^2k_2^2\mathcal{S}_{4,0}\right) \right\} \\
I_2 =& - I_1
\end{aligned}$$

The extrema of integration x_i and x_f correspond to τ_i and τ respectively. We want all the three wavelength corresponding to k_1, k_2, k_3 to be outside of the horizon when we integrate, hence $-k_i\tau \leq 1$ for the smallest wavelength or equivalently the largest k:

$$x_i = \frac{1}{k_{\max}}$$

We will want to compute the bispectrum at the end of inflation, $\tau = 0$, but for now we keep it there.

Putting together the pieces, (B.2) becomes:

$$
\begin{aligned}
&\langle \mathcal{R}_{\vec{k}_1}(\tau)\mathcal{R}_{\vec{k}_2}(\tau)\mathcal{R}_{\vec{k}_3}(\tau)\rangle\Big|_{\text{time-integrated piece}} \\
&= \frac{1}{2}\frac{1}{(2\pi)^{3/2}}\delta^{(3)}(\vec{k}_1+\vec{k}_2+\vec{k}_3)\frac{\pi}{2i}k_3(p-1)(-\tau)^{\nu}\theta_{k_1}(\tau)\theta_{k_2}(\tau)\left(H_\nu^{(2)}(-k_3\tau)I_1 - H_\nu^{(1)}(-k_3\tau)I_2\right) \\
&\quad + \vec{k}_2 \longleftrightarrow \vec{k}_3 + \vec{k}_1 \longleftrightarrow \vec{k}_3 \\
&= \frac{1}{(2\pi)^{3/2}}\delta^{(3)}(\vec{k}_1+\vec{k}_2+\vec{k}_3)\frac{\pi}{4i}k_3(p-1)c^2(-\tau)^{3\nu}H_\nu^{(1)}(-k_1\tau)H_\nu^{(1)}(-k_2\tau)2J_\nu(-k_3\tau)I_1 \\
&\quad + \vec{k}_2 \longleftrightarrow \vec{k}_3 + \vec{k}_1 \longleftrightarrow \vec{k}_3
\end{aligned} \tag{B.13}
$$

The additional factor $\frac{1}{2}$ comes from the definition of the second order perturbation $\mathcal{R}^{(2)}$.
Notice that the last step, where the Bessel function appears, is necessary: we cannot approximate for small argument before that, otherwise the two Hankel functions in parenthesis add up to zero. The Bessel function grasp the next order in the approximation.
The asymptotic behaviour of the Bessel functions is given in (A.3) and (A.4):

$$
J_\nu(z) \xrightarrow{z\longrightarrow 0} \frac{1}{\Gamma(\nu+1)}\left(\frac{z}{2}\right)^{\nu} \qquad 0 < z < \sqrt{\nu+1} \tag{B.14}
$$

$$
Y_\nu(z) \xrightarrow{z\longrightarrow 0} -\frac{1}{\pi}\Gamma(\nu)\left(\frac{z}{2}\right)^{-\nu} \qquad \text{Re}\nu > 0 \text{ or } \nu = -\frac{1}{2}, -\frac{3}{2}, -\frac{5}{2}, \ldots \tag{B.15}
$$

The condition on z translates into $-k_i\tau < \sqrt{\nu+1}$, but $\nu > 3/2$ so in the most restrictive case $-k_i\tau \leq 1.5$, which is true anyway since we are putting ourselves on superhorizon scales.

The time-integrated piece becomes:

$$
\begin{aligned}
&\langle \mathcal{R}_{\vec{k}_1}(\tau)\mathcal{R}_{\vec{k}_2}(\tau)\mathcal{R}_{\vec{k}_3}(\tau)\rangle\Big|_{\text{time-integrated piece}} \\
&= \frac{1}{(2\pi)^{3/2}}\delta^{(3)}(\vec{k}_1+\vec{k}_2+\vec{k}_3)\left(-\frac{2^{-5+4\nu}}{\pi^4}\right)(c^*c)^2\frac{k_3^{2+2\nu}}{(k_1k_2k_3)^{2\nu}}\frac{p^2-1}{3p-1}\left(\Gamma(\nu-1)\right)^4 \cdot \\
&\quad (-\tau)^{2\nu}\left(x^{2-2\nu}\Big|_{x_i}^{x^f}F_2(\vec{k}_3,\vec{k}_1,\vec{k}_2) + x^{4-2\nu}\Big|_{x_i}^{x^f}F_4(\vec{k}_3,\vec{k}_1,\vec{k}_2) + x^{6-2\nu}\Big|_{x_i}^{x^f}F_6(\vec{k}_3,\vec{k}_1,\vec{k}_2)\right) \\
&\quad + \vec{k}_2 \longleftrightarrow \vec{k}_3 + \vec{k}_1 \longleftrightarrow \vec{k}_3
\end{aligned} \tag{B.16}
$$

where:

$$
\begin{aligned}
F_2(\vec{k}_3,\vec{k}_1,\vec{k}_2) =& 4(\nu-1)\mathcal{S}_{1,2}(\vec{k}_3,\vec{k}_1,\vec{k}_2) - 2k_2^2\mathcal{S}_{2,3}(\vec{k}_3,\vec{k}_1,\vec{k}_2) - 2k_1^2\mathcal{S}_{3,3}(\vec{k}_3,\vec{k}_1,\vec{k}_2) + \\
&+ \frac{1}{\nu-1}k_1^2k_2^2\mathcal{S}_{4,4}(\vec{k}_3,\vec{k}_1,\vec{k}_2) \qquad \text{(B.17)} \\
F_4(\vec{k}_3,\vec{k}_1,\vec{k}_2) =& -\frac{1}{\nu-2}\Big(-4\mathcal{S}_{1,0}(\vec{k}_3,\vec{k}_1,\vec{k}_2)(\nu-1)^2 + 2k_2^2(\nu-1)\mathcal{S}_{2,1}(\vec{k}_3,\vec{k}_1,\vec{k}_2) \\
&+ 2k_1^2(\nu-1)\mathcal{S}_{3,1}(\vec{k}_3,\vec{k}_1,\vec{k}_2) - k_1^2k_2^2\mathcal{S}_{4,2}(\vec{k}_3,\vec{k}_1,\vec{k}_2)\Big) \qquad \text{(B.18)} \\
F_6(\vec{k}_3,\vec{k}_1,\vec{k}_2) =& \frac{1}{\nu-3}k_1^2k_2^2\mathcal{S}_{4,0}(\vec{k}_3,\vec{k}_1,\vec{k}_2) \qquad \text{(B.19)} \\
& \qquad \text{(B.20)}
\end{aligned}
$$

Then we have the other two terms in (B.2), the ones that we have always written very schematically $\vec{k}_2 \longleftrightarrow \vec{k}_3$ and $\vec{k}_1 \longleftrightarrow \vec{k}_3$. Their final contribution will be equal to the first one, that we have computed explicitly, but with the momenta exchanged.

The whole time-integrated piece, after adding up the three contributions, is:

$$
\begin{aligned}
&\langle \mathcal{R}_{\vec{k}_1}(\tau)\mathcal{R}_{\vec{k}_2}(\tau)\mathcal{R}_{\vec{k}_3}(\tau)\rangle\Big|_{\text{time-integrated piece}} \\
&= \frac{1}{(2\pi)^{3/2}}\delta^{(3)}(\vec{k}_1+\vec{k}_2+\vec{k}_3)\left(\frac{2^{-5+4\nu}}{\pi^4}\right)(c^*c)^2\frac{p^2-1}{3p-1}\left(\Gamma(\nu-1)\right)^4(-\tau)^{2\nu}\cdot \\
&\left(x^{2-2\nu}\Big|_{x_i}^{xf}\mathcal{F}_2(\vec{k}_1,\vec{k}_2,\vec{k}_3)+x^{4-2\nu}\Big|_{x_i}^{xf}\mathcal{F}_4(\vec{k}_1,\vec{k}_2,\vec{k}_3)+x^{6-2\nu}\Big|_{x_i}^{xf}\mathcal{F}_6(\vec{k}_1,\vec{k}_2,\vec{k}_3)\right)
\end{aligned} \tag{B.21}
$$

The functions $\mathcal{F}_i$ are symmetric under exchange of *any pair* of arguments.

$$
\begin{aligned}
\mathcal{F}_2(\vec{k}_1,\vec{k}_2,\vec{k}_3) &= -k_1^2(k_2k_3)^{-2\nu}F_2(\vec{k}_1,\vec{k}_3,\vec{k}_2)-k_2^2(k_1k_3)^{-2\nu}F_2(\vec{k}_2,\vec{k}_1,\vec{k}_3)-k_3^2(k_1k_2)^{-2\nu}F_2(\vec{k}_3,\vec{k}_1,\vec{k}_2) \\
\mathcal{F}_4(\vec{k}_1,\vec{k}_2,\vec{k}_3) &= -k_1^2(k_2k_3)^{-2\nu}F_4(\vec{k}_1,\vec{k}_3,\vec{k}_2)-k_2^2(k_1k_3)^{-2\nu}F_4(\vec{k}_2,\vec{k}_1,\vec{k}_3)-k_3^2(k_1k_2)^{-2\nu}F_4(\vec{k}_3,\vec{k}_1,\vec{k}_2) \\
\mathcal{F}_6(\vec{k}_1,\vec{k}_2,\vec{k}_3) &= -k_1^2(k_2k_3)^{-2\nu}F_6(\vec{k}_1,\vec{k}_3,\vec{k}_2)-k_2^2(k_1k_3)^{-2\nu}F_6(\vec{k}_2,\vec{k}_1,\vec{k}_3)-k_3^2(k_1k_2)^{-2\nu}F_6(\vec{k}_3,\vec{k}_1,\vec{k}_2)
\end{aligned} \tag{B.22}
$$

B.2 Approximation on superhorizon scales: non-integrated piece

Approximating the Hankel functions as in (A.6), the contribution from $\vec{k}_3$ is:

$$
\begin{aligned}
&\delta^{(3)}(\vec{k}_1+\vec{k}_2+\vec{k}_3)\frac{2^{-\frac{11}{2}+4\nu}}{\pi^{11/2}}(c^*c)^2\frac{1}{k_1^{2\nu}k_2^{2\nu}k_3^4}\frac{(p+1)^2}{(p-1)^4p^2}\left(\Gamma(\nu-1)\right)^4\cdot \\
&\left(G_0(\vec{k}_3,\vec{k}_1,\vec{k}_2)+(-\tau)^2G_2(\vec{k}_3,\vec{k}_1,\vec{k}_2)+(-\tau)^4G_4(\vec{k}_3,\vec{k}_1,\vec{k}_2)\right)
\end{aligned} \tag{B.23}
$$

where:

$$
\begin{aligned}
G_0(\vec{k}_3,\vec{k}_1,\vec{k}_2) &= p^2\left((1+p)\left(-3(k_1^4+k_2^4)+2(k_1^2+k_2^2)k_3^2+6k_1^2k_2^2\right)+(-19+13p)k_3^4\right) \\
G_2(\vec{k}_3,\vec{k}_1,\vec{k}_2) &= p(p-1)^2\left(-2(k_1^2+k_2^2)k_3^4+3p(k_1^2-k_2^2)^2(k_1^2+k_2^2)-p(3k_1^4+3k_2^4+2k_1^2k_2^2)k_3^2\right) \\
G_4(\vec{k}_3,\vec{k}_1,\vec{k}_2) &= (p-1)^4k_1^2k_2^2k_3^4
\end{aligned} \tag{B.24}
$$

Analogous contributions will come from $\vec{k}_2 \longleftrightarrow \vec{k}_3$ and $\vec{k}_1 \longleftrightarrow \vec{k}_3$ but with the momenta exchanged accordingly.
Adding up the three pieces and collecting all the powers of τ:

$$
\begin{aligned}
&\langle \mathcal{R}_{\vec{k}_1}(\tau)\mathcal{R}_{\vec{k}_2}(\tau)\mathcal{R}_{\vec{k}_3}(\tau)\rangle\Big|_{\text{non-integrated piece}} \\
&= \delta^{(3)}(\vec{k}_1+\vec{k}_2+\vec{k}_3)\frac{2^{-\frac{11}{2}+4\nu}}{\pi^{11/2}}(c^*c)^2\frac{1}{(k_1k_2k_3)^{2(2+\nu)}}\frac{(p+1)^2}{(p-1)^4p^2}\frac{1}{k_1^4k_2^4k_3^4}\left(\Gamma(\nu-1)\right)^4\cdot \\
&\left(\mathcal{G}_0(\vec{k}_1,\vec{k}_2,\vec{k}_3)+\mathcal{G}_2(\vec{k}_1,\vec{k}_2,\vec{k}_3)(-\tau)^2+\mathcal{G}_4(\vec{k}_1,\vec{k}_2,\vec{k}_3)(-\tau)^4\right)
\end{aligned} \tag{B.25}
$$

$$
\begin{aligned}
\mathcal{G}_0(\vec{k}_1,\vec{k}_2,\vec{k}_3) &= k_1^{2\nu}k_2^4k_3^4G_0(\vec{k}_1,\vec{k}_3,\vec{k}_2)+k_1^4k_2^{2\nu}k_3^4G_0(\vec{k}_2,\vec{k}_1,\vec{k}_3)+k_1^4k_2^4k_3^{2\nu}G_0(\vec{k}_3,\vec{k}_1,\vec{k}_2) \\
\mathcal{G}_2(\vec{k}_1,\vec{k}_2,\vec{k}_3) &= k_1^{2\nu}k_2^4k_3^4G_2(\vec{k}_1,\vec{k}_3,\vec{k}_2)+k_1^4k_2^{2\nu}k_3^4G_2(\vec{k}_2,\vec{k}_1,\vec{k}_3)+k_1^4k_2^4k_3^{2\nu}G_2(\vec{k}_3,\vec{k}_1,\vec{k}_2) \\
\mathcal{G}_4(\vec{k}_1,\vec{k}_2,\vec{k}_3) &= k_1^{2\nu}k_2^4k_3^4G_4(\vec{k}_1,\vec{k}_3,\vec{k}_2)+k_1^4k_2^{2\nu}k_3^4G_4(\vec{k}_2,\vec{k}_1,\vec{k}_3)+k_1^4k_2^4k_3^{2\nu}G_4(\vec{k}_3,\vec{k}_1,\vec{k}_2)
\end{aligned} \tag{B.26}
$$

The functions $\mathcal{G}_i$ are symmetric under exchange of *any pair* of momenta.

B.3 Full bispectrum: time-integrated piece and non-integrated piece together

Putting together the contribution from (B.21) and (B.25) we obtain:

$$\begin{aligned}&\langle \mathcal{R}_{\vec{k}_1}(\tau)\mathcal{R}_{\vec{k}_2}(\tau)\mathcal{R}_{\vec{k}_3}(\tau)\rangle \\ &= \delta^{(3)}(\vec{k}_1+\vec{k}_2+\vec{k}_3)\frac{2^{-\frac{13}{2}+4\nu}}{\pi^{11/2}}(c^*c)^2\left(\Gamma(\nu-1)\right)^4\Big(\mathcal{B}_0(\vec{k}_1,\vec{k}_2,\vec{k}_3)+(-\tau)^{2\nu}\mathcal{B}_{2\nu}(\vec{k}_1,\vec{k}_2,\vec{k}_3)+ \\ &\quad +(-\tau)^2\mathcal{B}_2(\vec{k}_1,\vec{k}_2,\vec{k}_3)+(-\tau)^4\mathcal{B}_4(\vec{k}_1,\vec{k}_2,\vec{k}_3)+(-\tau)^6\mathcal{B}_6(\vec{k}_1,\vec{k}_2,\vec{k}_3)\Big)\end{aligned} \tag{B.27}$$

$$\begin{aligned}\mathcal{B}_0(\vec{k}_1,\vec{k}_2,\vec{k}_3) &= \frac{(p+1)^2}{(p-1)^4p^2}\frac{1}{(k_1k_2k_3)^{2(2+\nu)}}\mathcal{G}_0(\vec{k}_1,\vec{k}_2,\vec{k}_3) \\ \mathcal{B}_{2\nu}(\vec{k}_1,\vec{k}_2,\vec{k}_3) &= -\frac{p^2-1}{3p-1}(-\tau_i)^{2-2\nu}\Big(\mathcal{F}_2(\vec{k}_1,\vec{k}_2,\vec{k}_3)+(-\tau_i)^2\mathcal{F}_4(\vec{k}_1,\vec{k}_2,\vec{k}_3)+(-\tau_i)^4\mathcal{F}_6(\vec{k}_1,\vec{k}_2,\vec{k}_3)\Big) \\ \mathcal{B}_2(\vec{k}_1,\vec{k}_2,\vec{k}_3) &= \frac{p^2-1}{3p-1}\mathcal{F}_2(\vec{k}_1,\vec{k}_2,\vec{k}_3)+\frac{(p+1)^2}{(p-1)^4p^2}\frac{1}{(k_1k_2k_3)^{2(2+\nu)}}\mathcal{G}_2(\vec{k}_1,\vec{k}_2,\vec{k}_3) \\ \mathcal{B}_4(\vec{k}_1,\vec{k}_2,\vec{k}_3) &= \frac{p^2-1}{3p-1}\mathcal{F}_4(\vec{k}_1,\vec{k}_2,\vec{k}_3)+\frac{(p+1)^2}{(p-1)^4p^2}\frac{1}{(k_1k_2k_3)^{2(2+\nu)}}\mathcal{G}_4(\vec{k}_1,\vec{k}_2,\vec{k}_3) \\ \mathcal{B}_6(\vec{k}_1,\vec{k}_2,\vec{k}_3) &= \frac{p^2-1}{3p-1}\mathcal{F}(\vec{k}_1,\vec{k}_2,\vec{k}_3)\end{aligned} \tag{B.28}$$

Writing down explicitly the coefficient of the modefunction c and the scale factor normalization A:

$$\begin{aligned}&\langle \mathcal{R}_{\vec{k}_1}(\tau)\mathcal{R}_{\vec{k}_2}(\tau)\mathcal{R}_{\vec{k}_3}(\tau)\rangle \\ &= \delta^{(3)}(\vec{k}_1+\vec{k}_2+\vec{k}_3)\frac{2^{-\frac{23}{2}+4\nu}}{\pi^{7/2}}\frac{e^{\frac{2C}{M_P}\sqrt{\frac{2}{p}}}V_0^2}{M_P^8}\frac{(p-1)^4}{(1-3p)^2}\left(\Gamma(\nu-1)\right)^4\Big(\mathcal{B}_0(\vec{k}_1,\vec{k}_2,\vec{k}_3)+ \\ &\quad +(-\tau)^{2\nu}\mathcal{B}_{2\nu}(\vec{k}_1,\vec{k}_2,\vec{k}_3)+(-\tau)^2\mathcal{B}_2(\vec{k}_1,\vec{k}_2,\vec{k}_3)+(-\tau)^4\mathcal{B}_4(\vec{k}_1,\vec{k}_2,\vec{k}_3)+(-\tau)^6\mathcal{B}_6(\vec{k}_1,\vec{k}_2,\vec{k}_3)\Big)\end{aligned} \tag{B.29}$$

Evaluating the full bispectrum (B.29) at the end of inflation $\tau = 0$ we obtain:

$$\begin{aligned}&\langle \mathcal{R}_{\vec{k}_1}\mathcal{R}_{\vec{k}_2}\mathcal{R}_{\vec{k}_3}\rangle \\ &= \frac{1}{(2\pi)^{3/2}}\delta^{(3)}(\vec{k}_1+\vec{k}_2+\vec{k}_3)\frac{4^{-5+2\nu}}{\pi^2}\frac{e^{\frac{2C}{M_P}\sqrt{\frac{2}{p}}}V_0^2}{M_P^8}\left(\Gamma(\nu-1)\right)^4\frac{(p-1)^4}{(1-3p)^2}\mathcal{B}_0(\vec{k}_1,\vec{k}_2,\vec{k}_3) \\ &= \frac{1}{(2\pi)^{3/2}}\delta^{(3)}(\vec{k}_1+\vec{k}_2+\vec{k}_3)\frac{4^{-5+2\nu}}{\pi^2}\frac{e^{\frac{2C}{M_P}\sqrt{\frac{2}{p}}}V_0^2}{M_P^8}\left(\Gamma(\nu-1)\right)^4\frac{(1+p)^2}{(1-3p)^2}\frac{1}{(k_1k_2k_3)^{2(2+\nu)}}\cdot \\ &\quad\left(\frac{1}{2}k_1^{2\nu}k_2^4k_3^4\left(4k_1^2k_2^2(1+p)-6k_2^2(k_2^2-k_3^2)(1+p)+k_1^4(-19+13p)\right)+5\text{ perm.}\right)\end{aligned} \tag{B.30}$$

Rewritten in terms of ϵ only:

$$\boxed{\begin{aligned}&\langle \mathcal{R}_{\vec{k}_1}\mathcal{R}_{\vec{k}_2}\mathcal{R}_{\vec{k}_3}\rangle = \frac{1}{(2\pi)^{3/2}}\delta^{(3)}(\vec{k}_1+\vec{k}_2+\vec{k}_3) \\ &\frac{2^{-9+\frac{4}{1-\epsilon}}}{\pi^2}\frac{e^{\frac{2C}{M_P}\sqrt{2\epsilon}}V_0^2}{M_P^8}\frac{(1+\epsilon)^2\left(\Gamma\left(\frac{1+\epsilon}{2(1-\epsilon)}\right)\right)^4}{(3-\epsilon)^2\epsilon}\frac{1}{(k_1k_2k_3)^{-1-\frac{2}{1-\epsilon}}}\cdot \\ &\Big(4k_1^{-1+\frac{2}{1-\epsilon}}k_2^2(1+\epsilon)-6k_1^{-3+\frac{2}{1-\epsilon}}k_2^2\left(k_2^2-k_3^2\right)(1+\epsilon)+k_1^{1+\frac{2}{1-\epsilon}}(13-19\epsilon) \\ &+5\text{ permutations}\Big)\end{aligned}} \tag{B.31}$$

In the slow-roll limit $\epsilon \to 0$ and introducing the would-be Hubble parameter in de Sitter case $H_{\rm DS}^2 \equiv V_0/3M_P^2$, the leading order contribution is:

$$\frac{1}{(2\pi)^{3/2}}\delta^{(3)}(\vec{k}_1+\vec{k}_2+\vec{k}_3)\frac{H_{\rm DS}^4}{32k_1^4k_2^4k_3^4M_P^4\epsilon}\Big(4k_1^3k_2^2k_3-6k_1^5k_2+6k_1^3k_2^3+13k_1^4k_2k_3+5\text{ perm.}\Big) \quad \text{(B.32)}$$

As we have mentioned, there are additional contributions coming from the definitions of the different gauge-invariant variables, see equation (10.32). However, even taking care of the extra terms, this result still does not reproduce Maldacena's in the slow-roll limit.
This could be due to the integration procedure: setting a cutoff and restricting our attention on superhorizon scales may result in missing some important contribution at horizon crossing. This point needs to be further investigated.

Bibliography

[1] E. Dudas, N. Kitazawa, and A. Sagnotti, "On Climbing Scalars in String Theory," *Phys. Lett. B*, vol. 694, pp. 80–88, 2011.

[2] E. Dudas, N. Kitazawa, S. P. Patil, and A. Sagnotti, "CMB Imprints of a Pre-Inflationary Climbing Phase," *JCAP*, vol. 05, p. 012, 2012.

[3] C. R. Contaldi, M. Peloso, L. Kofman, and A. D. Linde, "Suppressing the lower multipoles in the CMB anisotropies," *JCAP*, vol. 07, p. 002, 2003.

[4] F. Lucchin and S. Matarrese, "Power Law Inflation," *Phys. Rev. D*, vol. 32, p. 1316, 1985.

[5] D. Baumann, "Inflation," in *Theoretical Advanced Study Institute in Elementary Particle Physics: Physics of the Large and the Small*, 2011, pp. 523–686.

[6] D. H. L. Andrew R. Liddle, *Cosmological Inflation and Large-Scale Structure.* Cambridge University Press, 2008. [Online]. Available: https://www.ebook.de/de/product/3243388/andrew_r_liddle_david_h_lyth_cosmological_inflation_and_large_scale_structure.html

[7] M. V. Viatcehslav Mukhanov, *Physical Foundations of Cosmology.* Cambridge University Press, 2013. [Online]. Available: https://www.ebook.de/de/product/4016569/viatcehslav_mukhanov_mukhanov_viatcheslav_physical_foundations_of_cosmology.html

[8] D. Baumann, "Cosmology. part iii: Mathematical tripos," 2014, lecture notes.

[9] X. Chen, "Primordial Non-Gaussianities from Inflation Models," *Adv. Astron.*, vol. 2010, p. 638979, 2010.

[10] A. R. L. David H. Lyth, *The Primordial Density Perturbation.* Cambridge University Press, 2015. [Online]. Available: https://www.ebook.de/de/product/8167912/david_h_lyth_andrew_r_liddle_the_primordial_density_perturbation.html

[11] D. Baumann, "Open Problems in Inflationary Cosmology," proceedings of the international Workshop "Unsolved Problems in Astrophysics and Cosmology (UPAC)", 13th-19th Feb 2011, Centro de Ciencias de Benasque Pedro Pascual. [Online]. Available: http://benasque.org/2011Astrophysics/talks_contr/151_Baumann.pdf

[12] N. Bartolo, E. Komatsu, S. Matarrese, and A. Riotto, "Non-Gaussianity from inflation: Theory and observations," *Phys. Rept.*, vol. 402, pp. 103–266, 2004.

[13] A. Ortolan, F. Lucchin, and S. Matarrese, "Nongaussian Perturbations From Inflationary Dynamics," *Phys. Rev. D*, vol. 38, p. 465, 1988.

[14] L. F. Abbott and M. B. Wise, "Constraints on Generalized Inflationary Cosmologies," *Nucl. Phys. B*, vol. 244, pp. 541–548, 1984.

[15] I. P. C. Heard and D. Wands, "Cosmology with positive and negative exponential potentials," *Class. Quant. Grav.*, vol. 19, pp. 5435–5448, 2002.

[16] N. D. Birrell and P. C. W. Davies, *Quantum Fields in Curved Space*, ser. Cambridge Monographs on Mathematical Physics. Cambridge University Press, 1982.

[17] V. Mukhanov and S. Winitzki, *Introduction to quantum effects in gravity.* Cambridge University Press, 6 2007.

[18] K. A. Malik and D. Wands, "Cosmological perturbations," *Phys. Rept.*, vol. 475, pp. 1–51, 2009.

[19] M. Bruni, S. Matarrese, S. Mollerach, and S. Sonego, "Perturbations of space-time: Gauge transformations and gauge invariance at second order and beyond," *Class. Quant. Grav.*, vol. 14, pp. 2585–2606, 1997.

[20] S. Matarrese, S. Mollerach, and M. Bruni, "Second order perturbations of the Einstein-de Sitter universe," *Phys. Rev. D*, vol. 58, p. 043504, 1998.

[21] J. M. Bardeen, "Gauge Invariant Cosmological Perturbations," *Phys. Rev. D*, vol. 22, pp. 1882–1905, 1980.

[22] V. Acquaviva, N. Bartolo, S. Matarrese, and A. Riotto, "Second order cosmological perturbations from inflation," *Nucl. Phys. B*, vol. 667, pp. 119–148, 2003.

[23] K. A. Malik and D. Wands, "Gauge invariant variables on cosmological hypersurfaces," 4 1998.

[24] K. A. Malik and D. Wands, "Evolution of second-order cosmological perturbations," *Class. Quant. Grav.*, vol. 21, pp. L65–L72, 2004.

[25] T. Falk, R. Rangarajan, and M. Srednicki, "The Angular dependence of the three point correlation function of the cosmic microwave background radiation as predicted by inflationary cosmologies," *Astrophys. J. Lett.*, vol. 403, p. L1, 1993.

[26] A. Gangui, F. Lucchin, S. Matarrese, and S. Mollerach, "The Three point correlation function of the cosmic microwave background in inflationary models," *Astrophys. J.*, vol. 430, pp. 447–457, 1994.

[27] J. M. Maldacena, "Non-Gaussian features of primordial fluctuations in single field inflationary models," *JHEP*, vol. 05, p. 013, 2003.

[28] D. H. Lyth and Y. Rodriguez, "Non-Gaussianity from the second-order cosmological perturbation," *Phys. Rev. D*, vol. 71, p. 123508, 2005.

[29] H. Kodama and M. Sasaki, "Cosmological Perturbation Theory," *Progress of Theoretical Physics Supplement*, vol. 78, pp. 1–166, 01 1984. [Online]. Available: https://doi.org/10.1143/PTPS.78.1

[30] Y. Akrami *et al.*, "Planck 2018 results. IX. Constraints on primordial non-Gaussianity," *Astron. Astrophys.*, vol. 641, p. A9, 2020.

[31] N. Aghanim *et al.*, "Planck 2018 results. VI. Cosmological parameters," *Astron. Astrophys.*, vol. 641, p. A6, 2020, [Erratum: Astron.Astrophys. 652, C4 (2021)].

[32] L. F. Abbott and M. B. Wise, "Large Scale Anisotropy of the Microwave Background and the Amplitude of Energy Density Fluctuations in the Early Universe," *Astrophys. J. Lett.*, vol. 282, pp. L47–L50, 1984.

[33] M. Kamionkowski and A. Loeb, "Getting around cosmic variance," *Phys. Rev. D*, vol. 56, pp. 4511–4513, 1997.

[34] E. Yusofi and M. Mohsenzadeh, "Creation of Non-minimal Coupled Particle in Asymptotic de-Sitter Background," 6 2015.

[35] J. Grain and V. Vennin, "Canonical transformations and squeezing formalism in cosmology," *JCAP*, vol. 02, p. 022, 2020.

[36] V. Mukhanov, "Theory of cosmological perturbations," *Physics Reports*, vol. 215, no. 5-6, pp. 203–333, jun 1992.

[37] W. Greiner and J. Reinhardt, *Field Quantization.* Springer Berlin Heidelberg, 1996.

[38] Y. Wang, "Inflation, Cosmic Perturbations and Non-Gaussianities," *Commun. Theor. Phys.*, vol. 62, pp. 109–166, 2014.

[39] D. Baumann, "Primordial Cosmology," *PoS*, vol. TASI2017, p. 009, 2018.

[40] H. Collins, "Primordial non-Gaussianities from inflation," 1 2011.

[41] R. M. Wald, *General Relativity.* Chicago, USA: Chicago Univ. Pr., 1984.

[42] F. Arroja and T. Tanaka, "A note on the role of the boundary terms for the non-Gaussianity in general k-inflation," *JCAP*, vol. 05, p. 005, 2011.

[43] X. Chen, M.-x. Huang, S. Kachru, and G. Shiu, "Observational signatures and non-Gaussianities of general single field inflation," *JCAP*, vol. 01, p. 002, 2007.

[44] E. Tzavara, "Second-order cosmological perturbations in two-field inflation and predictions for non-Gaussianity," Ph.D. dissertation, Orsay, LPT, 2013.

[45] A. Gervois and H. Navelet, "Integrals of three bessel functions and legendre functions. i," *Journal of Mathematical Physics*, vol. 26, no. 4, pp. 633–644, apr 1985.

[46] G. A. Tyler, "Analysis of propagation through turbulence: evaluation of an integral involving the product of three bessel functions," *Journal of the Optical Society of America A*, vol. 7, no. 7, p. 1218, jul 1990.

[47] V. Fabrikant, "Computation of infinite integrals involving three bessel functions by introduction of new formalism," *ZAMM*, vol. 83, no. 6, pp. 363–374, jun 2003.

[48] I. S. Gradshteyn, *Table of integrals, series and products.* Oxford: Academic, 2007.

[49] "*NIST Digital Library of Mathematical Functions*," http://dlmf.nist.gov/, Release 1.1.2 of 2021-06-15, f. W. J. Olver, A. B. Olde Daalhuis, D. W. Lozier, B. I. Schneider, R. F. Boisvert, C. W. Clark, B. R. Miller, B. V. Saunders, H. S. Cohl, and M. A. McClain, eds. [Online]. Available: http://dlmf.nist.gov/

[50] E. A. Lim, "Advanced Cosmology: Primordial non-Gaussianities," 2017.

[51] D. Seery, K. A. Malik, and D. H. Lyth, "Non-gaussianity of inflationary field perturbations from the field equation," *JCAP*, vol. 03, p. 014, 2008.

[52] F. Vernizzi, "On the conservation of second-order cosmological perturbations in a scalar field dominated Universe," *Phys. Rev. D*, vol. 71, p. 061301, 2005.

[53] A. Gruppuso and A. Sagnotti, "Observational Hints of a Pre–Inflationary Scale?" *Int. J. Mod. Phys. D*, vol. 24, no. 12, p. 1544008, 2015.

[54] P. A. R. Ade *et al.*, "Planck 2013 results. XVI. Cosmological parameters," *Astron. Astrophys.*, vol. 571, p. A16, 2014.

[55] N. Aghanim *et al.*, "Planck 2015 results. XI. CMB power spectra, likelihoods, and robustness of parameters," *Astron. Astrophys.*, vol. 594, p. A11, 2016.

[56] N. Kitazawa and A. Sagnotti, "Pre-inflationary clues from String Theory?" *JCAP*, vol. 04, p. 017, 2014.

[57] A. Gruppuso, N. Kitazawa, M. Lattanzi, N. Mandolesi, P. Natoli, and A. Sagnotti, "The Evens and Odds of CMB Anomalies," *Phys. Dark Univ.*, vol. 20, pp. 49–64, 2018.

[58] A. Sagnotti, "Low-ℓ CMB from string-scale SUSY breaking?" *Mod. Phys. Lett. A*, vol. 32, no. 01, p. 1730001, 2016.

[59] P. Fré, A. Sagnotti, and A. S. Sorin, "Integrable Scalar Cosmologies I. Foundations and links with String Theory," *Nucl. Phys. B*, vol. 877, pp. 1028–1106, 2013.

[60] I. Wolfson, "Numerical Analysis of the Primordial Power Spectrum for (Small Field) Inflationary Potentials," Other thesis, 3 2021.

[61] M. Hazumi *et al.*, "LiteBIRD: JAXA's new strategic L-class mission for all-sky surveys of cosmic microwave background polarization," *Proc. SPIE Int. Soc. Opt. Eng.*, vol. 11443, p. 114432F, 2020.

[62] T. C. C. C. Armitage-Caplan, M. Avillez, D. Barbosa, A. Banday, N. Bartolo, R. Battye, J. Bernard, P. Bernardis, S. Basak, M. Bersanelli, P. Bielewicz, A. Bonaldi, M. Bucher, F. Bouchet, F. Boulanger, C. Burigana, P. Camus, A. Challinor, S. Chongchitnan, D. Clements, S. Colafrancesco, J. Delabrouille, M. Petris, G. Zotti, C. Dickinson, J. Dunkley, T. Ensslin, J. Fergusson, P. Ferreira, K. Ferrière, F. Finelli, S. Galli, J. García-Bellido, C. Gauthier, M. Haverkorn, M. Hindmarsh, A. Jaffe, M. Kunz, J. Lesgourgues, A. Liddle, M. Liguori, M. López-Caniego, B. Maffei, P. Marchegiani, E. Martinez-Gonzalez, S. Masi, P. Mauskopf, S. Matarrese, A. Melchiorri, P. Mukherjee, F. Nati, P. Natoli, M. Negrello, L. Pagano, D. Paoletti, T. Peacocke, H. Peiris, L. Perroto, F. Piacentini, M. Piat, L. Piccirillo, G. Pisano, N. Ponthieu, C. Rath, S. Ricciardi, J. Martín, M. Salatino, P. Shellard, R. Stompor, L. T. J. Urrestilla, B. Tent, L. Verde, B. D. Wandelt, and S. Withington, "Core (cosmic origins explorer) a white paper," *arXiv: Cosmology and Nongalactic Astrophysics*, 2011.

[63] J. Chluba *et al.*, "New Horizons in Cosmology with Spectral Distortions of the Cosmic Microwave Background," 9 2019.

[64] S. Matarrese and L. Verde, "The effect of primordial non-Gaussianity on halo bias," *Astrophys. J. Lett.*, vol. 677, pp. L77–L80, 2008.

[65] N. Dalal, O. Dore, D. Huterer, and A. Shirokov, "The imprints of primordial non-gaussianities on large-scale structure: scale dependent bias and abundance of virialized objects," *Phys. Rev. D*, vol. 77, p. 123514, 2008.

[66] A. J. Ross *et al.*, "The Clustering of Galaxies in SDSS-III DR9 Baryon Oscillation Spectroscopic Survey: Constraints on Primordial Non-Gaussianity," *Mon. Not. Roy. Astron. Soc.*, vol. 428, pp. 1116–1127, 2013.

[67] E. Sefusatti and E. Komatsu, "The Bispectrum of Galaxies from High-Redshift Galaxy Surveys: Primordial Non-Gaussianity and Non-Linear Galaxy Bias," *Phys. Rev. D*, vol. 76, p. 083004, 2007.

[68] J.-Q. Xia, A. Bonaldi, C. Baccigalupi, G. De Zotti, S. Matarrese, L. Verde, and M. Viel, "Constraining Primordial Non-Gaussianity with High-Redshift Probes," *JCAP*, vol. 08, p. 013, 2010.

[69] R. Laureijs, J. Amiaux, S. Arduini, J. L. Auguères, J. Brinchmann, R. Cole, M. Cropper, C. Dabin, L. Duvet, A. Ealet, B. Garilli, P. Gondoin, L. Guzzo, J. Hoar, H. Hoekstra, R. Holmes, T. Kitching, T. Maciaszek, Y. Mellier, F. Pasian, W. Percival, J. Rhodes, G. Saavedra Criado, M. Sauvage, R. Scaramella, L. Valenziano, S. Warren, R. Bender, F. Castander, A. Cimatti, O. Le Fèvre, H. Kurki-Suonio, M. Levi, P. Lilje, G. Meylan, R. Nichol, K. Pedersen, V. Popa, R. Rebolo Lopez, H. W. Rix, H. Rottgering, W. Zeilinger, F. Grupp, P. Hudelot, R. Massey, M. Meneghetti, L. Miller, S. Paltani, S. Paulin-Henriksson, S. Pires, C. Saxton, T. Schrabback, G. Seidel, J. Walsh, N. Aghanim, L. Amendola, J. Bartlett, C. Baccigalupi, J. P. Beaulieu, K. Benabed, J. G. Cuby, D. Elbaz, P. Fosalba, G. Gavazzi, A. Helmi, I. Hook, M. Irwin, J. P. Kneib, M. Kunz, F. Mannucci, L. Moscardini, C. Tao, R. Teyssier, J. Weller, G. Zamorani, M. R. Zapatero Osorio, O. Boulade, J. J. Foumond, A. Di Giorgio, P. Guttridge, A. James, M. Kemp, J. Martignac, A. Spencer, D. Walton, T. Blümchen, C. Bonoli, F. Bortoletto, C. Cerna, L. Corcione, C. Fabron, K. Jahnke, S. Ligori, F. Madrid, L. Martin, G. Morgante, T. Pamplona, E. Prieto, M. Riva, R. Toledo, M. Trifoglio, F. Zerbi, F. Abdalla, M. Douspis, C. Grenet, S. Borgani, R. Bouwens, F. Courbin, J. M. Delouis, P. Dubath, A. Fontana, M. Frailis, A. Grazian, J. Koppenhöfer, O. Mansutti, M. Melchior, M. Mignoli, J. Mohr, C. Neissner, K. Noddle, M. Poncet, M. Scodeggio, S. Serrano, N. Shane, J. L. Starck, C. Surace, A. Taylor, G. Verdoes-Kleijn, C. Vuerli, O. R. Williams, A. Zacchei, B. Altieri,

I. Escudero Sanz, R. Kohley, T. Oosterbroek, P. Astier, D. Bacon, S. Bardelli, C. Baugh, F. Bellagamba, C. Benoist, D. Bianchi, A. Biviano, E. Branchini, C. Carbone, V. Cardone, D. Clements, S. Colombi, C. Conselice, G. Cresci, N. Deacon, J. Dunlop, C. Fedeli, F. Fontanot, P. Franzetti, C. Giocoli, J. Garcia-Bellido, J. Gow, A. Heavens, P. Hewett, C. Heymans, A. Holland, Z. Huang, O. Ilbert, B. Joachimi, E. Jennins, E. Kerins, A. Kiessling, D. Kirk, R. Kotak, O. Krause, O. Lahav, F. van Leeuwen, J. Lesgourgues, M. Lombardi, M. Magliocchetti, K. Maguire, E. Majerotto, R. Maoli, F. Marulli, S. Maurogordato, H. McCracken, R. McLure, A. Melchiorri, A. Merson, M. Moresco, M. Nonino, P. Norberg, J. Peacock, R. Pello, M. Penny, V. Pettorino, C. Di Porto, L. Pozzetti, C. Quercellini, M. Radovich, A. Rassat, N. Roche, S. Ronayette, E. Rossetti, B. Sartoris, P. Schneider, E. Semboloni, S. Serjeant, F. Simpson, C. Skordis, G. Smadja, S. Smartt, P. Spano, S. Spiro, M. Sullivan, A. Tilquin, R. Trotta, L. Verde, Y. Wang, G. Williger, G. Zhao, J. Zoubian, and E. Zucca, "Euclid Definition Study Report," *arXiv e-prints*, p. arXiv:1110.3193, Oct. 2011.

[70] O. Doré *et al.*, "Cosmology with the SPHEREX All-Sky Spectral Survey," 12 2014.

[71] S. Camera, M. G. Santos, and R. Maartens, "Probing primordial non-Gaussianity with SKA galaxy redshift surveys: a fully relativistic analysis," *Mon. Not. Roy. Astron. Soc.*, vol. 448, no. 2, pp. 1035–1043, 2015, [Erratum: Mon.Not.Roy.Astron.Soc. 467, 1505–1506 (2017)].